

Matthias Leopold Schroeter: Enlightening the Brain: Optical Imaging in Cognitive Neuroscience. Leipzig: Max Planck Institute for Human Cognitive and Brain Sciences, 2006 (MPI Series in Human Cognitive and Brain Sciences; 72)

Enlightening the Brain – Optical Imaging in Cognitive Neuroscience

Der Hohen Medizinischen Fakultät
der Universität Leipzig
eingereichte

HABILITATIONSSCHRIFT

zur Erlangung des akademischen Grades

Doctor medicinae habilitatus
(Dr. med. habil.)

vorgelegt von

Dr. med. Matthias Leopold Schroeter, M.A.
geboren am 22.10.1965 in Döbeln

Datum des Verleihungsbeschlusses:

18.04.2006

Gutachter

Prof. Dr. med. Hans Förstl
Prof. Dr. med. Christoph Hock
Prof. Dr. med. Arno Villringer

Bibliographische Beschreibung

Matthias Leopold Schroeter: *Enlightening the Brain – Optical Imaging in Cognitive Neuroscience [Optische Bildgebung in der kognitiven Neurowissenschaft]*

Die vorliegende Habilitationsschrift befaßt sich mit der Etablierung der optischen Bildgebung (funktionelle Nahinfrarot-Spektroskopie) in der kognitiven Neurowissenschaft. Im ersten Teil wird in die Methode eingeführt. Hierbei werden im besonderen die Vorteile der Methode dargestellt. Im zweiten Teil werden die Ergebnisse der eigenen Experimente vorgestellt. Diese zeigen, daß mit der optischen Bildgebung kortikale Aktivierungen zuverlässig erfaßt werden können. In der Anwendung auf kognitive Studien wird dargestellt, daß ereigniskorrelierte Stimulationsdesigns, am günstigsten mit einer randomisierten Stimuluspräsentation, möglich sind. Die weiteren Experimente etablieren die Methode für kognitive Studien mit Kindern (Entwicklungsneuropsychologie), mit älteren Probanden (Neuropsychologie des Alterns) und mit Patienten (kognitive Neuropsychiatrie). Im letzten Experiment werden Standardanalyseverfahren für die Methode untersucht. Der letzte Teil bettet die eigenen Experimente in die internationalen Studien ein. Im Ergebnis trägt die Arbeit zu einer Etablierung der optischen Bildgebung in den kognitiven Neurowissenschaften bei.

Danksagung

Zuallererst möchte ich mich dafür bedanken, daß mir die Durchführung der Experimente am Max-Planck-Institut für Kognitions- und Neurowissenschaften in Leipzig mit seinen exzellenten Arbeitsbedingungen durch Herrn Prof. D. Yves von Cramon ermöglicht wurde.

Die vorliegende Arbeit hätte nicht ohne die Kooperationspartner vom Berlin-NeuroImaging Center an der Berliner Charité (Herrn PD Dr. Hellmuth Obrig und Herrn Dr. Kamil Uludag) entstehen können, welche mir immer hervorragende Diskussionspartner bezüglich methodischer Fragen waren.

Weiterhin gilt mein besonderer Dank Herrn Dr. Stefan Zysset, der mich in die Kognitionswissenschaften einführte, meinen Doktoranden Herrn Thomas Kupka und Frau Barbara Ettrich und meinem ehemaligen Mitarbeiter Herrn Dr. Markus Bücheler für ihre begeisterte Mitarbeit. Herrn Stephan Liebig danke ich für die langmütige Unterstützung meiner graphischen Sonderwünsche.

Zuletzt möchte ich meiner Frau Margarethe Wahl und meinen Kindern Moritz und Emilia danken, welche mich immer unterstützten und welche sich trotz meiner jahrelangen Arbeit an der Habilitation entschieden das Licht der Welt zu erblicken.

Contents

1.	Introduction	1
1.1.	<i>Neuroimaging Methods</i>	1
1.2.	<i>Non-Invasive Optical Neuroimaging</i>	2
1.2.1.	Basic Concept	2
1.2.2.	Comparison with other Imaging Techniques	3
1.2.3.	Physical Basis of Optical Imaging	6
1.2.3.1.	The Optical Window	6
1.2.3.2.	Interactions of Photons with Tissue	6
1.2.3.3.	The (modified) Lambert-Beer Law	8
1.2.3.4.	Determining the Differential Pathlength Factor	9
1.2.3.5.	Limitations of the (modified) Lambert-Beer Law	9
1.2.4.	Optical Measurement Devices	10
1.2.5.	One Channel Measurements vs. Optical Imaging	11
1.2.6.	Placement of Optodes	12
1.3.	<i>Neurovascular Coupling</i>	14
1.3.1.	Changes in Hemoglobin Oxygenation due to Activation	15
1.3.2.	Changes in the Redox-State of the Cytochrome-c-Oxidase due to Activation	17
2.	Experiments	19
2.1.	<i>Main Issues of Current Research</i>	19
2.2.	<i>Neurovascular Coupling & Origin of the Optical Signal</i>	22
2.3.	<i>Establishing Optical Imaging as a Tool for Cognitive Neuroscience</i>	30
2.4.	The Stroop Interference Task	30
2.4.1.	The Color-Word Matching Stroop Interference Task	31
2.5.	Event-Related Designs for Cognitive fNIRS Studies	32
2.5.1.	Stroop Interference activates the Lateral Prefrontal Cortex	32
2.5.2.	Searching the Optimal Intertrial Interval for fNIRS	40
2.6.	Development & Aging	46
2.6.1.	Prefrontal Activation due to Stroop Interference increases during Development	46
2.6.2.	Prefrontal Activation due to Stroop Interference declines with Aging	52
2.6.3.	Spontaneous Low Frequency Oscillations decline in the Aging Brain	59
2.7.	Patient Studies	66
2.7.1.	Brain Activation declines in Cerebral Microangiopathy during a Stroop Interference Task	66
2.7.2.	Spontaneous Slow Hemodynamic Oscillations are impaired in Cerebral Microangiopathy	70
2.8.	<i>Towards Standard Analyses for Functional Near-Infrared Imaging</i>	79
3.	Embedding Optical Imaging into Cognitive Neuroscience	89
3.1.	<i>Previous Optical Studies in Cognitive Neuroscience</i>	89
3.2.	<i>Prospects for Optical Imaging in Cognitive Neuroscience</i>	95
4.	References	97
5.	Appendix	115

Abbreviations

AD	Alzheimer's disease
ANOVA	analysis of variance
BOLD	blood-oxygenation level dependent (signal)
CBF	cerebral blood flow
CBV	cerebral blood volume
CMA	cerebral microangiopathy
Cyt-Ox	cytochrome-c-oxidase
DPF	differential pathlength factor
EEG	electroencephalography
EPI	echo planar imaging
ERP	event related potential
fNIRS	functional near-infrared spectroscopy
fMRI	functional magnetic resonance imaging
Hb	hemoglobin
HbD	hemoglobin difference
ITI	intertrial interval
LFO	low frequency oscillation
LPFC	lateral prefrontal cortex
MD	major depression
MDEFT	modified driven equilibrium Fourier transform
MEG	magnetoencephalography
MNI	Montreal neurological institute
MRI	magnetic resonance imaging
NIRS	near-infrared spectroscopy
PET	positron emission tomography
PSD	power spectral density
PTSD	posttraumatic stress disorder
rCBF	regional cerebral blood flow
rCBV	regional cerebral blood volume
SD	standard deviation
SEM	standard error of the mean
SPECT	single-positron emission computed tomography
tHB	total hemoglobin
TMS	transcranial magnetic stimulation
VLFO	very low frequency oscillation

1. Introduction

The main aim of the work is to establish optical imaging¹ as a standard tool for cognitive neuroscience. Cognitive neuroscience emerged over the past two decades (Gazzaniga, 2004). By attributing mental functions to brain structures it aims at understanding the relationship between mind and brain. Traditionally, patients with brain lesions were examined psychologically to infer brain function. Recent technological advances, such as functional imaging techniques, have allowed neuroscientists to measure and localize brain activity in healthy individuals. In the result, cognitive functions such as attention, perception, learning, memory, language, and executive functions could be related to brain structures. Moreover, by applying cognitive neuroscience to psychiatry and neurology, clinical symptoms might be explained in terms of deficits to normal cognitive mechanisms (David & Halligan, 2000; Halligan & David, 2001). Hence, cognitive neuropsychiatry attempts to establish the functional organization of neuropsychiatric disorders within a framework of human cognitive neuropsychology. After shortly outlining cognitive neuroscience the next chapters give an introduction to imaging methods and emphasize particularly the importance of optical approaches.

1.1. Neuroimaging Methods

Several non- or minimally-invasive neuromonitoring techniques for examining functional brain activity are currently available (Frackowiak et al., 2002). Historically, electroencephalography (EEG) was the first to appear, followed by other technologies including positron emission tomography (PET) and single-positron emission computed tomography (SPECT), magnetoencephalography (MEG), and most recently functional magnetic resonance imaging (fMRI). These methods are often categorized in terms of whether they provide direct or indirect information about brain function (Figure 1). Direct methods include MEG, EEG, and event-triggered EEG (also called event related potentials; ERPs), each of which monitors brain electromagnetic activity directly. In particular, EEG and ERP record the electrical fields generated by neuronal activity, while MEG records the magnetic fields induced by such activity. PET, SPECT and fMRI, on the other hand, are indirect methods in that they generally monitor hemodynamic changes consequent to brain electrical activity. PET and SPECT brain imaging operate by monitoring the decay of blood-borne radioactive isotopes as they pass through the brain. fMRI, in contrast, detects changes in the local concentration of deoxyhemoglobin via its effect on imposed magnetic fields. While each of these techniques has its own distinct advantages, at present the direct methods tend to have

¹ The term 'optical imaging' will be used generally as synonymously with near-infrared spectroscopic imaging, although, in a broader meaning, it includes fast optical signals (Gratton & Fabiani, 2001) and intrinsic optical signals (Pouratian et al., 2003).

limited spatial resolution, whereas the indirect methods can only detect neuronal activity after it has been filtered by a complex and poorly-understood neurovascular coupling function (described in more detail in chapter 2.2.).

1.2. Non-Invasive Optical Neuroimaging

1.2.1. Basic Concept

Optical imaging capitalizes on the absorption and scattering properties of near-infrared light to provide information about brain activity. It was long thought that the scattering of light by tissue made it impossible to recover information from anything but the most superficial layers of tissue (e.g., microscopy). Accordingly, most long-standing optical techniques in use in the neurosciences are for superficial tissues only (Villringer & Chance, 1997). Some 30 years ago, however, it was discovered that useful information could be obtained from thick tissue samples, including brain monitoring using light applied to and detected from the scalp (Jöbsis, 1977). This finding accelerated the development of optical imaging as a technique for human brain monitoring. The technique is called variously near-infrared spectroscopy (NIRS), (diffuse) optical tomography or topography or near-infrared imaging. All of the techniques are based on essentially the same concept - shining light onto the scalp, detecting it as it exits the head, and using the absorption spectra of the light absorbing molecules (chromophores) present in tissue to interpret the detected light levels as changes in chromophore concentrations.

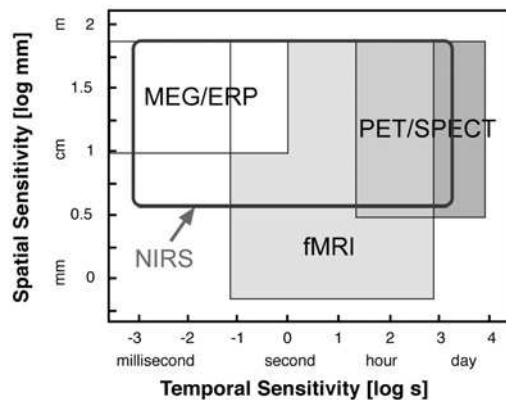


Figure 1 Comparison of the spatial and temporal sensitivities of the several neuroimaging techniques. Methods provide either direct (white) or indirect (gray) information about brain function (Strangman et al., 2002a).

1.2.2. Comparison with other Imaging Techniques

Figure 1 compares the spatial and temporal sensitivity of the various brain imaging techniques, modeled after a similar figure by Churchland & Sejnowski (1988). Obviously, MEG and ERPs are characterized by a high temporal sensitivity but relatively weak spatial sensitivity. In contrast, fMRI, PET and SPECT enable a higher spatial sensitivity but are weak in terms of temporal resolution. Optical techniques, in comparison, can provide excellent temporal sensitivity as well as reasonable spatial sensitivity. When multiple wavelengths of light are used simultaneously, moreover, spectroscopic information about the sampled tissue also becomes available, thereby affording the promise of quantifying the concentrations of the various hemoglobin species – oxyhemoglobin, deoxyhemoglobin, and the sum of these (total hemoglobin, which is proportional to blood volume).

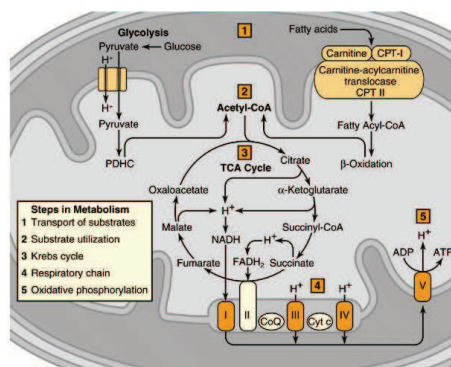


Figure 2 Schematic representation of mitochondrial metabolism. Respiratory chain complexes or components I-V. CoQ coenzyme Q, Cyt c cytochrome-c (Siegel et al., 1999).

In addition to hemoglobin-based measures of brain activity, optical techniques can measure other tissue chromophores, including cytochrome-c-oxidase (EC 1.9.3.1; Figure 2). The enzyme, which is located in complex IV of the respiratory chain in mitochondria, is tightly coupled to the production of adenosine triphosphate by oxidative phosphorylation (Siegel, et al., 1999; Wong-Riley, 1989). Because neurons depend strongly on oxidative energy metabolism, cytochrome-c-oxidase is considered as an endogenous metabolic marker for neuronal activity. Hence, cytochrome-c-oxidase measurements can provide more direct information about neuronal activity than hemoglobin changes (Heekeren et al., 1999; Jöbsis et al., 1977). There is also evidence to suggest that optical methods can detect cell swelling that occurs in the 50–200 milliseconds following neuronal firing, which would be an even more direct measure of neuronal activity than the hemodynamic or metabolic markers (Gratton et al., 2003; Gratton & Fabiani, 2001; Steinbrink et al., 2000; Stepnoski et al., 1991). This type of ‘fast’ signal appears to be significantly smaller than the hemodynamic signals (on the order of a 0.01% signal change). With sufficiently fast and sensitive electronics,

however, such signals could be feasibly recorded by the same equipment as the hemodynamic signals (Figure 3).² Thus, optical techniques may be simultaneously capable of providing both indirect and more direct methods of neuronal activity monitoring complementary sources of information about brain function.

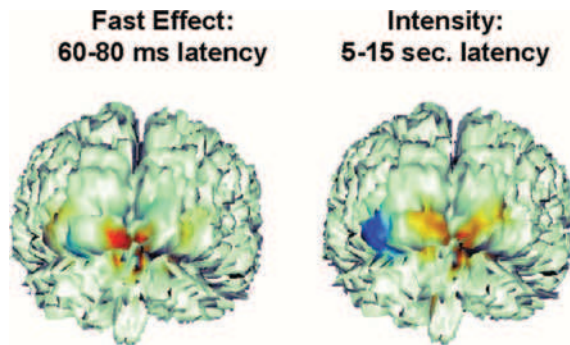


Figure 3 Maps of the neuronal ('fast') and hemodynamic ('slow') optical responses during visual stimulation. Areas in red indicate maximum increase in phase delay (left) and maximum increase in the light reaching the detector (right) indicating increased activity (blue indicates the opposite) (from Gratton et al., 2001).

Advantages of optical approaches are illustrated in Figure 4. In particular, the instrumentation - which is completely non-invasive - can be made portable, unobtrusive, low-cost, low-power, and can even be made robust to motion artifacts (e.g., Totaro et al., 1998). For the cognitive neuroscientist, these strengths can bring previously unthinkable projects into the realm of possibility. For example, with proper fiber coupling, extensive movement can be tolerated, opening up the possibility of studying neonates and infants (Meek et al., 1998; Pena et al., 2003; Taga et al., 2003; Zaramella et al., 2001), children (Baird et al., 2002), patients with severe movement disorders, moving patients, for instance walking on a tread mill (Miyai et al., 2001, 2002, 2003; Suzuki et al., 2004) or other highly animated subjects, without sedation, such as patients suffering from mania, schizophrenia or Alzheimer's disease (Eschweiler et al., 2000; Fallgatter et al., 1997; Fallgatter & Strik, 2000; Fladby et al., 2004). Recently, Vaithianathan et al. (2004) designed even a portable optical imaging system for infants. Moreover, it was suggested to use optical imaging for brain-computer interfaces (Coyle et al., 2004). The portability and near-zero run-time cost of the instrument enables bedside monitoring for extended periods, which could be useful for monitoring the effects of

² Although, as discussed above, near-infrared light might be used to detect the highly promising 'fast' optical signal, this issue will not be considered further as almost all of these studies examined activations in primary brain regions only (sensorimotor cortex: DeSoto et al., 2001; Franceschini & Boas, 2004; Gratton et al., 1995b; Maclin et al., 2004; Morren et al., 2004; Steinbrinck et al., 2000; Wolf et al., 2002a; visual cortex: Fabiani et al., 2003; Gratton, 1997; Gratton et al., 1995a, 1997, 1998, 2000, 2001; Gratton & Fabiani, 2003; Wolf et al., 2003; auditory cortex: Rinne et al., 1999). Further, detectability of the 'fast' optical signal is even controversial (Syre et al., 2003). Highly invasive imaging of intrinsic optical signals can be detected in the near-infrared range if the skull is removed (Pouratian et al., 2003). However, only two cognitive studies have been conducted with this method, whereas one of them was even a case study (Cannestra et al., 2000; Pouratian et al., 2000). Whether the limitation of these techniques is a general one, has to be explored in future studies.

slowly acting drugs, or slowly evolving pathologies. The fact that near-infrared light is non-ionizing³ means that there is no limit to the number of scans one can undergo. Patients may be examined several times opening a window to studies of development and treatment effects. Moreover, patients and children who might not stand the confined environment of fMRI experiments can be examined, which is particularly relevant for imaging studies with patients suffering from anxiety disorders. Because of its high temporal sensitivity Fourier and power spectral analysis approaches might easily be applied to optical signals (Obrig et al., 2000a). Moreover, optical measurements are not influenced by magnetic or electric fields, if long enough fibers are supplied. Accordingly, optical imaging can easily be combined with electrical stimulation (Sakatani et al., 1999; Tanosaki et al., 2001, 2003), (visually) evoked potentials (Obrig et al., 2002), EEG (Buchheim et al., 2004; Fabbri et al., 2003; Haginoya et al., 2002; Moosmann et al., 2003), MEG (Mackert et al., 2004), transcranial magnetic stimulation (TMS) (Noguchi et al., 2003), Doppler (Terborg et al., 2000), fMRI (Kleinschmidt et al., 1996) and PET (Hock et al., 1997). Combining biochemically specific optical imaging with other imaging methods may further enable studies on neurovascular coupling, particularly because it is sensitive to the microvasculature (Boushel et al., 2001; Liu et al., 1995a,b), whereas for instance the blood-oxygenation level dependent (BOLD) signal represents all spatial scales of venous vessels (Lee et al., 2001; Strangman et al., 2002b; Weisskoff, 1999). The most decisive drawback of the method is that it can not detect brain activation in areas distant from the skin surface, such as the frontomedian cortex and basal ganglia (see Figure 8).

Pros and Cons of Optical Imaging

- | | |
|---|--|
| <ul style="list-style-type: none"> • Portable, unobtrusive, low-cost • Biochemical specificity • Vascular and intracellular signal • 'Fast' and 'slow' response • Sensitive to microvasculature • High temporal sensitivity • Easy combination with other imaging methods • Robust to motion artifacts • Patient studies • Children studies | <ul style="list-style-type: none"> • Low spatial resolution (increased by mapping) • Cortex without deeper areas |
|---|--|

Figure 4 Advantages and disadvantages of optical imaging.

³ Unlike MEG and EEG, which are passive recording techniques, optical techniques - like MRI and PET - operate by depositing energy into the subject and recording changes in that energy when remitted. Near-infrared light is non-ionizing (unlike, for example, ultraviolet and shorter light wavelengths). The primary side effect is tissue heating, which is for brain monitoring most relevant for the skin of the scalp, as the vast majority (>95 %) of the near-infrared power is deposited in this layer. The power required for optical measurements remains well below the level where tissue damage from heating might occur (Ito et al., 2000). However, at present, there is little information on the direct effects of near-infrared light on brain tissue.

1.2.3. Physical Basis of Optical Imaging

1.2.3.1. The Optical Window

Optical recordings depend on two critical characteristics of the electromagnetic spectrum as it interacts with biological tissue. Biological tissue is relatively opaque to visible light. Contrary, near-infrared light - from approximately 650-950 nm - is more weakly absorbed by tissue. As a result, this range of wavelengths is often called an “optical window” into biological tissue. This property allows light of these wavelengths to penetrate several centimeters through tissue and still be detected.

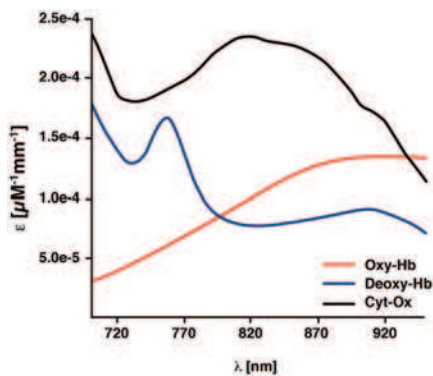


Figure 5 Extinction coefficient (ϵ) spectra of oxygenated and deoxygenated hemoglobin (Oxy-Hb, Deoxy-Hb) and the difference spectrum of oxidized minus reduced cytochrome-c-oxidase (Cyt-Ox) (Uludag et al., 2004).

The second critical characteristic of near-infrared light as it interacts with biological tissue is also apparent in Figure 5. The two dominant chromophores for the near-infrared wavelength range just happen to be two biologically relevant markers for brain activation: oxy- and deoxyhemoglobin. Thus, near-infrared wavelengths pass relatively easily through tissue, and their absorption can provide information relevant to brain function.

1.2.3.2. Interactions of Photons with Tissue

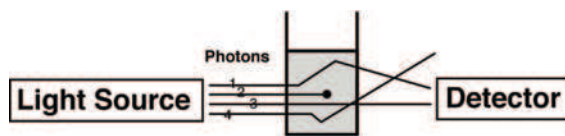
As illustrated in Figure 6, photons that enter tissue may undergo, in principle, the following types of interaction with tissue (Villringer & Chance, 1997). Absorption leads to radiationless loss of energy to the medium. Further, photons may induce either fluorescence (or delayed fluorescence) or phosphorescence. Lastly, scattering may occur at unchanged frequency when occurring in stationary tissue or accompanied by a Doppler shift due to scattering by moving particles in the tissue (for example, blood cells).

Absorption	Radiationless loss of energy to the medium
Scattering	Direction change of photons at borders of media with different refractive indices
Fluorescence/ Phosphorescence	Results in photons with longer pathlength (<math>< > 10^{-6}< /math> s delay)

Figure 6 Possible interactions of light with tissue.

Typically, an optical apparatus consists of a light source by which the tissue is irradiated, and a light detector that receives light after it has been reflected from or transmitted through the tissue (Figure 7). Light that has traveled through tissue is attenuated mainly due to absorption and scattering. By analogy with a photometer, this can then be expressed mathematically in a modified Lambert–Beer law. Separating light of different wavelengths using certain filter designs is the basis for the detection of fluorescent or phosphorescent light, which has a longer wavelength than the irradiated (and reflected) light. The detection of the Doppler frequency shift of scattered light is the basis of laser Doppler flowmetry devices (Stern, 1975).

Absorption changes of near-infrared light within the head are predominantly driven by changes in hemoglobin concentrations (Strangman et al., 2002a). Sources of scattering changes, in contrast, are only partly understood. For example, scattering may be higher in regions with dense fiber tracts. Presently, most optical brain monitoring experiments assume scattering remains essentially constant during the experiment and that all observed signal fluctuations are due to changes in absorption.



Modified Lambert-Beer Law

$$A = \epsilon \times c \times d \times B + G$$

- A:** Lg [I₀/I]: Light extinction
- ε:** Specific extinction coefficient
- c:** Substance concentration
- d:** Distance (width of cuvette)
- B:** Differential path length factor (DPF)
- G:** Signal loss due to light scattering

Figure 7 Influence of light absorption and scattering on optical measurement as described with the modified Lambert–Beer law (Villringer & Chance, 1997).

1.2.3.3. The (modified) Lambert-Beer Law

The concentration of a light absorbing molecule in tissue is determined similarly to the determination of a substance concentration in a photometer (Figure 7; Cope et al., 1987). Assuming infinitesimal substance concentrations, and therefore negligible light scattering, a concentration can be determined according to the original Lambert–Beer law,

$$A = \varepsilon * c * d \quad (1)$$

in which the extinction of light (the logarithm of the ratio of incident versus measured light, $\lg(I_0/I)$) is proportional to the concentration c of the absorber multiplied by the constant extinction coefficient ε for the particular absorber and the distance d corresponding to the width of the cuvette. This law holds as long as photons are either absorbed (photon 2 in Figure 7) or transmitted in a straight line directly to the detector (photon 3 in Figure 7).

With higher substance concentrations and significant light scattering, the formula must be modified to take into account the longer pathlength of light (see photon 1 in Figure 7) and the loss of light (photon 4 in Figure 7) due to light scattering.

$$A = \varepsilon * c * d * B + G \quad (2)$$

Therefore, a term B (differential pathlength factor) which accounts for the longer pathlength and a term G , which is a measure of the signal loss due to light scattering and which depends mainly on geometrical factors are introduced in the modified Lambert–Beer law (Figure 7). It has to be mentioned, that ε , B and G are wavelength dependent. Further, G is usually not known and, therefore, absolute chromophore concentration cannot be assessed.

In certain situations only the difference c between two situations is of interest and under the assumption of a constant light scattering loss the term G cancels out in the subtraction.

$$\Delta A = \varepsilon * \Delta c * d * B \quad (3)$$

If the pathlength $d * B$ can be determined, absolute changes in concentration can be calculated.

$$\Delta c = \frac{\Delta A}{\varepsilon * d * B} \quad (4)$$

In the result, one may determine concentration changes of one chromophore. The simultaneous assessment of several chromophores relies on measuring absorption changes ΔA at several wavelengths in the near-infrared range (Cope et al., 1991). Changes of the relevant chromophores can be separated by relying on their differential extinction coefficients (Figure 5). Hence, changes in hemoglobin concentrations and in the redox state of the cytochrome-c-oxidase enable to detect the underlying brain activity (Villringer & Chance, 1997).

1.2.3.4. Determining the Differential Pathlength Factor

For absolute measurements of the pathlength there are several types of optical approaches (Elwell, 1995; Villringer & Chance, 1997). One uses the measurement of the direct time of flight of a short (ps) light pulse traveling through tissue. In another approach the phase shift of a light source that is intensity-modulated at a certain frequency is measured. A third approach measures water absorption that, assuming a constant water concentration in tissue, should change with the pathlength of light. The above mentioned approaches for the determination of pathlength may not only serve for a more accurate determination of a substance concentration, but they may also serve to measure light scattering (or changes in light scattering) as another optical parameter.

1.2.3.5. Limitations of the (modified) Lambert-Beer Law

Although the (modified) Lambert-Beer law provides a reasonable approximation to calculating concentration changes, it depends on several strong assumptions (Obrig & Villringer, 2003).

The first one is that scattering is high but changes are negligible during the measurement. This assumption permits the investigator to disregard the loss of light intensity due to scattering G as long as *changes* in attenuation are assessed. It allows the investigator to assume the differential pathlength factor B at a certain wavelength to be constant. The assumption is plausible because changes in blood flow will more strongly change, owing to changes in hemoglobin oxygenation and concentration, the absorption coefficient μ_a of the tissue rather than the scatter coefficient μ_s (i.e., changes in scattering particles in the sampling volume and ultrastructural changes in the neuronal tissue).

Second, one has to assume that the medium in which changes are monitored is homogeneous. This assumption is one of the reasons for the low spatial resolution of

noninvasive NIRS when compared with invasive optical techniques. Third, applying the (modified) Lambert-Beer law includes the assumption that the change in the volume sampled is homogeneous within the sampling volume. This assumption, related to the second assumption, is also wrong and introduces an additional source of error that stems from the wavelength dependence of the differential pathlength factor. In an adult human, the scalp and skull range from approximately 1 to 2 cm thick, depending on the subject and the region on the head (Okamoto et al., 2004a). Moreover, a lack of significant findings in these layers from whole-head fMRI scanning suggests that these layers generally exhibit little or no change in hemodynamic variables during task performance. Thus, the region of hemoglobin change will typically be focal relative to the entire sampling region for a given source-detector pair (partial volume effect). The consequences of violating the global-change assumption are only beginning to be characterized (Uludag et al., 2002). Thus far, the validity of the technique has tested favorably against several other monitoring modalities (for instance Kleinschmidt et al., 1996; Terborg et al., 2000; Villringer et al., 1997; for a detailed discussion see chapter 2.2.). Theoretical studies suggest that any resulting errors can be limited to less than 10% (Strangman et al., 2002a). One way to further reduce such focal-change errors is to use imaging instruments with associated image reconstruction algorithms as proposed for instance by Strangman et al. (2002a). Limitations of the three assumptions of optical approaches, and respective proposed solutions are no further discussed in the present paper. Please, refer to extensive discussions in the literature (Boas et al., 2001, 2004; Strangman et al., 2002a, 2003).

Another limitation is related to the question, whether one may detect redox changes in cytochrome-c-oxidase in response to cerebral activation by non-invasive NIRS. Some experiments suggested that these changes are hampered by methodological spectroscopic issues (cross talk with oxyhemoglobin), and can therefore be fully explained as an artifact of changes of oxyhemoglobin (Uludag et al., 2002). Other studies support the detectability of redox changes in cytochrome-c-oxidase, if full-spectrum approaches are applied (Cooper et al., 1997; Cooper & Springett, 1997; Hekeeren et al., 1999; Uludag et al., 2004).

1.2.4. Optical Measurement Devices

Three main categories of optical measurements have been developed: time domain, frequency domain and continuous wave measurements (Strangman et al., 2002a). Time domain, or time-resolved, systems introduce extremely short (ps) incident pulses of light into tissue, which are broadened and attenuated by the various tissue layers (e.g., skin, skull, cerebrospinal fluid and brain). A time domain system detects the temporal distribution of

photons as they leave the tissue, and the shape of this distribution provides information about tissue absorption and scattering. In frequency domain systems, the light source shines continuously but is amplitude-modulated at frequencies on the order of tens to hundreds of MHz. Information about the absorption and scattering properties of tissue are obtained by recording the amplitude decay and phase shift (delay) of the detected signal with respect to the incident signal. In continuous-wave systems, light sources emit light continuously, like frequency domain systems, but at constant amplitude, or modulated at frequencies not higher than a few tens of kHz (which provides stray-light rejection). Continuous-wave systems measure only the amplitude decay of the incident light. Absorption and scattering can not be separated.

Each of these techniques has intrinsic advantages and drawbacks. The choice of measurement mode is basically determined by the type of information one needs to collect. For the neuroimaging researcher interested in monitoring brain function changes over time, a frequency domain or continuous wave instrument is sufficient; the added spatial specificity of time domain instruments and the ability to separate absorption and scattering effects is not clearly necessary for such measurements.

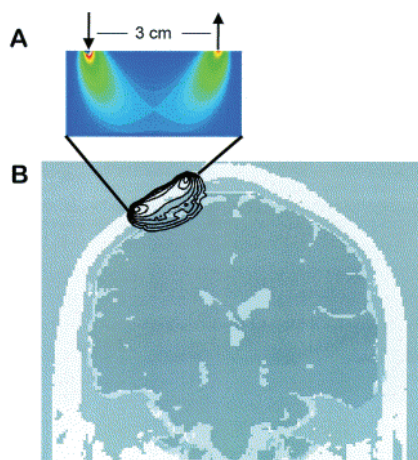


Figure 8 **A** An example sensitivity plot for light traveling in a homogeneous, highly scattering medium for a continuous-wave or frequency-domain measurement. Colors indicate the number of detected photons that reached any given point in the homogeneous medium (white/reds/yellows indicate highest numbers, and hence sensitivities, blues/purples indicate lower sensitivities). **B** A similar plot for light traveling through the head of an example subject. (Strangman et al., 2002a).

1.2.5. One Channel Measurements vs. Optical Imaging

Each of the three instrument types can in theory be deployed as either point (one channel) measurement or imaging devices. Figure 8 illustrates a one channel instrument. Optical imaging instruments have been available for a few years only (Eda et al., 1999; Hoshi et al., 2000; Watanabe et al., 1998). Fundamentally, the difference between a point-measurement

instrument and an imaging instrument lies merely in the number and geometrical arrangement of sources and detectors. In particular, a point-measurement instrument requires only one source location and one or more detector locations. In contrast, a true imaging instrument requires that each detector be able to detect light from two or more source locations. To increase spatial sensitivity, the multiple source and detector locations may even overlap. If data from multiple colors are simultaneously gathered at every detector location, spectroscopic images (of both oxy- and deoxyhemoglobin) can be generated.

Obviously, imaging systems with multichannel NIRS may offer several advantages. In case of multichannel imaging, it is not necessary to know a priori the location of brain activation. The grid of optodes may roughly be placed over a brain region. After the measurement the relation of the optodes to the cortical areas may be examined by structural MRI. Thus, activations as revealed by functional NIRS (fNIRS) may be projected onto the cortex. Contrary, single channel approaches require a priori knowledge of location of brain activation by previous fMRI studies or results from the literature. This limitation is particularly evident for studies examining brain plasticity. If brain areas are injured, it is almost impossible to predict the cortical network, which takes over the task of the injured region. The same is the case for studies in developmental cognitive neuroscience. To avoid this limitation of ‚self-fulfilling prophecies‘ in one (or two) channel approaches, imaging approaches should generally be preferred.

Recently, three-dimensional optical tomography had been developed for the human brain (Bluestone et al., 2001; Hielscher et al., 2002). Although technically a breakthrough, its practical importance for human brain imaging is currently low due to limited depth penetration of near-infrared light.

1.2.6. Placement of Optodes

As with EEG, MEG and PET, optical methods cannot provide anatomical images or other direct measures of anatomy. To afford between-subject comparisons for functional brain changes, therefore, an extrinsic frame of reference is required. EEG researchers have developed an external referential system, namely the international 10/20 system that provides 21 standardized electrode placement positions (Harner & Sannit, 1974), and has been expanded even to dense sensor grids of 256 detectors (Suarez et al., 2000). While such a system is technically only self-consistent, efforts have been made to determine the location of various major anatomical landmarks relative to the standard 10/20 system locations (Homan et al., 1987; Okamoto et al., 2004a; Steinmetz et al., 1989). The most

comprehensive study by Okamoto et al. (2004a) examined cranio-cerebral correlation via the 10/20 system using MRI. They projected the 10/20 standard cranial positions over the cerebral cortical surface. After examining the cranio-cerebral correspondence for 17 healthy adults, they normalized the individual 10/20 cortical projection points to the standard Montreal Neurological Institute (MNI) and Talairach stereotactic coordinates. They found that the locations of the 10/20 cortical projection points in the standard MNI or Talairach space could be estimated with an average standard deviation of 8 mm (Figure 9). Further, they examined the distance between the cortical surface and the head surface along the scalp and created a cortical surface depth map (Figure 10).

Depth penetration of near-infrared light depends strongly on source-detector distance. As an approximate rule of thumb the depth of maximum brain sensitivity is approximately half the source-detector separation distance. Thus, for a source-detector separation of 3 cm, the region of maximum brain sensitivity will be found between the source and detector fiber tip locations, and roughly 1.5 cm below the surface of the scalp, though banana-shaped region of sensitivity extends both above and below this depth (Figure 8; Strangman et al., 2002a).

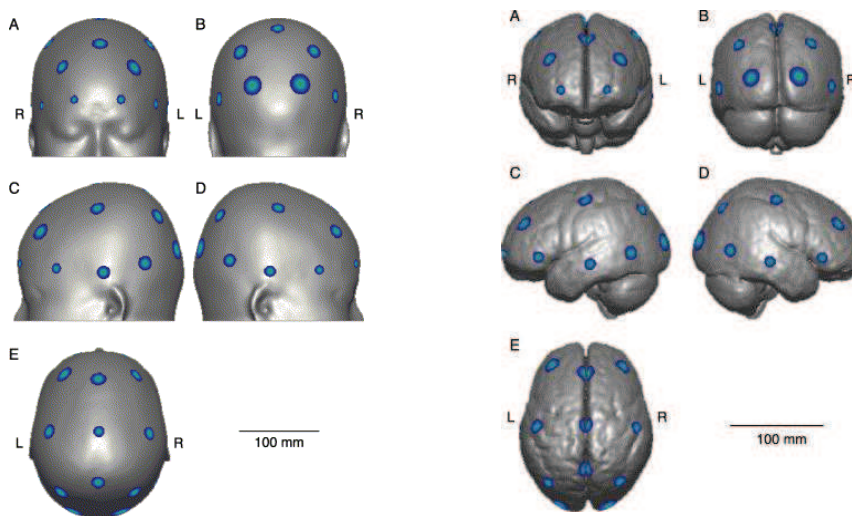


Figure 9 Locations of the 10/20 standard positions on the surface of the head (left) and the brain (right). All positions are overlaid on the averaged image of 17 subjects normalized to the MNI152 standard template. The centers of color gradients represent the locations of the most likely MNI coordinates for the 10/20 standard positions. The edges of color gradients represent the respective standard deviation (Okamoto et al., 2004a).

If one increases source-detector separations, sensitivity to cortical areas is increased whereas influences of changes in extracranial tissues is reduced (Germon et al., 1999). Hence, signal-to-noise ratios might be improved. If one takes into account a skin-cortex distance of at least 11 mm (see Figure 10), one may conclude that the source-detector distance has to be at least 3 cm. Currently available optical instruments operate with approximately such a source-detector distance (ETG-100 by Hitachi 3 cm, NIRO-300 by Hamamatsu 4 to 5 cm). One may conclude that positioning optodes according to the 10/20 system is sufficient for optical imaging, because spatial resolution of current optical instruments is maximally 2-3 cm.

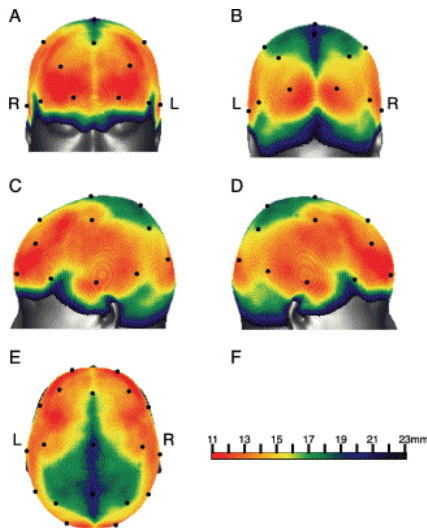


Figure 10 Cortical surface depth map as averaged head surface image of 17 subjects normalized to the MNI152 standard template. The locations of the 10/20 standard positions are indicated as dots. Color gradient bar indicates cortical depth (Okamoto et al., 2004a).

As shown in Figure 10, skin-cortex distance varies in several brain regions. Superficial cortices, including lateral frontal, temporal, occipital, and inferior parietal cortex, are easily accessible. For superior parietal cortex, longer source-detector separations have to be recommended. However, localizing activation to deeper brain structures, such as fronto- and parietomedian regions, and basal ganglia, is not feasible, and has to be done by other imaging methods, such as fMRI or PET.

1.3. Neurovascular Coupling

After describing the principles of optical imaging, the following chapter explores how brain activation changes blood oxygenation. Generally, brain activity induces a local arteriolar vasodilatation and consequently an increase in regional cerebral blood volume (rCBV) and blood flow (rCBF), termed neurovascular coupling (Anderson & Nedergaard, 2003; Roy &

Sherrington, 1890; Villringer & Dirnagl, 1995). This tight spatial and temporal coupling of neuronal activity with blood-borne energy substrate delivery is a well-established hallmark of brain function and forms the basis for indirect neuroimaging methods (Figure 1). Temporally, increased blood flow occurs a few seconds after neuronal stimulation, resulting in rapid satisfaction of energy demand. Spatially, increased blood flow is limited to intraparenchymal radii of ~250 μm from the site of enhanced neuronal activity, and corresponds nearly identically to areas of increased metabolism. In addition, functional hyperemia appears to involve coordinated changes in blood flow upstream, at the level of pial resistance arterioles, aimed at improving parenchymal blood flow in the stimulated area. Mechanisms that induce functional hyperemia include neuronal release of vasoactive metabolic factors such as H^+ , K^+ , lactate, and adenosine, direct innervation by nerves of the peripheral and central nervous system, and glutamate-induced activation of neuronal nitric oxide synthase. Recently, it was shown that astrocytes, which constitute the blood-brain barrier together with endothelial cells (Nedergaard et al., 2003; Schroeter et al., 1998, 1999, 2001) are also involved in blood flow regulation (Anderson & Nedergaard, 2003).

At the capillary level, the increase in rCBF is achieved mainly by higher blood flow per capillary, associated with higher blood flow velocity rather than with opening and closing of previously unperfused capillaries. The increase in rCBF and oxygen delivery exceeds the increase in local oxygen consumption (Fox et al., 1988). Therefore, cerebral blood oxygenation rises locally (Villringer & Dirnagl, 1995).

1.3.1. Changes in Hemoglobin Oxygenation due to Activation

Theoretically, as illustrated in Figure 11, concentrations of oxy- and deoxyhemoglobin can be influenced by rCBF, rCBV, and/or oxygen consumption. Assuming a one-compartment model, an isolated increase in rCBF will lead to an increase in oxyhemoglobin, and a (symmetrical) decrease in deoxyhemoglobin, because more oxygenated than deoxygenated blood will fill the compartment. This effect is often described as the 'washout effect'. An isolated elevation of cerebral metabolic rate of oxygen will lead to exactly opposite changes compared to the first pattern. Namely, decreasing oxyhemoglobin is mirrored by symmetrical elevations of deoxyhemoglobin because oxygen is consumed without being replaced. If rCBV (and accordingly total hemoglobin) increases, one may expect asymmetrical elevations of oxyhemoglobin and deoxyhemoglobin. More specifically, the concentration of oxyhemoglobin rises more than that of deoxyhemoglobin, because hemoglobin is generally mainly oxygenated.

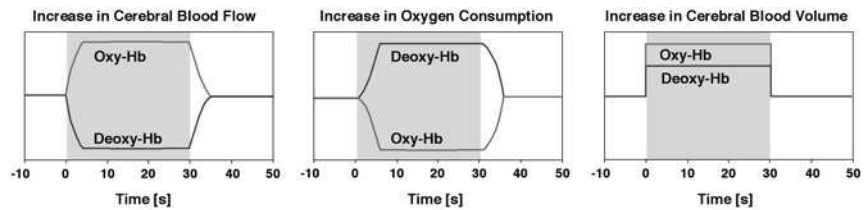


Figure 11 Changes in the concentration of oxy- and deoxyhemoglobin due to increases in cerebral blood flow, cerebral metabolic rate of oxygen, and cerebral blood volume. The shaded area indicates the period when the respective parameter is increased (according to Wolf et al., 2002b).

Studies on exposed brain tissue (Malonek & Grinvald, 1996) suggest that increased brain activity is associated with an early decrease in hemoglobin oxygenation. This phenomenon, producing the so called 'initial dip' of the BOLD signal, occurs within the first 3 seconds and is highly localized. It was suggested that it is related to a rapid increase in oxygen consumption without changes in rCBF or rCBV. However, it was shown for optical measurements directly on the brain surface only (Mayhew et al., 1999, 2000), and is highly controversial (Lindauer et al., 2001).

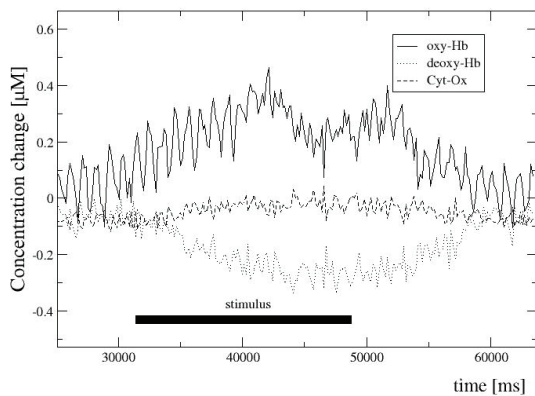


Figure 12 Changes in the concentration of oxy-, deoxy-hemoglobin and the redox-state of the cytochrome-c-oxidase in the visual cortex during stimulation with a checkerboard. Average of 8 stimulation cycles in one subject.

The early decrease in hemoglobin oxygenation is followed by a subsequent longlasting increase in hemoglobin oxygenation (Figure 12; Malonek & Grinvald, 1996). The delayed phase of the vascular response starts approximately 2-3 s after stimulation onset, peaks after ~6 s, and is less localized. Similar to the increasing BOLD contrast in fMRI (Frahm et al., 1992; Kwong et al., 1992; Ogawa et al., 1992) these signals reflect the fact that the blood flow response to functional activation is larger than the increase in total hemoglobin, and in

oxygen consumption (Fox et al., 1988). Therefore, brain activation leads to a localized increase in oxyhemoglobin and a decrease in deoxyhemoglobin (Figure 12). Consistent with this notion, in simultaneous PET-fNIRS studies, during stimulation tasks positive correlations between changes in oxyhemoglobin and rCBF, and between changes in total hemoglobin and rCBF along with a negative correlation between changes in deoxyhemoglobin and rCBF were observed (Hock et al., 1997; Villringer et al., 1997). Furthermore, in a study employing simultaneous fNIRS and BOLD fMRI (which is inversely related to deoxyhemoglobin), a good spatial agreement between the BOLD measurement and the drop in deoxyhemoglobin by fNIRS was noted (Kleinschmidt et al., 1996).

1.3.2. Changes in the Redox-State of the Cytochrome-c-Oxidase due to Activation

Measurements of the redox-state of the cytochrome-c-oxidase would be a very interesting marker of intracellular energy metabolism. However, measurements are the most difficult to interpret (see above). Measurements on exposed brain tissue using visible light have indicated a transient oxidation of cytochrome-c-oxidase during electrical stimulation (LaManna et al., 1987; Lockwood et al., 1984). Using non-invasive NIRS systems similar findings of transient oxidation were obtained in humans, indicating increased oxidation of the (presumably already highly oxidized) cytochrome-c-oxidase with increasing brain activity (Figure 12; Heekeren et al., 1999; Uludag et al., 2004).

2. Experiments

2.1. Main Issues of Current Research

We argued in the Introduction section that optical imaging could be developed to a valuable tool for functional studies of the human brain. Several studies showed that functional optical imaging can measure activations in primary cortices (Obrig & Villringer, 2003; Villringer & Chance, 1997). Only a few studies applied optical imaging to cognitive neuroscience.

To further establish optical approaches in cognitive neuroscience we conducted nine experiments at the Max-Planck-Institute for Human Cognitive and Brain Sciences in Leipzig from 2000 to 2005. The experiments covered issues of physiology, methodology, development, aging, patient studies, and analysis approaches.

More precisely, the following questions had to be answered:

- What is the origin of the optical signal? How do the optical parameters change during stimulation? Is multimodal imaging possible?

Before applying optical imaging to cognitive neuroscience, we wanted to explore the origin of the optical signal. fMRI is currently considered as the 'golden standard' for cognitive experiments. Measuring the hemodynamic response with fMRI together with fNIRS may overcome limitations of single-method approaches. Hence, such multimodal imaging experiments may yield a framework to understand neurovascular coupling and the origin of the optical signal. Particularly, depth penetration of fNIRS may be investigated. Accordingly, we measured the hemodynamic response with both, fMRI and fNIRS simultaneously during visual stimulation.

The following series of experiments aimed at establishing optical imaging as a tool for cognitive neuroscience. Generally, the well-known Stroop interference task was chosen for stimulation as it activates reliably lateral prefrontal regions (Zysset et al., 2001).

- Can optical imaging be used in cognitive studies with event-related designs?

Event-related approaches, which allow the analysis of events of the stimulation protocol whose duration is much shorter than the latency of the vascular response, are generally advantageous in studies with cognitive paradigms (Leung et al., 2000; Pollmann et al., 1998). Hence, the study examined the feasibility of fNIRS for the event-related approach in studies with cognitive paradigms.

- Can intertrial intervals be reduced to increase statistical power?

In most former optical studies trials were separated by an intertrial interval of at least 12 s, to minimize an overlap of the vascular response. Reducing the length of the intertrial interval can increase statistical power, and enables a better control over subject's mental activity (Pollmann et al., 1998, 2000). Further, many short-lived between-trials effects can not be investigated with long intertrial intervals. Therefore, the study investigated whether the length of the intertrial interval may be reduced to 2 s in cognitive studies as it has been shown for simple motor and visual tasks (Jasdzewski et al., 2003).

- Are measurements in children possible?

The next experiment aimed at applying optical imaging to developmental studies in cognitive neuroscience, because the method is robust to artifacts, and, therefore, well suited for children studies.

- Are measurements in elderly people and patients possible?

The next four experiments applied optical imaging to elderly subjects and patients, because of its robustness to artifacts, and easy replicability. Patients with cerebral microangiopathy were chosen, because executive functions, as measured by the Stroop task, are particularly impaired in this disease (McPherson & Cummings, 1996). Furthermore, pathological alterations affect the microvasculature of the brain, which might be easily examined by fNIRS (Roman et al., 2002).

After showing that optical imaging is well suited for cognitive neuroscience, still one methodological question had to be answered.

- Which statistical approaches may yield standard analyses?

Until now no standardized approach for fNIRS data analysis has been established, although this has to be regarded as a precondition for future application. Hence, we applied the well-established general linear model, and spatially resolved spectral analysis to optical imaging data. These approaches offer the advantage being independent of the highly variable differential pathlength factor.

The following chapters summarize the results of the experiments, which were designed to answer these questions. Detailed information on methods, statistical analysis and results can be found in the respective articles.

2.2. Neurovascular Coupling & Origin of the Optical Signal

Several recent studies compared the hemodynamic response to brain activation as measured by fNIRS with another imaging method, such as fMRI (Kennan et al., 2002b; Kleinschmidt et al., 1996; Mehagnoul-Schipper et al., 2002; Obrig et al., 2000b; Seiyama et al., 2004; Siegel et al., 2003; Strangman et al., 2002b; Toronov et al., 2001a, 2001b, 2003; Wenzel et al., 2000) or PET (Hock et al., 1997; Villringer et al., 1997). While optical measurements are poorer in spatial resolution and depth penetration than fMRI, they are, as discussed above, biochemical specific. Consequently, they provide information about changes in oxy-, deoxy- and total hemoglobin with a high temporal resolution (Hoshi, 2003; Villringer & Chance, 1997). Moreover, fNIRS is particularly sensitive to the microvasculature (Boushel et al., 2001; Liu et al., 1995a,b), whereas the BOLD signal represents all spatial scales of venous vessels (Lee et al., 2001; Strangman et al., 2002b; Weisskoff, 1999). These advantages of fNIRS can be used to better understand the nature of the hemodynamic response to neuronal activation, and the origin of the BOLD signal. On the other hand, optical studies are limited because anatomical information is not obtained. Simultaneously acquired optical and fMRI data may synergize and overcome this limitation as the MRI data provide information about the location of the optical probes.

The study aimed at comparing the temporal behavior of the hemodynamic response between fMRI and fNIRS in the visual cortex of young healthy humans. We hypothesized a strong correlation between the BOLD signal and deoxyhemoglobin, because the BOLD signal arises mainly from magnetic disturbances caused by the paramagnetic deoxyhemoglobin (Buxton et al., 1998; Ogawa et al., 1993). Almost all previous studies that combined fNIRS with another imaging method used block designs and did not investigate the post-stimulus period of the hemodynamic response. An event-related approach was employed as it is advantageous compared with block designs (Burock et al., 1998; Schroeter et al., 2002b, 2003, 2004c, 2004d). A long intertrial interval of 60 s was chosen to include the prolonged post-stimulus undershoot of the BOLD signal (Mildner et al., 2001). Further, we examined depth penetration of near-infrared light as it has been investigated in previous fNIRS/PET studies in elderly or diseased subjects only (Hock et al., 1997; Villringer et al., 1997).

For task-induced activation, a simple visual task was employed (array of red L-shapes randomly rotating as a strong full-field visual stimulus). The duration of the visual stimulus was 6 s, and the recovery period after each stimulus was 54 s. 10 complete cycles of visual stimulation were recorded. Further, fMRI and fNIRS data were obtained during a resting condition of 10 min (closed eyes).

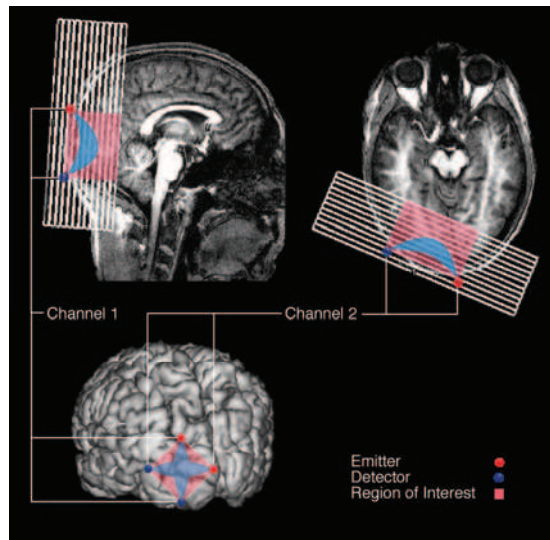


Figure 13 Sampling volume (blue) between the two emitter-detector pairs of fNIRS in relation to the slices of fMRI (white). The two emitter-detector pairs were placed in a cross shape, and centered at position O1 of the international 10/20 system. The fMRI slices were oriented parallel to the plane spanned between the four optodes. The BOLD signal was analyzed for each slice in the respective region of interest. Highest correlation between oxy-/deoxyhemoglobin and the BOLD signal is expected for the slice in the center of the banana-shaped fNIRS sampling volume. Note that illustration is schematically only.

Changes in the concentration of oxy-, deoxyhemoglobin and the redox state of the cytochrome-c-oxidase were measured by a NIRO-300 spectrometer (Hamamatsu Photonics K.K., Japan) and expressed in nM. Values were calculated according to Cope & Delpy (1988). Moreover, we calculated changes in the concentration of total hemoglobin (sum of oxy- and deoxyhemoglobin) as a measure for changes in rCBV. The emitter-detector spacing was 4 cm, and a differential pathlength factor of 6.26 was used (Duncan et al., 1995). Two emitter-detector pairs were placed in a cross shape, one oriented vertically, the other horizontally, and centered at the position O1 of the international 10/20 system localized over the left visual cortex (Figure 13, 14; Homan et al., 1987; Okamoto et al., 2004a).

fMRI experiments were performed using a 3.0 T whole-body scanner (Medspec Scanner, Bruker, Germany). Anatomical images were obtained with a T1-weighted modified driven equilibrium Fourier transform (MDEFT) sequence (Lee et al., 1995; Norris, 2000; Thevenaz et al., 2000; Ugurbil et al., 1993). For functional imaging, an echo planar imaging (EPI) sequence was used. Optodes were visualized by vitamin E capsules on individual MRIs (Figure 14). 12 oblique slices were oriented parallel to the plane spanned between the two emitter detector pairs (Figure 13).

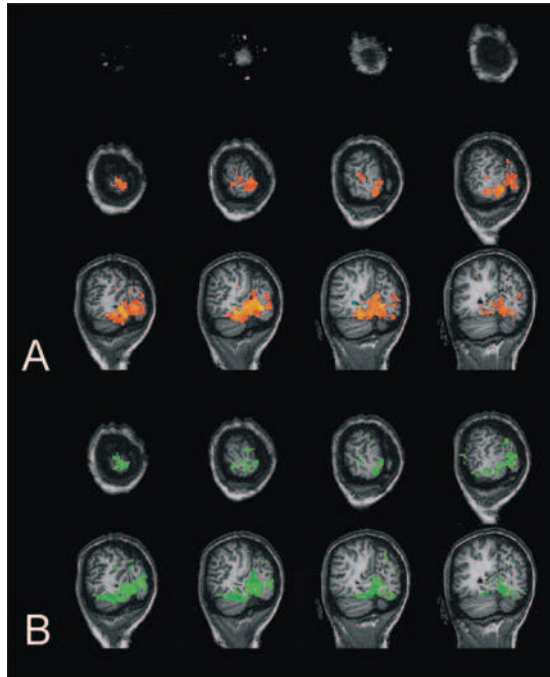


Figure 14 Averaged correlation maps for one subject. BOLD contrast. **A** If a boxcar function was used as a design function (delay of 6 s; $0.85 \leq r \leq 0.95$). **B** If the time course of deoxyhemoglobin as measured by fNIRS was used as a design function ($0.8 \leq r \leq 0.83$). Optode positions are marked by vitamin E capsules (see first row in A).

As illustrated in Figure 15, the BOLD signal, oxy-, total hemoglobin, and cytochrome-c-oxidase increased, whereas deoxyhemoglobin decreased during stimulation in accordance with recent studies (Buxton et al., 1998; Heekeren et al., 1999; Obrig et al., 2000b; Schroeter et al., 2004a; Seiyama et al., 2004; Wobst et al., 2001), indicating an increase in rCBF and rCBV due to neurovascular coupling (Villringer & Dirnagl, 1995). The post-stimulus undershoot of the BOLD signal was accompanied by a decrease of oxyhemoglobin, and an increase of deoxyhemoglobin. Interestingly, a few previous fNIRS studies reported similar changes of oxy- and deoxyhemoglobin during the post-stimulus period. These studies investigated whisker deflection in the rat (Lindauer et al., 2001, 2003), or visual and motor stimulation in humans (Jaszewski et al., 2003; Schroeter et al., 2004a).

Generally, three mechanisms may contribute to the post-stimulus undershoot of the BOLD signal (Aubert & Costalat, 2002; Buxton et al., 1999). First, rCBV may return later to baseline than rCBF due to delayed venous compliance as proposed by the Balloon and Windkessel models. Second, the undershoot may reflect the persistence of a high oxygen consumption after rCBF has returned to baseline. Third, an undershoot of the rCBF could contribute to the BOLD signal undershoot.

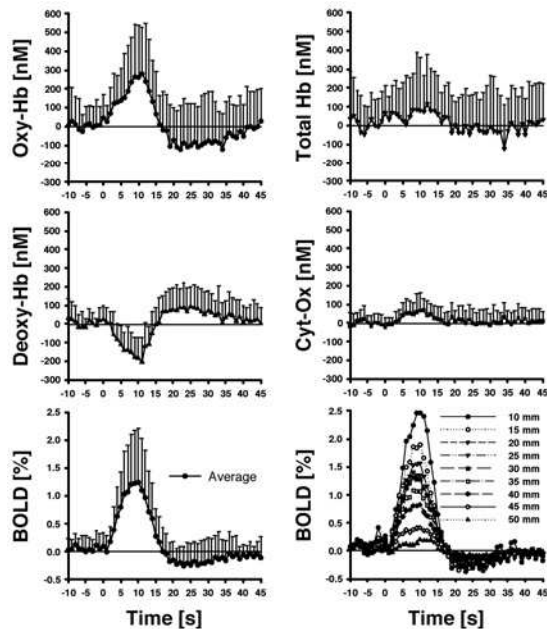


Figure 15 Concentration changes of oxy-, deoxy-, total hemoglobin (Hb), and cytochrome-c-oxidase (Cyt-Ox) as measured by fNIRS, and the BOLD signal as measured by fMRI (time courses for the square area between the four optodes, averaged over all measured slices and for every slice separately). Visual stimulation started at 0 s and continued till 6 s. Mean \pm SD.

In accordance with the Balloon (Buxton et al., 1998) and Windkessel models (Mandeville et al., 1998, 1999), the post-stimulus undershoot of the BOLD signal was accompanied by reverse changes of deoxyhemoglobin, namely a post-stimulus overshoot of that chromophore in our study. However, there are three inconsistencies with the assumption of a delayed venous compliance. Firstly, in our experiments total hemoglobin did not show significant post-stimulus changes, although it may be regarded as an equivalent of (corpuscular) rCBV. Second, concentration of oxyhemoglobin fell below baseline levels during the post-stimulus period, whereas one could expect from the Balloon and Windkessel models values above baseline. Finally, the ratio between post-stimulus and stimulus changes was much higher for oxy- and deoxyhemoglobin compared with the averaged BOLD signal, which indicate relatively higher post-stimulus effects for the optical parameters.

It is known from literature, that different vascular compartments contribute to optical parameters and the BOLD signal. Optical methods such as fNIRS are sensitive to the microvasculature, namely to arterioles, capillaries and venules (Boushel et al., 2001; Cannestra et al., 2001; Schroeter et al., 2004b), because for larger vessels such as arteries and veins entering light cannot escape (Liu et al., 1995a,b). The BOLD signal represents, on the other hand, all spatial scales of venous vessels (Lee et al., 2001; Strangman et al.,

2002b; Weisskoff, 1999). Interestingly, the Balloon model neglects the capillary compartment by assuming that the BOLD signal stems from postcapillary venous vessels (Buxton et al., 1998). Recently, Lu et al. (2003, 2004) showed by vascular space occupancy dependent fMRI that, in the human brain, rCBV returned immediately after visual stimulation to baseline values, if the signal's origin was limited to the microvasculature. Jaszewski et al. (2003) reported similar results for total hemoglobin after visual and motor stimulation in humans. Moreover, total hemoglobin as measured by fNIRS represents changes in corpuscular rCBV, because hemoglobin is mainly localized in erythrocytes. Hematocrit, and red blood cell concentration are directly correlated with flow velocity (Barfod et al., 1997; Mchedlishvili, 1986; Mchedlishvili & Varazashvili, 1987). Hence, total hemoglobin follows directly rCBF and falls immediately after stimulation to baseline levels. These results fit very well with our data.

During the post-stimulus period, we observed a significant undershoot of oxyhemoglobin (beside the overshoot of deoxyhemoglobin) that cannot be explained by delayed decreases in rCBV. Hence, the post-stimulus changes of oxy-, and deoxyhemoglobin may reflect the persistence of a high-level oxygen consumption after rCBF has returned to baseline (Aubert & Costalat, 2002; Buxton et al., 1999; Frahm et al., 1996). A high oxygen consumption diminishes the BOLD signal, concentrations of oxyhemoglobin, and elevates deoxyhemoglobin without influencing total hemoglobin. Therefore, it can explain the post-stimulus events. This argument is strongly supported by a recent multimodal fMRI study (Lu et al., 2003, 2004). Investigating visual stimulation in humans the authors reported that the long post-stimulus undershoot of the BOLD signal of approximately 30 s, such as in our study, was accompanied by a prolonged elevation of oxygen utilization with the same time course. Microvascular rCBV, in contrast, returned immediately after stimulation to baseline values (see above).

Lastly, it needs an explanation why the post-stimulus effects (as measured by the ratio between post-stimulus and stimulus changes) were relatively stronger for the optical parameters in comparison with the BOLD signal in our study. Obviously, oxygen is consumed mainly in capillaries. If optical methods are particularly sensitive to the microvasculature (Boushel et al., 2001; Cannestra et al., 2001; Liu et al., 1995a,b; Schroeter et al., 2004b) whereas the BOLD signal represents all spatial scales of venous vessels (Lee et al., 2001; Strangman et al., 2002b), a prolonged post-stimulus elevation of oxygen utilization would be more visible in the optical parameters. A recent study found a negligible signal attenuation of the BOLD signal by diffusion weighting at 3.0 Tesla during the post-stimulus undershoot supporting the assumption of an extravascular origin of the BOLD signal (Mildner et al., 2001). Results suggest that the post-stimulus undershoot of the BOLD signal

is related to an elevated vessel volume as suggested by the Balloon and Windkessel models, and exclude an increase in the concentration of deoxyhemoglobin in post-capillary venous vessels. Jones (1999) measured changes in the relaxation times R_2 and R_2^* at 1.5 Tesla during the post-stimulus period of the BOLD signal. He concluded that intravascular signals, if present in this period, stem from small vessels (not affected by diffusion weighting). Although this fits well with our assumptions, the elevation in the concentration of deoxyhemoglobin by an increased oxygen consumption in capillaries without affecting the concentration of deoxyhemoglobin in post-capillary veins remains difficult to explain.

The post-stimulus changes of oxy- and deoxyhemoglobin may also be explained by a reduced post-stimulus rCBF (Aubert & Costalat, 2002; Buxton et al., 1999), which is possibly preceded by an inhibition of neural activity after stimulation (Logothetis et al., 2001; Wenzel et al., 2000). However, the post-stimulus undershoot of rCBF occurs only in a minority of subjects, is highly variable (Irikura et al., 1994; Ma et al., 1996), task dependent (Hoge et al., 1999a), and can even be explained as an artifact of delayed rCBV changes (Mandeville et al., 1999). Further, the ratio between post-stimulus and stimulus changes of rCBF, as calculated from these studies, reaches only small values (Hoge et al. 1999a; Irikura et al., 1994; Ma et al., 1996). Hence, it cannot explain the fNIRS data of our study. One can conclude that the above mechanisms cannot be the main source for the post-stimulus changes.

During visual stimulation, we found the strongest correlation between the BOLD signal and deoxyhemoglobin, which was highest in a depth of 15 mm beneath the skin (Figure 16). Oxyhemoglobin, total hemoglobin, and cytochrome-c-oxidase were correlated with the BOLD signal as well, although with smaller correlation coefficients. Our data agree well with Buxton et al. (1998) and Ogawa et al. (1993), which assume that the BOLD signal arises mainly from magnetic disturbances caused by the paramagnetic deoxyhemoglobin. Our data are also consistent with simultaneous fMRI and fNIRS experiments showing a high correlation between the BOLD signal and deoxyhemoglobin (Kida et al., 1996; Mehagnoul-Schipper et al., 2002; Punwani et al., 1997, 1998; Toronov et al., 2003), and with Pouratian et al. (2002) who showed a high temporal and spatial correlation between the BOLD signal and optical intrinsic signals measured at 610 nm (particularly sensitive to deoxyhemoglobin) in humans. Differences to Strangman et al. (2002b), who found a lower correlation of the BOLD signal with deoxy- compared with oxyhemoglobin during finger flexion/extension motor activation, may be explained by their less (three) subjects, different (block) design, their shorter emitter-detector separation (Germon et al., 1999), and non-linear changes of oxyhemoglobin in relation to deoxyhemoglobin in the motor cortex (Wolf et al., 2002b). Because of the known

linear relationship between changes of oxy-, and deoxyhemoglobin in the visual cortex (Figures 15 and 16; Wolf et al., 2002b), we decided to apply a visual paradigm in contrast to their study.

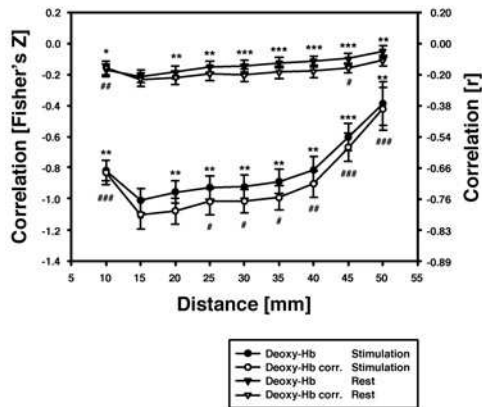


Figure 16 Depth penetration of fNIRS. Time courses of deoxy-hemoglobin (Deoxy-Hb) as measured by fNIRS were correlated with the BOLD signal as measured by fMRI for every layer separately. Correlation is shown for visual stimulation and rest (closed eyes). Pearson correlation coefficients and partial correlation coefficients (adjusted for changes in total hemoglobin; corr.) were normalized with a Fisher's Z transformation. Distance to optode layer. Mean \pm SEM. *** ### $p < 0.001$, ** ## $p < 0.01$, * # $p < 0.05$ 2-tailed paired Student's t-test vs. values at 15 mm.

Crucially, we investigated for the first time simultaneously the BOLD signal and changes of fNIRS chromophores during rest, and found that deoxyhemoglobin was again tightly related to the BOLD signal. This analysis covered un-averaged data and was independent of functional stimulation that may bias results. Correlation during rest may be based on spontaneous vascular oscillations related to vasomotion, such as low and very low frequency oscillations, and on oscillations related to respiration (Colantuoni et al., 1994; Obrig et al., 2000a; Schroeter et al., 2004b). With an effective sampling rate of 1 Hz, oscillations due to heart pulsations did not influence our measurements.

We found the highest correlation between deoxyhemoglobin and the BOLD signal during visual stimulation and rest, when a depth penetration of 1.5 cm from skin surface was assumed. These results are in good accordance with two simultaneous fNIRS/H₂¹⁵O-PET studies measuring the hemodynamic response in the parietal cortex of patients with Alzheimer's disease during a Stroop task (Hock et al., 1997), and in the forehead of healthy elderly subjects during calculation and a Stroop task (Villringer et al., 1997). In both studies, rCBF in a hemisphere shaped volume beneath the optodes was correlated strongest with total hemoglobin, with lower values for oxy-, and deoxyhemoglobin. Applying an emitter-detector spacing of 4 cm the authors concluded that fNIRS covers the outer 1 to 3 cm of the

brain cortex (Hock et al., 1997), with a maximal correlation in the outer 0.9 cm (Villringer et al., 1997). Our study differs in several aspects from the mentioned studies. We used an advantageous event-related design in comparison with the block design in their studies, and examined primary cortical areas in young healthy subjects. It is well known that the hemodynamic response declines in associative cortices with aging as examined in both PET studies whereas primary cortices are unaltered (Schroeter et al., 2003, 2004b). Hence, aging effects may have biased the results of both PET studies. We found the highest correlation between deoxyhemoglobin and the BOLD signal, whereas both PET studies reported maximal correlation between total hemoglobin and rCBF, presumably caused by the fact that total hemoglobin as a measure of corpuscular rCBV is crucially confounded by rCBF (Barford et al., 1997; Mchedlishvili, 1986; Mchedlishvili & Varazashvili, 1987). Both PET studies assumed a semisphere shaped volume to calculate changes in rCBF. We defined the square between the two emitter-detector pairs as the region of interest in every slice to avoid any assumption on depth penetration and sampling volume of near-infrared light, and to allow a specific correlation analysis for each slice separately.

The study investigated for the first time the post-stimulus undershoot in a simultaneous fMRI/fNIRS study in humans during visual stimulation. This multimodal approach investigates simultaneously events in the microvascular (fNIRS) and the postcapillary venous compartment (BOLD fMRI). Results suggest that post-stimulus events are dominated by a prolonged high-level oxygen consumption in the microvasculature. Compared with the BOLD signal, relatively higher post-stimulus effects were found for fNIRS data. This and the contribution of a delayed return of rCBV in post-capillary veins to the BOLD post-stimulus undershoot as suggested by the Balloon and Windkessel models remain to be explored. Concerning depth penetration of near-infrared light our results confirm the assumption that the depth of maximum brain sensitivity is approximately half the source-detector separation distance (Strangman et al., 2002a).

2.3. Establishing Optical Imaging as a Tool for Cognitive Neuroscience

In the next experiments we wanted to explore whether optical imaging might be applied to the cognitive neurosciences, particularly for studies on executive functions supported by the frontal lobe. We applied a Stroop interference task, which is known to involve executive functions and showed reliable brain activation in recent fMRI studies (Zysset et al., 2001). After description of the task, we summarize the main findings of our experiments on methodological issues (event-related designs, optimizing the length of the intertrial interval), as well as studies on development, aging, and patients.

2.4. The Stroop Interference Task

The Stroop color-word task, introduced by Stroop 1935, has been a classic measure of frontal lobe function (MacLeod, 1991). In the task, a color word such as GREEN appears in an ink color such as red. If the subject's task is to read the word and ignore the color (i.e., say 'green'), there is no difficulty relative to reading the word in standard black ink. However, if the subject's task is to name the ink color and ignore the word (i.e., say 'red'), there is considerable difficulty relative to naming a color patch. Reading the word interferes with naming the color. This phenomenon is called Stroop interference, requiring the inhibition of competing responses. Hence, it was suggested that executive processes, namely interference resolution and response inhibition, may be examined with this task (Adleman et al., 2002).

COLOR-WORD STROOP		
neutral	congruent	incongruent
XXXX BLUE	RED BLUE	GREEN BLUE
XXXX BLUE	BLUE BLUE	GREEN BLUE

Figure 17 Examples of single trials for the neutral, congruent and incongruent condition of the color-word matching Stroop task. 'Does the color of the upper word correspond with the meaning of the lower word?' For the upper three examples, the correct answer would be 'NO'; for the lower three examples, the correct answer would be 'YES' (according to Zysset et al., 2001).

2.4.1. The Color-Word Matching Stroop Interference Task

In our experiments we decided to use the color-word matching Stroop task (Stroop, 1935; Treisman & Fearnley, 1969; modified according to Zysset et al., 2001) in an event-related version. This version of the Stroop task was chosen because of two reasons. Firstly, response preparation and interference processes may not confound each other in this version, because they are separated into two modalities (button press vs. verbal). Second, this version mainly activates the lateral prefrontal cortex (LPFC) (Schroeter et al., 2002b, 2003, 2004c,d; Zysset et al., 2001) as frontomedian regions cannot be captured by fNIRS due to limited depth penetration (Villringer & Chance, 1997).

During an experimental run, two rows of letters appeared on the screen and subjects were instructed to decide, whether the color of the top row letters corresponded to the color name written on the bottom row (Figure 17). Response was given by a button press with the index (YES-response) and middle (NO-response) fingers of the right hand. During neutral trials, the letters in the top row were 'XXXX' printed in red, green, blue or yellow, and the bottom row consisted of the color words 'RED', 'GREEN', 'BLUE' and 'YELLOW' printed in black. For congruent trials, the top row consisted of the color words 'RED', 'GREEN', 'BLUE' and 'YELLOW' printed in the congruent color. For the incongruent condition, the color word was printed in a different color to produce interference between color word and color name (see above). To shift visual attention to the top word, it was presented 100 ms before the lower word (MacLeod, 1991). Generally, in half of the trials in all conditions the color in the top row corresponded to the color name of the bottom row. Words remained on the screen until the response was given. The screen was blank between the trials.

Contrasting incongruent with neutral trials yields a measure for Stroop interference (MacLeod, 1991). Although the contrast between incongruent and congruent trials also contains interference processes, facilitation effects as measured with the congruent/neutral contrast may bias them. Hence, we compared mainly incongruent with neutral trials, where interference is not confounded by facilitation processes.

2.5. Event-Related Designs for Cognitive fNIRS Studies

2.5.1. Stroop Interference activates the Lateral Prefrontal Cortex

Event-related approaches, which allow the analysis of events whose duration is much shorter than the latency of the vascular response, are advantageous in studies with cognitive paradigms (Leung et al., 2000; Pollmann et al., 1998). First, they enable randomized presentation of experimental conditions in contrast to blocked designs. Second, only event-related designs allow the analysis of the time course of activation over a single trial. However, until 2002 cognitive fNIRS studies had employed solely blocked designs with presentation of the stimulus for 1 to 10 min (Obrig & Villringer, 1997). Only one fNIRS study had examined premotor potentials in a single trial design (Go/NoGo task) and showed a difference between the Go and NoGo condition with respect to the post-stimulus undershoot of oxyhemoglobin (Obrig et al., 2000b). Thus, the authors demonstrated the feasibility of the single trial approach for fNIRS in a motor paradigm study. The aim of our study was to examine the feasibility of fNIRS for event-related cognitive studies (Schroeter et al., 2002b). Therefore, changes in the concentration of oxy-, deoxy- and total hemoglobin as well as changes in the redox state of the cytochrome-c-oxidase were measured by fNIRS (NIRO-300 spectrometer; Hamamatsu Photonics K.K.) in young adults during performance of a Stroop paradigm as described above in an event-related version.

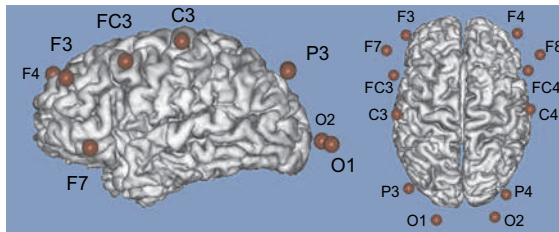


Figure 18 Optode positions according to the international 10/20 system, in relation to the corresponding cortical areas. Magnetic resonance image of one test subject. Results by Homan et al. (1987) are summarized in the table.

Optode position	Brodman location	Cortical location
F3/4	46	Middle frontal gyrus, near superior frontal sulcus; rostro-caudal location.
F7/8	45/46	Inferior frontal gyrus rostral portion of pars triangularis.
FC3/4	6/8/9	Posterior part of the middle frontal gyrus.
C3/4	4	Precentral gyrus, shoulder to wrist area, caudal to middle frontal gyrus.
P3/4	7	Superior parietal lobule near intraparietal sulcus, superior to posterior portion of supramarginal gyrus.
O1/2	17	Occipital lobe, lateral and superior to occipital pole, overlapping calcarine fissure.

Optodes were placed symmetrically at positions F7/8, F3/4, FC3/4, C3/4, P3/4, and O1/2 of the international 10/20 system (Figure 18; Homan et al., 1987; Steinmetz et al., 1989). For better visualization of optode positions, optodes were replaced by vitamin E containing capsules in one test subject. Optode positions included the LPFC (F7/8, F3/4, FC3/4), intraparietal sulcus (P3/4), primary visual (O1/2), and primary motor cortices (C3/4).

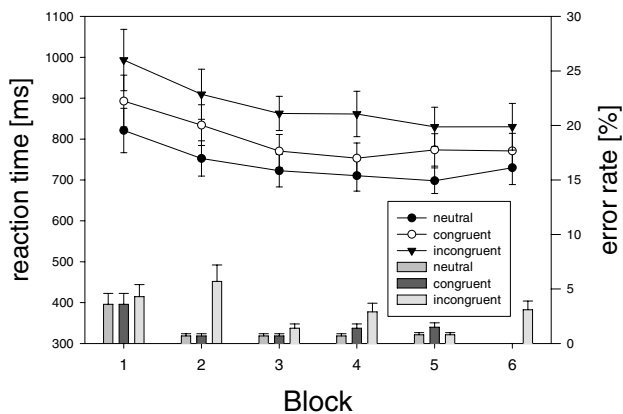


Figure 19 Reaction time (lines and symbols) and error rates (bars) for the color-word matching Stroop task, averaged over all subjects for each of the 6 runs. Mean \pm SEM.

As illustrated in Figure 19, mean reaction times were shorter in the neutral than in the congruent or incongruent conditions. Mean error rates (percentage of all respective trials) were smaller in the neutral than in the congruent or incongruent conditions. Hence, behavioral results of the Stroop task were in accordance with the literature (MacLeod, 1991), as demonstrated by a clear interference effect (incongruent vs. neutral condition).

According to the response with the right index or middle finger, there was a significantly stronger increase of oxyhemoglobin and decrease of deoxyhemoglobin in the left motor cortex in comparison with the right one (Figure 20A). When subjects responded with the left hand, the vascular response was inverted between the left and right side (Figure 20B). Therefore, a specifically stronger vascular response was found in the respective contralateral primary motor cortex. The differences in activation between the motor cortices were more pronounced for deoxy- compared with oxyhemoglobin in accordance with previous reports (Hirth et al., 1996; Kleinschmidt et al., 1996; Obrig et al., 2000b).

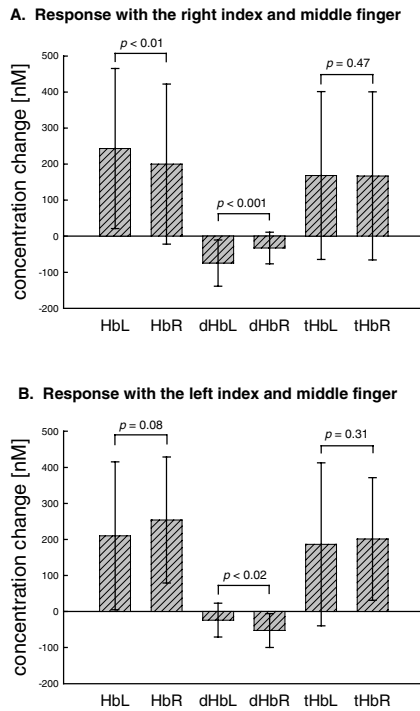


Figure 20 Brain activation in comparison between the left (C3) and right (C4) primary motor cortices during the Stroop task. Values are represented as averages of all neutral, congruent and incongruent trials. **A** Response with the right index and middle finger. **B** Response with the left index and middle finger. Hb oxy-, dHb deoxy-, tHb total hemoglobin. R right, L left side. Mean \pm SD. Paired 1-tailed students t-test.

During the Stroop task, concentrations of oxy- and total hemoglobin increased, whereas deoxyhemoglobin decreased in the LPFC (Figure 21). The increase of oxy- and total hemoglobin and the decrease of deoxyhemoglobin were significantly higher in the LPFC during the incongruent compared with the neutral condition. Thus, incongruent trials led to a stronger vascular response than neutral trials, corresponding to a stronger brain activation due to interference reduction. At the parietal and occipital cortex, changes in the concentration of oxy-, deoxy- and total hemoglobin did not differ between the three conditions.

In a second analysis approach, the hemodynamic response for each trial was modeled according to the nonlinear regression model by Kruggel & von Cramon (1999). A Gaussian function was fitted to each single hemodynamic response (Figure 23), yielding gain (in nM, the 'height' of the hemodynamic response), dispersion (in seconds, the duration of the hemodynamic response), and lag (in seconds, the time delay from stimulation onset to the peak of the hemodynamic response).

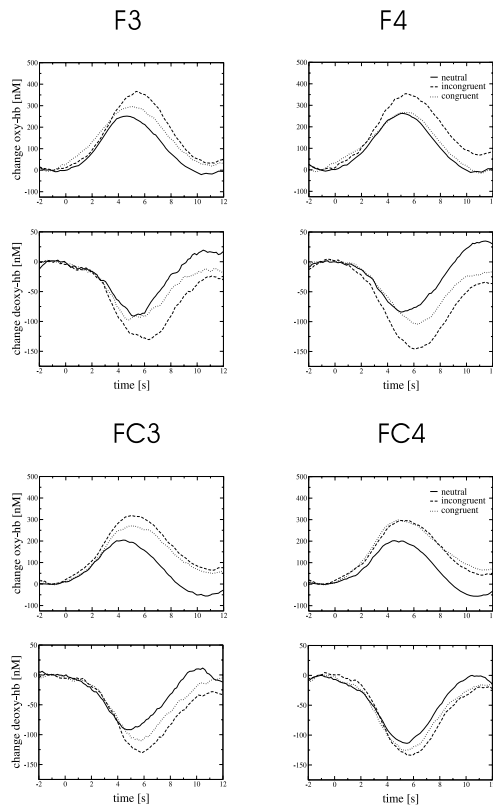


Figure 21 Time courses for concentrations of oxy- and deoxy-hemoglobin (hb) during the color-word matching Stroop task at the positions F3/4 and FC3/4. Beginning of the Stroop task at 0 s. Running averages over 2 s.

The gain of deoxy- and oxyhemoglobin was higher in the left compared with the right motor cortex, if subjects responded with the right index or middle finger (Figure 22A), and the lag was significantly shorter in the left than right motor cortex. If subjects responded with the left index or middle finger, the vascular response was inverted (Figure 22B). Thus, the analysis confirmed that the vascular response was stronger in the primary motor cortex contralateral to the motor response.

Like for the first analysis method, the gain was higher in the LPFC during the incongruent compared with the neutral and congruent conditions in the case of oxyhemoglobin, and lower concerning deoxyhemoglobin. Results correspond to a stronger brain activation due to interference. No significant differences were found for lag and dispersion.

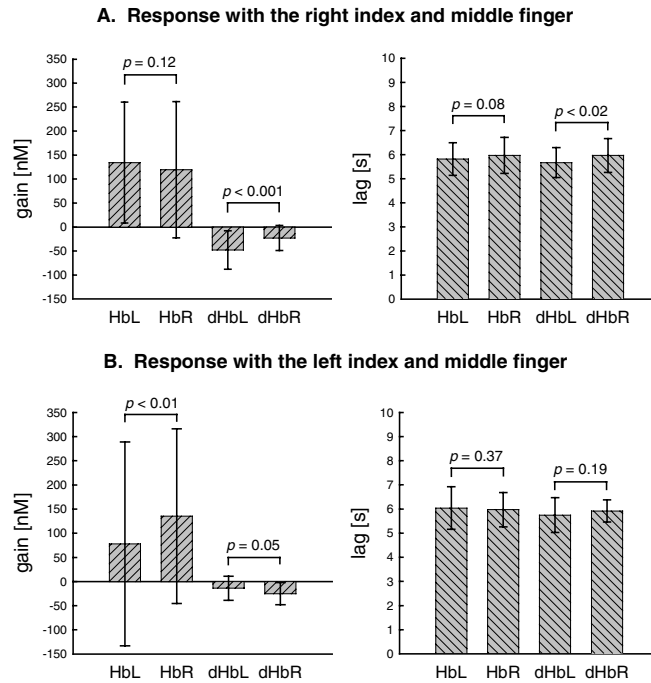


Figure 22 The parameters gain and lag of the respective fitted Gaussian function in comparison between the left (C3) and right (C4) primary motor cortices. Values are averages of all neutral, congruent and incongruent trials. **A** Response with the right index and middle finger. **B** Response with the left index and middle finger. Hb oxy-, dHb deoxyhemoglobin. R right, L left side. Mean \pm SD. Paired 1-tailed students t-test.

As illustrated in Figure 23, the lag (time-to-peak) for deoxyhemoglobin was longer than the lag for oxyhemoglobin at the positions over the LPFC. To further compare the hemodynamic responses between the conditions of the Stroop task, the difference between the lag of deoxyhemoglobin and oxyhemoglobin at the same position was calculated for the neutral and incongruent condition and compared with each other. Interference reduction may lead to a higher neuronal activity in the LPFC, and, consequently to a higher oxygen consumption in this region when incongruent trials are compared with neutral ones. Therefore, we hypothesized that deoxyhemoglobin reaches its minimum later than oxyhemoglobin reaches its maximum during incongruent compared with neutral trials. Accordingly, the time interval between the lag of deoxyhemoglobin and oxyhemoglobin was longer in the incongruent than the neutral condition at the LPFC (Figure 23).

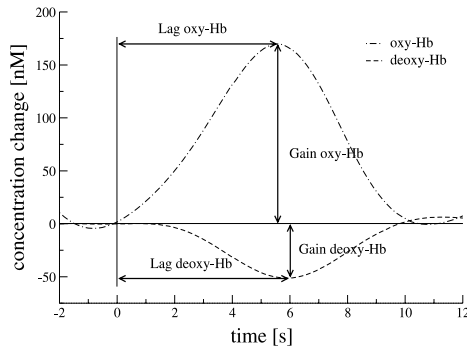


Figure 23 Graph Lag and gain of the Gaussian function as fitted to the time course of oxy- and deoxyhemoglobin at the left LPFC (F3) during the incongruent condition. Beginning of the Stroop task at 0 s. **Table** Differences between the lag of deoxy- and oxyhemoglobin (Hb), and the changes in the gain of oxy- and deoxyhemoglobin at F3/4 and FC3/4. Mean±SD. The incongruent and neutral condition was compared with paired students t-test.

Position	Lag $_{\text{deoxy-Hb}} - \text{Lag}_{\text{oxy-Hb}}$ (s)		Gain $_{\text{oxy-Hb}} - \text{Gain}_{\text{deoxy-Hb}}$ (nM)	
	Neutral	Incongruent	Neutral	Incongruent
F3	-0.17±0.5	0.31±0.9*	182±150	226±176*
F4	-0.11±0.8	0.31±0.44*	198±214	219±187
FC3	0.21±0.75	0.39±0.84	154±112	215±129**
FC4	0.02±0.62	0.09±0.68	178±83	225±103*

Note: * $p < 0.05$, ** $p < 0.01$ incongruent in comparison with neutral condition, paired 1-tailed students t-test, N=14.

Brain activation leads to an increase in rCBF, which exceeds the increase in oxygen consumption (Villringer & Dirnagl, 1995). Consequently, the concentration of oxyhemoglobin increases whereas the concentration of deoxyhemoglobin decreases (Villringer & Chance, 1997). The sum of the absolute changes in the gain of oxyhemoglobin and deoxyhemoglobin may characterize these changes for each position, revealing a parameter including deoxy- and oxyhemoglobin (Figure 23). Values were specifically higher during incongruent than neutral trials in particularly the left LPFC.

So far the analysis showed significant differences between neutral and incongruent trials of the Stroop task concerning either the hemodynamic response or behavioral data. If changes in oxygen consumption and CBF in the LPFC are specific for the Stroop task, one may assume that reaction time and error rate are correlated with the difference between the lag of deoxyhemoglobin and oxyhemoglobin, and with the sum of the absolute changes in the gain of oxyhemoglobin and deoxyhemoglobin in the LPFC. Accordingly, reaction time was positively correlated with the gain difference, and error rate was positively correlated with the lag difference at the left LPFC, respectively.

The study demonstrates the feasibility of fNIRS to monitor brain activation using a cognitive paradigm in an event-related design. The second analysis approach modeled the hemodynamic response trialwise by a nonlinear regression model (Kruggel & von Cramon, 1999) taking advantage of the good temporal resolution of the method. Modeling the response has advantages in comparison to the first method. It reveals three parameters (gain, lag and dispersion) which characterize each hemodynamic response, and which may be related to behavioral results (for instance, reaction time and error rate) and compared between different conditions. Our study shows that interference during the color-word matching Stroop task leads to specific brain activation in the LPFC in the vicinity of the inferior and middle frontal gyrus (Homan et al., 1987). Thus, results agree with recent adult imaging studies with fMRI (Banich et al., 2000; Carter et al., 2000; Fan et al., 2003; Leung et al., 2000; Milham et al., 2002; Ruff et al., 2001; Zysset et al., 2001), and PET (George et al., 1994; Taylor et al., 1997), which revealed a left sided frontomedian and frontolateral network for the Stroop task. The activations in the anterior cingulate cortex (summarized in Barch et al., 2001) cannot be captured by fNIRS because of limited depth penetration (Villringer & Chance, 1997). Therefore, we selected a color-word matching Stroop task that mainly activates the LPFC (Zysset et al., 2001). Furthermore, Adelman et al. (2002) reported that Stroop task-related activations were observed more consistently in the LPFC than in the anterior cingulate cortex in former studies.

Simultaneous measurement of several chromophores is an advantage of fNIRS (Villringer & Chance, 1997). Our study demonstrates that fNIRS may contribute additional information concerning the vascular response in comparison with other functional imaging methods, such as fMRI. We found a specific delay between the lag of oxy- and deoxyhemoglobin in the incongruent condition compared with the neutral one at F3/4. Such a temporal shift between the peaks of deoxy- and oxyhemoglobin can be detected by fNIRS only, in contrast to fMRI. The concentration of deoxyhemoglobin decreased more whereas the concentration of oxyhemoglobin increased more during incongruent compared with neutral trials, specifically at positions over the LPFC. These results may indicate that interference leads to a higher neuronal activity, and, thus to a higher oxygen consumption in the LPFC with a subsequent increase in rCBF due to neurovascular coupling (Gratton et al., 2001; Villringer & Dirnagl, 1995). At F3/4, oxygen consumption increased more than the rise of rCBF in the early phase. The decrease of deoxyhemoglobin was postponed and deoxyhemoglobin reached its minimum later than oxyhemoglobin reached its maximum during incongruent compared with neutral trials. Thereafter, the increase in rCBF exceeded the oxygen consumption. Consequently, the concentration of oxyhemoglobin increased whereas the concentration of deoxyhemoglobin decreased, such as in the other parts of the LPFC. Data suggest that brain

activation due to interference was higher in the cortical areas at F3/4 than at FC3/4, because oxygen consumption increases with brain activation (Hoge et al., 1999b), and the increase of oxygen consumption is more localized than the increase of blood flow (Malonek & Grinvald, 1996). The specificity of the hemodynamic response in the LPFC was supported by the correlation with behavioral data.

The analysis of the hemodynamic response in the superior parietal lobe (P3/4) revealed no significant differences between the experimental conditions. Whereas the fMRI study of Zysset et al. (2001) demonstrated a stronger brain activation along the intraparietal sulcus, depth penetration of fNIRS is limited (Germon et al., 1999) and may not be sensitive enough to detect differences within the depth of the intraparietal sulcus (Okamoto et al., 2004a). Generally, no significant differences were found between the conditions of the Stroop-task concerning cytochrome-c-oxidase, presumably due to smaller changes in the redox state of cytochrome-c-oxidase in comparison with oxy- and deoxyhemoglobin, and due to a relatively short trial length in our study (Wobst et al., 2001).

In summary, it was shown that fNIRS is a valuable tool for event-related cognitive brain activation studies, as demonstrated for the color-word matching Stroop task. A new method was introduced for fNIRS data evaluation in event-related studies that enables the analysis of the hemodynamic response for each single trial utilizing good temporal sensitivity of the method.

2.5.2. Searching the Optimal Intertrial Interval for fNIRS

As raised above event-related approaches are advantageous in studies with cognitive paradigms (Pollmann et al., 1998). Recent cognitive fNIRS studies demonstrated the feasibility of event-related approaches (Kennan et al., 2002a; Noguchi et al., 2002; Schroeter et al., 2002b, 2003). In these studies trials were separated by an intertrial interval of at least 12 s, to minimize an overlap of the vascular response. Expected between-condition effects are often small for event-related designs in cognitive neuroscience. Thus, an increase in statistical power by reducing the length of the intertrial interval, and consequently increasing the trial number, is considered as a prerequisite for a broad range of applications. Further, control over subject's mental activity is better achieved during short intertrial intervals, and many short-lived between-trials effects cannot be investigated with long intertrial intervals (Pollmann et al., 1998, 2000).

Therefore, the primary aim of the study (Schroeter et al., 2004c) was to investigate whether the length of the intertrial interval may be reduced to 2 s in cognitive studies, as previously shown for simple motor and visual tasks (Jasdzewski et al., 2003). Changes in the concentration of oxy- and deoxyhemoglobin as well as changes in the redox state of the cytochrome-c-oxidase were again measured by event-related fNIRS (NIRO-300 spectrometer; Hamamatsu Photonics K.K., Japan) during performance of a color-word matching Stroop task (Zysset et al., 2001). The intertrial interval was varied between 12, 6, 4, and 2 s. For an intertrial interval of 6, 4 and 2 s, non-events, consisting of a blank screen, were inserted between the neutral and incongruent trials according to the randomized event-related design as proposed by Burock et al. (1998). For analysis, averaged time lines for the non-events were subtracted from the averaged time lines of the neutral and incongruent condition to correct for the overlap of the hemodynamic response.

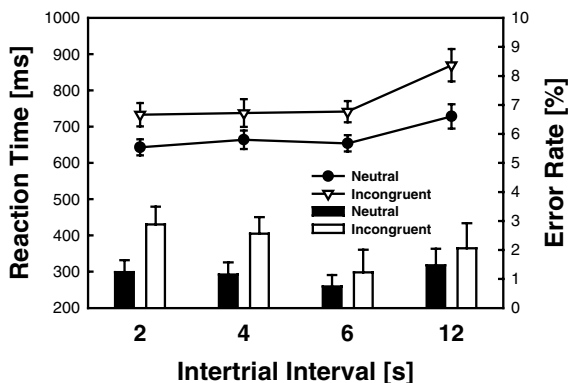


Figure 24 Reaction time (lines and symbols), and error rate (bars). Mean \pm SEM.

Recent results by fNIRS (Schroeter et al., 2002b) and fMRI (Zysset et al., 2001) demonstrated activations particularly in the left LPFC along the inferior frontal sulcus of young subjects, if the incongruent and neutral trials of the color-word matching Stroop task were compared (interference effect). Thus, optodes were placed over the LPFC (F3/4 of the international 10/20 system; Homan et al., 1987). We hypothesized that the Stroop interference effect may be detected down to an intertrial interval of 2 s, if a randomized design is applied (Burock et al., 1998). Further, we supposed that reducing the intertrial interval leads to a concomitant reduction of the vascular response during a trial, because of saturation of rCBF and rCBV.

As illustrated in Figure 24, mean reaction times were longer and mean error rates were higher in the incongruent compared with the neutral condition. Hence, the Stroop task produced a clear interference effect for every intertrial interval.

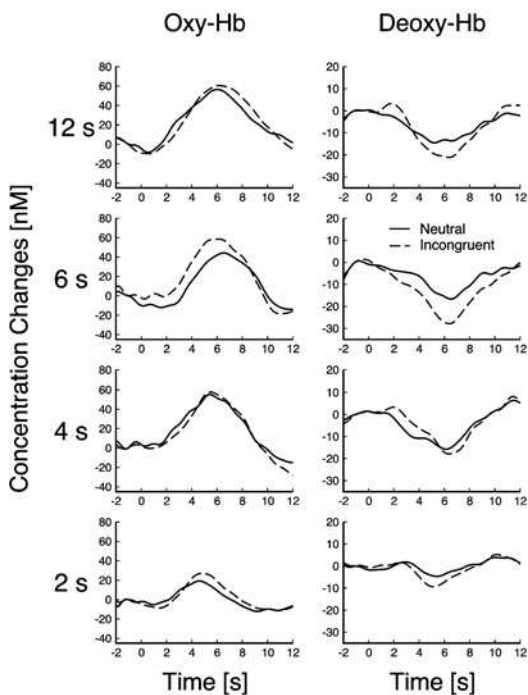


Figure 25 Concentration changes of oxy- and deoxyhemoglobin (Hb) during the color-word matching Stroop task in the left LPFC. Beginning of the Stroop task at 0 s. Running averages over 2 s.

Concentration of deoxyhemoglobin decreased more during incongruent trials compared with neutral ones in the left LPFC, except for an intertrial interval of 4 s. Data indicate that coping with interference elicits a stronger brain activation in the left LPFC (Figure 25 and 26). For

oxyhemoglobin no significant interference effect was detected, as for deoxyhemoglobin in the right LPFC. Results reveal that adults utilized particularly the left LPFC to cope with Stroop-related interference, consistent with the verbal nature of the Stroop task, and in agreement with previous studies with fMRI (Banich et al., 2000; Carter et al., 2000; Fan et al., 2003; Leung et al., 2000; Milham et al., 2002; Ruff et al., 2001; Zysset et al., 2001), and PET (George et al., 1994; Taylor et al., 1997). In the aforementioned study (Schroeter et al., 2002b), we reported additionally a significant interference effect for oxyhemoglobin with an intertrial interval of 12 s. This discrepancy may be explained by differences in the experimental design and analysis methods, and by the lower signal-to-noise ratio of oxyhemoglobin in comparison with deoxyhemoglobin (Obrig & Villringer, 2003).

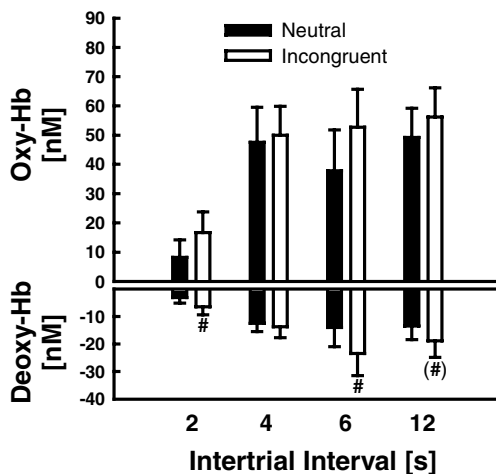


Figure 26 Comparison of the hemodynamic response during neutral and incongruent trials of the Stroop task in the left LPFC for the different intertrial intervals. Oxy- and deoxyhemoglobin (Hb). 1-tailed paired Student's t-test ([#] $p < 0.05$, ^(#) $p = 0.05$). Mean \pm SEM.

Pollmann et al. (1998) reported in an fMRI study that the effect size of the hemodynamic response may depend on the length of the intertrial interval. To compare the detectability of the interference effect between the several intertrial intervals, effect sizes were calculated for deoxyhemoglobin, and related to effect sizes of reaction time and error rate. As shown in Figure 27, effect sizes were large for behavioral data, whereas they reached small to medium values for hemodynamic data. This difference indicates a lower signal-to-noise ratio for the hemodynamic signal. Effect size of deoxyhemoglobin was highest for an intertrial interval of 2 s, followed by 6 and 12 s. The value was lowest for 4 s. Interestingly, effect size for reaction time was also lowest for 4 s. Thus, at 4 s the behavioral performance might have

reached its optimum, leading to a very small additional brain activation due to interference, and thus a non-detectable hemodynamic interference effect.

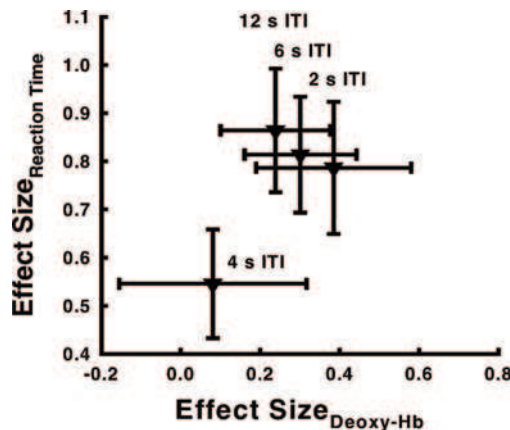


Figure 27 Effect sizes of the Stroop interference effect for reaction time, and deoxyhemoglobin (Deoxy-Hb) for the different intertrial intervals (ITI). Effect sizes were calculated according to Cohen (1988). Mean \pm SEM.

It is reasonable to compare methodological approaches for fNIRS studies with fMRI experiments, as fNIRS and fMRI (BOLD contrast) measure both the hemodynamic response to a stimulus (particularly deoxyhemoglobin). Our results for deoxyhemoglobin agree with fMRI data (Burock et al., 1998; Miezin et al., 2000; Pollmann et al., 1998) and results obtained with mathematical simulations (Dale, 1999). Burock et al. (1998) reported that the hemodynamic response overlap limits the maximum presentation rate with event-related fMRI, when fixed intertrial intervals are used. Thus, the transient information decreases with decreasing intertrial intervals. Accordingly, Pollmann et al. (1998) demonstrated an almost constant effect size as the ratio of task-related signal changes and error variance from 12 s down to 6 s (fixed) intertrial intervals in several cortical regions during a visual search task. However, at 4 s intertrial intervals, effect size was reduced by about 50%. Thus, with fixed intertrial intervals, it may be argued that the optimal intertrial interval for event-related fMRI experiments is 12 to 6 s. At shorter intertrial intervals, methods for overlap correction are necessary. When intertrial intervals are randomized (e. g., by inserting non-events as in our study), event-related experiments with extremely rapid presentation rates are possible (Burock et al., 1998). Our data might support the assumption that the hemodynamic effect size increases generally with a reduction of the intertrial interval, if the values at 4 s are regarded as an effect of reaction time. That effect is in accordance with fMRI studies and mathematical simulations showing that the transient information increases with decreasing mean intertrial interval with randomized designs (Burock et al., 1998; Dale, 1999; Miezin et

al., 2000). Further, data for 4 s suggest that the optimal intertrial interval has to be chosen for each cognitive imaging study individually, because effect size may increase with decreasing intertrial interval in a non-linear manner.

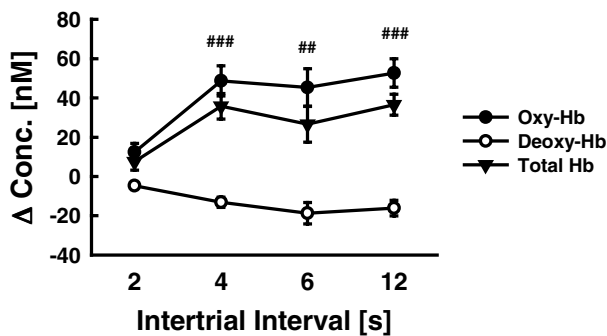


Figure 28 Concentration changes of oxy-, deoxy-, and total hemoglobin (Hb) in the left LPFC in relation to the length of the intertrial interval. Averages of all trials, respectively (neutral and incongruent trials were pooled). Significance values in comparison with 2 s intertrial interval for oxyhemoglobin ($##p<0.01$, $###p<0.001$). 1-tailed paired Student's t-test. Mean \pm SEM.

One may suppose that shorter intertrial intervals lead to a smaller hemodynamic response, because the rCBF and rCBV may not return to baseline during short intertrial intervals and the 'reserve' to increase both after one trial is reduced ('ceiling effect'). Indeed, changes of oxyhemoglobin declined with an intertrial interval of 2 s, without significant effects on deoxyhemoglobin (Figure 28). Moreover, the length of the intertrial interval was positively correlated with concentration changes of oxy-, and total hemoglobin. No significant correlation with intertrial interval was found for deoxyhemoglobin. If concentration changes of the chromophores were analyzed over the whole experiment, oxyhemoglobin increased, and deoxyhemoglobin decreased continuously, reaching a plateau at almost 1 or -0.5 μ M. These data further support the assumption of a 'ceiling effect'. It may be concluded that shortening the intertrial interval reduces the increase of oxyhemoglobin during a single trial, particularly with an intertrial interval shorter than 4 s. This effect may be due to a saturation of rCBF and rCBV with short intertrial intervals, whereas the latter is indicated by smaller changes in total hemoglobin (Figure 28). In contrast, we found almost constant changes of deoxyhemoglobin with the several intertrial intervals in agreement with fMRI data (Pollmann et al., 2000). Data suggest that changes of deoxyhemoglobin are closer related to brain activity during short intertrial intervals than changes of oxyhemoglobin, which is in agreement with a higher signal-to-noise ratio of deoxyhemoglobin (Wobst et al., 2001; Obrig & Villringer, 2003).

In summary, using a randomized presentation design by inserting non-events, this experiment shows that event-related cognitive fNIRS experiments are feasible with intertrial intervals as short as 2 s, particularly if changes in deoxyhemoglobin are considered.

2.6. Development & Aging

2.6.1. Prefrontal Activation due to Stroop Interference increases during Development

The Stroop color-word task has been a classic measure of frontal lobe function (MacLeod, 1991). Behavioral Stroop interference declines during development, which may indicate maturation of executive functions (Comalli et al., 1962; Daniel et al., 2000; Schiller, 1966). In conjunction with the behavioral development of executive functions, previous studies showed post-adolescent structural development particularly of the frontal lobes (Giedd et al., 1999; Sowell et al., 1999, 2001). Although the developmental parallelism between function and structure is well known for the frontal lobes, only one imaging study with fMRI has used the Stroop task to investigate this relationship from a developmental point of view. Adleman et al. (2002), covering an age range from 7 to 22 years, revealed that brain activation increased in a frontoparietal network with development. Because subjects were requested to respond vocally potentially resulting in head movements, Adleman et al. separated the behavioral investigation from the imaging study. Hence, they could not relate behavioral and hemodynamic results, and control the behavioral performance during the imaging experiment. Because of this limitation, we applied fNIRS which is known to be more insensitive to movement artifacts, and, therefore, particularly suitable for developmental studies.

We hypothesized that frontal brain activation during the Stroop task increases with development, together with the improvement of behavioral performance. Simultaneously, we measured changes in the concentration of oxy-, and deoxyhemoglobin as well as changes in the redox state of cytochrome-c-oxidase by fNIRS (NIRO-300 spectrometer, Hamamatsu Photonics K.K.) in the LPFC (F7/8, F3/4, FC3/4) of children (range 7-13 years; Schroeter et al., 2004d), and related results to an identical study involving young adults (range 19-29; Schroeter et al., 2003). An age dependent differential pathlength factor was applied (Duncan et al., 1996).

Children reacted slower and made more errors during the incongruent condition compared with the neutral one, such as adults. Generally, children reacted slower than adults. As illustrated in Figure 29 oxyhemoglobin increased and deoxyhemoglobin decreased more during the incongruent compared with the neutral condition in the left LPFC of children. Results reveal that children utilized particularly the left LPFC to cope with Stroop-related interference, consistent with the verbal nature of the Stroop task and results of recent studies with fMRI (Banich et al., 2000; Carter et al., 2000; Fan et al., 2003; Leung et al., 2000;

Milham et al., 2002; Ruff et al., 2001; Zysset et al., 2001), PET (George et al., 1994; Taylor et al., 1997), and fNIRS (Schroeter et al., 2002b, 2004c).

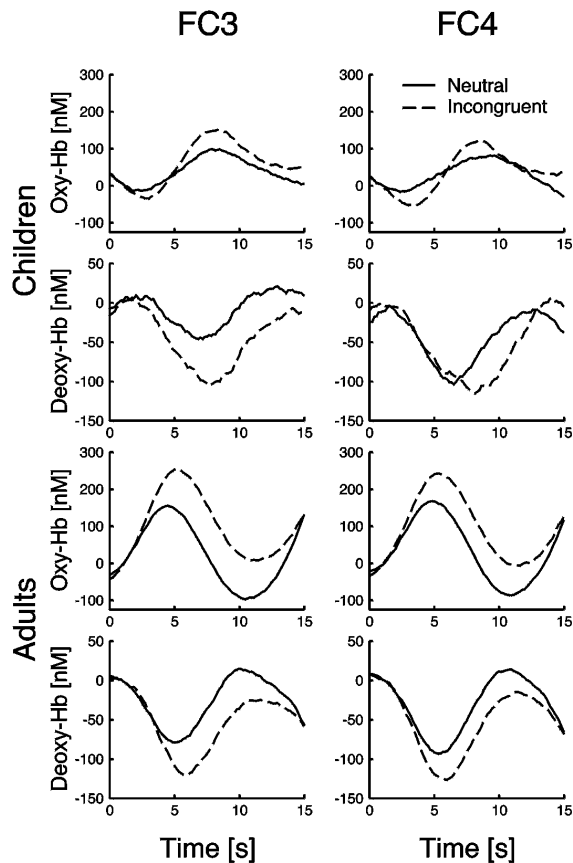


Figure 29 Time courses for concentrations of oxy- and deoxyhemoglobin (Hb) in the LPFC of children and adults (FC3/4) during the neutral and incongruent condition of the Stroop task starting at 0 s. Running averages over 3 s.

Analyzing the whole age range from 7 to 29 years (Figure 30), the interference effect of reaction time declined with aging in correspondence with previous behavioral studies (Comalli et al., 1962; Daniel et al., 2000; Schiller, 1966). These studies showed an interference effect, namely that word reading was faster than color naming except for first Graders, which were excluded from our study. More precisely, absolute interference as measured by the reaction time difference between incongruent and neutral trials was highest in young children as reading skills developed (Grades 2 and 3), and decreased with

increasing age to adulthood with higher reading proficiency. The authors suggested that young children have more difficulty than young adults in screening out interfering stimuli.

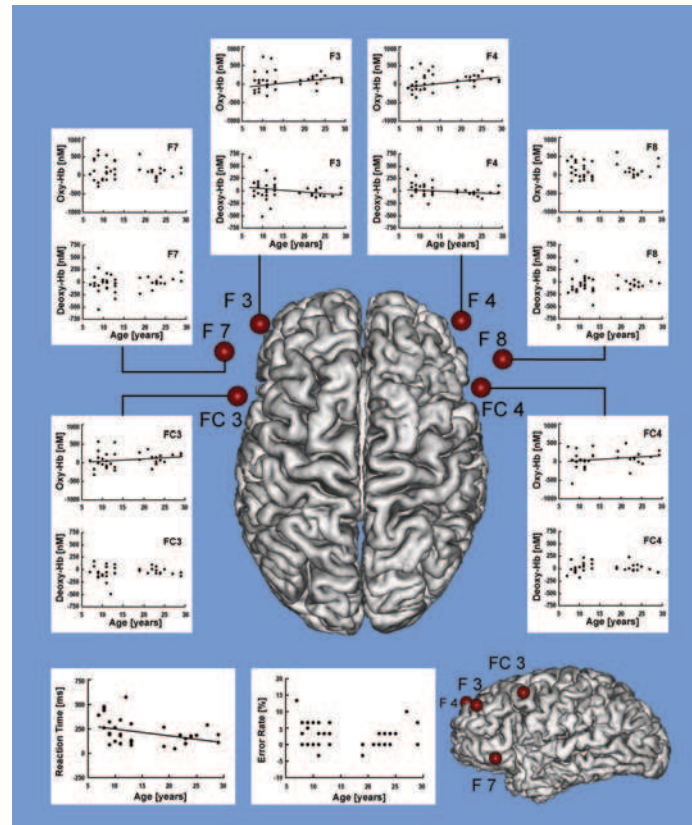


Figure 30 The impact of age on the behavioral, and the hemodynamic interference effect (incongruent minus neutral condition, respectively). Hb hemoglobin. Results for young adults were obtained from Schroeter et al. (2003). Regression lines are shown only, if the correlation analysis yielded significant results. Red spheres correspond with optode positions mapped onto an adult reference brain (Schroeter et al., 2002b).

As further illustrated in Figure 30, interference induced activation in the dorsolateral prefrontal cortex increased during development (Herwig et al., 2003; Okamoto et al., 2004a). Data agree with the fMRI study by Adelman et al. (2002) investigating brain activation in children, adolescents, and young adults with an almost similar age range of 7-22 years during a Stroop color-word task. They reported that, during development, brain activation

increased in the left (particularly dorso-) LPFC, anterior cingulate, parietal and parieto-occipital cortices. They discussed that lateral prefrontal activation may be related to interference processing/response inhibition, and word reading/production, and parietal(-occipital) activation to maintenance of sustained attention, and reading skills. Activation in the anterior cingulate was attributed to interference resolution and executive control processes. They concluded that Stroop-task-related functional development of the parietal lobe occurs by adolescence, whereas that of the prefrontal cortex continues to develop into adulthood. Although fNIRS is inferior to fMRI in spatial resolution, and our region of interest is confined to frontolateral areas, the results prove that fNIRS is particularly suitable for developmental studies because of its easy applicability to children. The increase of brain activation at FC3/4 with development was paralleled by a specifically decreasing interference effect of reaction time. Thus, our study is the first to provide evidence for ongoing developmental changes in Stroop-processing networks that correspond to improvements in behavioral task performance.

Development of executive functions has been examined, beside the Stroop interference task, in a few fMRI studies with the Go/NoGo (Booth et al., 2003; Bunge et al., 2002; Casey et al., 1997; Durston et al., 2002; Tamm et al., 2002), and the stop paradigm (Rubia et al., 2000) applying mainly block designs. Whereas a motor response has to be executed or inhibited in the Go/NoGo task, the motor response to a go-stimulus has to be retracted in the stop signal task. Hence, both tasks involve response inhibition. Go/NoGo studies reported controversial findings, namely stronger prefrontal activations in children (Booth et al., 2003; Casey et al., 1997), in adults (Bunge et al., 2002), or a region-specific increase and decline of prefrontal activation with development (Durston et al., 2002; Tamm et al., 2002). These controversial results may be related to differences in design and a small number of included subjects (≤ 24). Interestingly, the only study that involved more subjects (Bunge et al., 2002) showed a stronger ventro- and dorsolateral prefrontal activation in 16 adults (age range 19-33 years) compared with 16 children (age range 8-12 years) in accordance with our study. This fMRI study investigated additionally interference suppression with an Eriksen flanker task. Interference suppression activated the left ventrolateral prefrontal cortex in children, and the right ventrolateral prefrontal cortex of adults. Further, prefrontal activation increased with development during the stop signal task (Rubia et al., 2000), and, as shown in another fMRI study, during an oculomotor response-suppression (antisaccadic) task (Luna et al., 2001). Both studies support the hypothesis that prefrontal activation increases with development. However, comparability of the aforementioned tasks with the Stroop task is limited. These tasks involve mainly inhibition and/or interference control on the response level, whereas there is growing evidence that the Stroop task requires additionally interference control on

the task level (Monsell et al., 2001). Moreover, two fMRI studies observed a positive correlation between age and brain activity related to visuospatial working memory particularly in dorsolateral prefrontal regions (Klingberg et al., 2002; Kwon et al., 2002).

Interestingly, performance matures at approximately 12 years of age in the Go/NoGo task (Levin et al., 1991), at 13-17 years of age in the stop signal task (Williams et al., 1999), at 15-20 years of age in the antisaccadic task (Fischer et al., 1997; Munoz et al., 1998), and at ~17-19 years of age in the Stroop task (Comalli et al., 1962). Working memory performance also improves into young adulthood (Kwon et al., 2002). Hence, conducting imaging studies with the several tasks opens a window to the neurodevelopment of executive functions.

In conjunction with behavioral development of executive processes, several histological and morphometric studies reported that the frontal lobe develops structurally into adulthood. Genesis and organization of synapses, as well as myelination occur mainly postnatally (Rivkin, 2000). First, synapse number initially exceeds the final adult number. Thereafter, synapses are selectively eliminated to yield the final number found in adulthood (synaptic pruning). The temporal pattern differs in several cortices due to heterochronous development. For instance, synaptic densities reach maxima in visual, auditory, and prefrontal cortex at 7 to 8 months, 4 years, and 4 years. Adult numbers of synapses are attained in the visual cortex by about 10 years of age, in auditory regions by about 13 years, and in the prefrontal cortex until the age of ~18. These developmental patterns may correspond to the changing functional importance of these cortical regions, i. e. frontally supported executive functions develop gradually throughout adulthood in distinction to the rapid development of perceptual skills. Comparable different temporal patterns were reported for myelination, lasting in dorsofrontal regions into adolescence. The histological changes are mirrored in morphometric studies. Gray matter density decreases specifically in the frontal lobes between adolescence and young adulthood, in contrast to other cortices remaining unchanged (Sowell et al., 1999). Sowell et al. (2001), including additionally children, focused the inverse relationship between continued post-adolescent decline in gray matter density and brain growth to dorsofrontal areas. They argued that both processes might be related to cellular maturational events, such as myelination and synaptic pruning. Histological and morphometric studies fit very well with our findings, namely that activation increased during development in the dorsolateral prefrontal cortex. In summary, data support the assumption of a protracted frontal development.

Obviously, in our study, individual values of behavioral (reaction time) and hemodynamic interference varied much more in the children group compared with the adult sample (Figure

30), which can be explained by the fact that children differ in their individual cognitive development independent of their chronological age more than adults (Gaillard et al., 2001). Both, children and adults showed qualitatively the same hemodynamic response in our study in agreement with Gaillard et al. (2001). They reported that healthy children older than 5 years show activation maps comparable to adults for similar cognitive paradigms. However, the hemodynamic response occurred later in children compared with adults in our study, probably due to longer reaction times.

In summary the study shows that fNIRS is well suited for imaging studies in developmental cognitive neuroscience. Brain activation as elicited by Stroop interference increases from 7 to 29 years of age specifically in the dorsolateral prefrontal cortex in conjunction with an improvement in behavioral performance. Our results and data from literature suggest that the developmental trajectory of cognitive processing needed for the Stroop task is characterized by increasing ability to recruit additional frontal neural resources.

2.6.2. Prefrontal Activation due to Stroop Interference declines with Aging

Recent studies reported altered rCBF in elderly in comparison with young adults. During rest, rCBF decreases with advancing age in both association and limbic cortex as shown by PET (Martin et al., 1991) and SPECT (Nakano et al., 2000) (age range 30-85, 18-87 years, respectively). Further, in fMRI studies, less voxels were activated in elderly (>60 years) in comparison with young adults (<40 years) during a motor task (Mehagnoul-Schipper et al., 2002), a simple reaction time task (D'Esposito et al., 1999), and visual stimulation (Huettel et al., 2001). However, the amplitude of the hemodynamic response was equal in both age groups. Two fMRI studies (Buckner et al., 2000; Ross et al., 1997) demonstrated that the amplitude is reduced in elderly (mean 75 years) compared to young subjects (mean 24, 21 years, respectively) during visual stimulation. Mehagnoul-Schipper et al. (2002) showed by fNIRS that oxyhemoglobin increased less and deoxyhemoglobin decreased less during finger tapping in elderly compared with young adults, which was in agreement with the smaller number of activated voxels as shown by simultaneous fMRI. Hock et al. (1995) demonstrated by fNIRS that oxy- and total hemoglobin increased less in the anterior frontolateral cortex of elderly (mean 52 years) compared with young subjects (mean 28 years) during a calculation task, although they did not correct for the age dependency of the differential pathlength factor (Duncan et al., 1996).

The aim of the study (Schroeter et al., 2003) was to investigate age dependency of brain activation in primary and association cortices. fNIRS is particularly appropriate to examine brain function in elderly people, because it is relatively insensitive to movement artifacts in comparison with other imaging methods, such as fMRI. Therefore, changes in the concentration of oxy-, and deoxyhemoglobin as well as changes in the redox state of the cytochrome-c-oxidase were measured by fNIRS (NIRO-300 spectrometer, Hamamatsu Photonics K.K.) in the LPFC (F7/8, F3/4, FC3/4) during performance of an event-related Stroop task (Stroop, 1935; Zysset et al., 2001). Moreover, we examined age dependency of brain activation in the motor cortex (C3/4). Elderly subjects (range 62-71 years) were compared with young adults (range 19-29 years). Again, an age dependent differential pathlength factor was applied (Duncan et al., 1996).

Additionally to total hemoglobin as a measure of rCBV we calculated hemoglobin difference (oxy- minus deoxyhemoglobin) as a measure for changes in rCBF (Tsuji et al., 1998). As a second statistical approach we calculated effect sizes for behavioral and hemodynamic results according to Winer et al. (1991), additionally to concentration changes of the chromophores. These effect sizes are measures of the signal-to-noise ratio, and are age

independent as the age dependent differential pathlength factor is canceled during calculation.

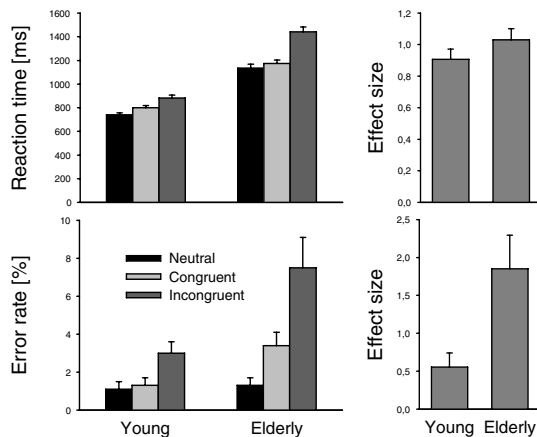


Figure 31 Reaction time, error rate and effect size of the Stroop interference effect (Incongruent vs. neutral condition), averaged over all young and elderly subjects. Mean \pm SEM.

Figure 31 illustrates behavioral results. The mean reaction time was significantly longer in the incongruent compared with the congruent and neutral condition in both age groups. Elderly subjects reacted more slowly than young subjects during all conditions. Mean error rates were significantly higher in both age groups in the incongruent condition, when compared with the congruent and neutral ones. Further, elderly subjects made more errors than younger ones in the incongruent and congruent condition, whereas there was no difference during the neutral condition. Hence, behavioral results of the Stroop task are in accordance with the literature (MacLeod, 1991), as demonstrated by a clear interference effect. Verhaeghen & De Meersman (1998) demonstrated that the age sensitivity of the Stroop interference effect is an artifact of general slowing. Accordingly, there was no significant difference for effect size of reaction time, whereas effect size of error rate was higher in the elderly subjects.

Like young adults, elderly subjects showed a stronger vascular response in the contralateral primary motor cortex during the response with the index or middle finger. As shown in Figure 32, oxyhemoglobin increased and deoxyhemoglobin decreased during the Stroop task, although the vascular response was generally lower in elderly in comparison with young subjects. Contrary, the mean change of cytochrome-c-oxidase was higher in elderly subjects. Incongruent trials led to a stronger vascular response than neutral trials at F3/4 in the young

adults, and at FC3/4 for both age groups. Regarding cytochrome-c-oxidase in the elderly, incongruent trials led to a stronger increase in its redox state compared with neutral trials at P3 and F4, which was not the case for young subjects. One may conclude that, although elderly subjects used a lateral prefrontal network like young adults (F3/4, F7/8, FC3/4) to cope with interference, brain activation was higher during incongruent than neutral trials in the elderly at F7/8 and FC3/4 only.

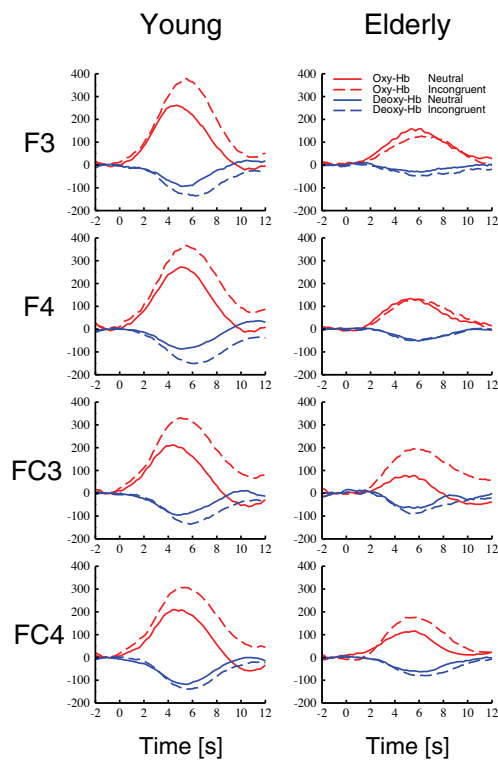


Figure 32 Time courses for concentrations of oxy- and deoxyhemoglobin (Hb) in nM in the dorsolateral prefrontal cortex (F3/4 and FC3/4) during the neutral and incongruent condition of the Stroop task. The Stroop task started at 0 s. Running averages over 2 s.

Additionally to the concentration changes of the chromophores, we compared age independent effect sizes for the hemodynamic response and changes in cytochrome-c-oxidase. Calculation of effect sizes included data from the right and left side, as the vascular response was approximately symmetrical during the Stroop task (Figure 32). We hypothesized a smaller vascular response in elderly compared with young subjects (Hock et al., 1995; Mehagnoul-Schippier et al., 2002). Accordingly, as illustrated in Figure 33, effect sizes for total hemoglobin and hemoglobin difference were reduced in the elderly in comparison with young subjects specifically in the LPFC (F3/4, F7/8) indicating smaller

changes in rCBF and rCBV (Tsuji et al., 1998). No age related difference was observed in primary motor cortex. Interestingly, effect sizes for cytochrome-c-oxidase were higher for elderly compared to young subjects at P3/4, and F3/4. So far it was shown that age significantly affects effect sizes of the Stroop task concerning either the hemodynamic response or behavioral data. If changes in rCBF and rCBV at F3/4 and F7/8 are specific for the Stroop task, one may assume that behavioral effect sizes (reaction time and error rate) are correlated with the calculated hemodynamic effect sizes. Indeed, effect size of error rate was negatively correlated with hemodynamic effect sizes, and positively correlated with effect size of cytochrome-c-oxidase in the LPFC (Figure 33). Moreover, effect size of reaction time was positively correlated with hemodynamic effect sizes in the parietal cortex (P3/4).

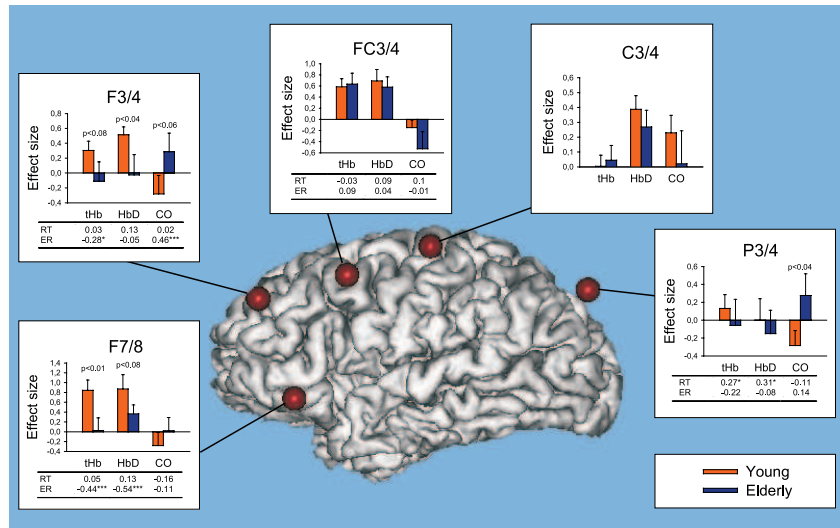


Figure 33 Effect sizes of total hemoglobin (tHb), hemoglobin difference (HbD), and cytochrome-c-oxidase (CO) in young and elderly subjects during the Stroop task. Mean \pm SEM. 1-tailed unpaired Student's t-test. Spearman correlation coefficients are reported for correlation between hemodynamic (tHb/HbD/CO) and behavioral effect sizes (reaction time [RT], and error rate [ER]; 1-tailed p). * $p < 0.05$, *** $p < 0.001$. Red spheres correspond with opode positions mapped onto a reference brain (Schroeter et al., 2002b).

In both young and elderly subjects, the LPFC was involved in coping with interference during the Stroop task in accordance with recent studies using fMRI (Banich et al., 2000; Carter et al., 2000; Fan et al., 2003; Leung et al., 2000; Milham et al., 2002; Zysset et al., 2001) and PET (Carter et al., 1995; George et al., 1994; Taylor et al., 1997). Our analysis of

hemodynamic effect sizes shows that rCBF and rCBV are specifically reduced in the LPFC of elderly compared to young subjects. These data are in agreement with PET, SPECT and fMRI studies reporting altered CBF in elderly in comparison with young adults. Martin et al. (1991) and Nakano et al. (2000) found a reduction of rCBF in association and limbic cortices with advanced age during rest by PET and SPECT. We show that age reduces rCBF in the prefrontal association cortex, whereas it is unaltered in the primary motor cortex and visual cortex (see next chapter). Kawahata et al. (1997) and Slosman et al. (2001) demonstrated by SPECT a decrease in global CBF with aging during rest (age range 50-99 and 18-71 years, respectively). However, this effect resolved after correction for partial-volume effects from cerebral atrophy (Meltzer et al., 2000; age range 19-76 years). In accordance with Kawahata et al. (1997) and Slosman et al. (2001) we found that mean vascular responses were smaller in elderly in comparison with young subjects at most of the examined optode positions. Analyzing effect sizes resolved this effect for P3/4 (lateral parietal), C3/4 (motor) and FC3/4 (prefrontal cortex, roughly on the border to the premotor cortex), whereas the effect was confirmed for F3/4 and F7/8 above the LPFC. Thus, our data may support the assumption that a reduction in CBF with aging is regionally limited and not a global phenomenon. The negative correlation between the effect size of error rate and hemodynamic response in the LPFC in our study may support the specificity of the aging effect.

Interestingly, Raz et al. (1997) reported a substantial decline in prefrontal gray matter volume in subjects from 18 to 77 years of age, in contrast to the precentral (primary motor) cortex and the pericalcarine (primary visual) cortex. Tisserand et al. (2002) confirmed these results and located the decline particularly to the lateral and orbital frontal gray matter in subjects from 21 to 81 years of age. Further, dendrites of pyramidal layer V neurons start to shrink in the prefrontal cortex from the fifth decade onwards (de Brabander et al., 1998). These alterations were described for Brodman area 9 and 46, which are roughly located beneath the optode positions F3/4 and F7/8 (Homan et al., 1987; Steinmetz et al., 1989). Thus, reductions of rCBF and rCBV in the LPFC as found in our study might be caused by this region-specific decline in cortical thickness and shrinkage of neuronal dendrites.

Further, fMRI and fNIRS studies reported that the hemodynamic response is altered during functional activation by age. Comparing age dependent hemodynamic responses between fMRI and fNIRS studies is complicated, because fNIRS measures the whole volume beneath the optodes, and, therefore, might not distinguish between changes of amplitude and number of activated voxels like fMRI. On the other hand, fNIRS measures changes of several chromophores and (indirectly) rCBV and rCBF. Combining our results and reports from literature one may suppose that the hemodynamic response declines in association cortices

starting from roughly 50 years of age. Hock et al. (1995) and our results support this hypothesis for the (prefrontal) association cortex, as they demonstrate a reduction of the hemodynamic response in subjects with a mean age of 52 and 65 years, respectively. However, the fNIRS study by Hock et al. had methodological limitations as they did not correct for the age dependency of the differential pathlength factor (Duncan et al., 1996), measured the hemodynamic response at only one location, and used a block design in contrast to the event-related design of our study, which is advantageous for cognitive studies (Pollmann et al., 2000).

For the primary motor cortex (and visual cortex) we did not find influences of age when effect sizes of the hemodynamic response were compared. Thus, one may assume that the hemodynamic response declines in primary cortices after 65 years of age. Firstly, the number of activated voxels decreases with age as shown by fMRI, which might be caused by a higher variability or a smaller active brain volume in the elderly. Concomitantly, the hemodynamic response as measured by fNIRS may be reduced (Buckner et al., 2000; D'Esposito et al., 1999; Huettel et al., 2001; Mehagnoul-Schipper et al., 2002; Mean age 75, 71.3, 66, 73 years, respectively). Later, starting from roughly 75 years of age, the amplitude of the hemodynamic response declines in the primary cortex, at least in visual areas (Buckner et al., 2000; Ross et al., 1997).

Differences between our results and Mehagnoul-Schipper et al. (2002) can be explained by the different mean age of the subjects. On the other hand, designs (event-related vs. block) and fNIRS analysis methods also contribute to differences. Mehagnoul-Schipper et al. (2002) showed that oxyhemoglobin increased less and deoxyhemoglobin decreased less during finger tapping in the motor cortex of elderly compared with young adults. Interestingly, we found also a smaller mean vascular response in elderly in comparison with young subjects in the primary motor cortex. However, when effect sizes were calculated, the age related difference disappeared.

We suggest that effect sizes are one valid approach for analyzing age related effects in fNIRS studies because of three reasons: (i) The age dependent differential pathlength factor is currently not known for subjects older than 50 years (Duncan et al., 1996). (ii) This factor has generally a high inter- (Essenpreis et al., 1993) and intrasubject variation (Zhao et al., 2002). (iii) Partial volume effects may change with aging as cortical thickness decreases at least in specific brain regions (Raz et al., 1997; Tisserand et al., 2002). (iv) Effect sizes as a measure of the signal-to-noise ratio are independent from the assumed differential pathlength factor, and may correct for these partial volume effects. Therefore, by calculating

effect sizes, one may avoid these pitfalls for all fNIRS studies investigating changes during aging. Further, this approach might be feasible for patient studies and fNIRS studies, which do not measure the individual differential pathlength factor.

During the Stroop task, effect sizes for cytochrome-c-oxidase were higher for elderly compared to young subjects at the lateral parietal cortex (P3/4) and tended to be higher at the LPFC (F3/4). These results correspond with human post mortem studies analyzing activity and protein content of cytochrome-c-oxidase. The enzyme's activity decreases in the frontal cortex, superior temporal cortex, cerebellum and putamen (Ojaimi et al., 1999b), and in human hippocampal neurons with age (Cottrell et al., 2001). The decreasing activity is accompanied by a reduction of some cytochrome-c-oxidase subunits as shown for the cerebellum (Ojaimi et al., 1999a). As cytochrome-c-oxidase is primarily localized in dendrites near excitatory synapses (Wong-Riley et al., 1998), decline in its activity might be related to shrinking of dendrites of pyramidal layer V neurons starting from the fifth decade onwards (de Brabander et al., 1998). Consequently, the alterations lead to a failure of the mitochondrial respiratory chain and decline in oxidative phosphorylation (Ojaimi et al., 1999b). One may assume, that although cytochrome-c-oxidase activity is decreased in the frontal cortex of elderly subjects, they have to make a stronger effort to cope with Stroop interference resulting in higher changes of cytochrome-c-oxidase. The higher effect size for error rate in elderly subjects and the positive correlation between effect sizes of error rate and cytochrome-c-oxidase in the prefrontal cortex (F3/4) support this assumption.

Our experiments reveal two effects of aging on brain activation during a color-word matching Stroop task. (i) Elderly and young subjects use the LPFC to cope with interference. A hemodynamic interference effect was found in the elderly at F7/8 and FC3/4 only, whereas it was detected in the young subjects at all prefrontal positions. (ii) The hemodynamic response is reduced in elderly in comparison with young subjects in the lateral prefrontal (association) cortex in contrast to the (primary) motor and visual cortex. Thus, combining our results and reports from literature one may hypothesize that the hemodynamic response declines in association cortices starting from roughly 50 years of age, and declines in primary cortices after 65 years of age.

2.6.3. Spontaneous Low Frequency Oscillations decline in the Aging Brain

Aging leads to a degeneration of the vascular system, probably beginning as early as the fourth decade (D'Esposito et al., 2003; Farkas & Luiten, 2001; Kalaria, 1996; Marin, 1995; Shimokawa, 1999). rCBF decreases especially in cortical areas, related to a shift in vasoregulatory capacity towards the domination of vasoconstrictive processes, may be due to the decline of vasodilatory mechanisms. Further, vessel stiffness is enhanced with aging. These phenomena are accompanied by a reduction in the cerebral metabolic rate for oxygen, cerebral glucose utilization, and cellular energy status. Interestingly, the aging brain also shows a compromised microvascular anatomy, which may interact with cerebral brain perfusion and metabolism, contributing to a suboptimal cognitive performance in the elderly. More precisely, aging leads to a decrease in capillary density, thickening of the basement membrane of cerebral microvessels, and microvascular fibrosis. Further, endothelial function and responsiveness of vascular smooth muscle cells is altered. These changes may hinder nutrient and electrolyte transport through the blood-brain barrier.

It is well known, that slow oscillations happen in cerebral hemodynamics and metabolism (Intaglietta, 1990; Mayhew et al., 1996; Obrig et al., 2000a). Although their origin is controversial, (i) they are characterized by their spontaneity, i. e. they occur without any overt stimulus, (ii) they can be differentiated from other oscillatory phenomena such as the heart beat at around 1 Hz, and respiratory cycles at about 0.2-0.3 Hz called high frequency oscillations by their slowness, and (iii) they are influenced by pharmacological (inhibitor of the NO synthase), pathological conditions (ischemia, large and small artery disease), hypercapnia, and by functional stimulation (reviewed in Obrig et al., 2000a). Particularly, spontaneous low frequency oscillations (LFOs) occurring at around 0.1 Hz might be distinguished from spontaneous very low frequency oscillations (VLFOs) centered at about 0.04 Hz. These spontaneous oscillations were observed with fNIRS, laser Doppler flowmetry, transcranial Doppler sonography and fMRI. Hudetz et al. (1998) discuss that spontaneous oscillations in cerebral hemodynamics may represent autoregulatory processes of rCBF, and be of myogenic origin.

Taken together, one may hypothesize that spontaneous oscillations decrease in the cerebral microvasculature with aging. Accordingly, we investigated the age dependency of spontaneous oscillations during rest, and visual activation with a checkerboard (Schroeter et al., 2004b). We applied fNIRS (NIRO-300 spectrometer, Hamamatsu Photonics K.K.), because it is particularly sensitive to the microvasculature (Boushel et al., 2001; Liu et al., 1995a, 1995b), has a high temporal sensitivity that is decisive for analysis in the frequency domain, and can measure specifically changes in the concentration of oxy-, deoxy- and total

hemoglobin (Hoshi et al., 2003; Obrig & Villringer, 2003; Schroeter et al., 2002b; Strangman et al., 2002a). Optodes were placed at O1/2 of the international 10/20 system localized over the calcarine fissure (Homan et al., 1987; Steinmetz et al., 1989). Elderly subjects (range 62-71 years) were compared with young adults (range 19-29 years). Again, an age dependent differential pathlength factor was applied (Duncan et al., 1996).

Young subjects did not suffer from any other diseases and did not take any medication. Elderly subjects suffered from arterial hypertension, ischemic heart disease, hypercholesterolemia, diabetes, thyroid dysfunction, pancreatitis in history, trigeminal neuralgia, arthrosis, and prostate hyperplasia. Accordingly, they received angiotensin-converting enzyme inhibitors/receptor blockers, beta-adrenergic blockers, calcium channel blockers, estrogens, isosorbide dinitrate, digitoxin, acetyl salicylic acid, statins, salbutamol, L-thyroxin, pancreatin, carbamazepine, tamsulosin.

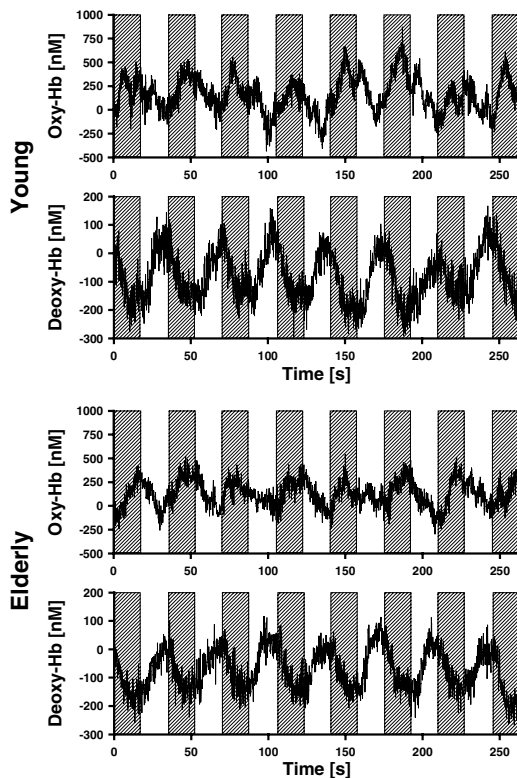


Figure 34 Concentration changes of oxy- and deoxyhemoglobin (Hb) in the right visual cortex during stimulation with a checkerboard (marked by gray boxes).

Visual stimulation was performed with a full-field checkerboard. The resting condition consisted of a black screen. Fixation was maintained by instructing subjects to fixate a gray point in the screen center that was shown during the whole experiment. Each stimulation period lasted 18 s, known to elicit a maximal hemodynamic response (Panczel et al., 1999), and was preceded by a resting period of 17 s. As illustrated in Figure 34, eight cycles were performed in each block and all subjects underwent two blocks in one session. Moreover, subjects were examined during rest without undergoing any stimulation with closed eyes for 6 min.

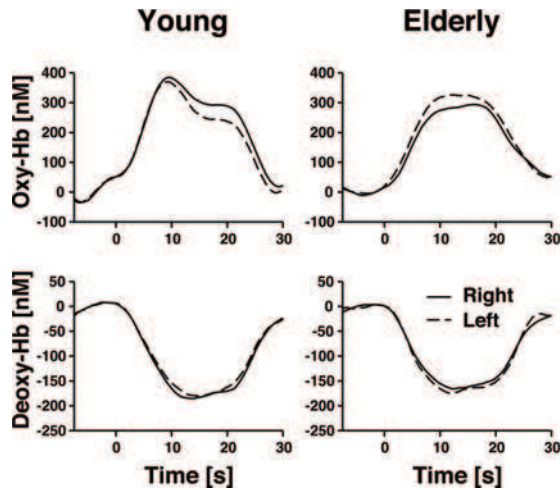


Figure 35 Epoch-related concentration changes of oxy- and deoxyhemoglobin (Hb) in the right and left visual cortex during stimulation with a checkerboard. Stimulation lasted from 0 to 18 s. Running averages over 5 s.

For analysis in the frequency domain, power spectral density was calculated with a frequency range from 0.018 to 3 Hz as peaks appeared in that range in our and previous studies (Obrig et al., 2000a). Power spectral density was normalized for every subject to 1 (integral normalization) as proposed by Schroeter et al. (2004a). This procedure matches with normalization by dividing the absolute amplitude of the power spectral density at particular frequencies by the mean amplitude of the entire spectrum (Kvandal et al., 2003; Kvernmo et al., 1998). Because both the numerator and denominator contain the same (age dependent) differential pathlength factor, it may be canceled. Hence, results are almost independent from the assumed differential pathlength factors (Schroeter et al., 2004a). To exclude that diagnoses or medication biased our results, we investigated their influence. Factors were included only, if an effect on the vascular system was assumed, and at least three subjects were affected. Hence, one diagnosis (arterial hypertension), and one group of

drugs (angiotensin-converting enzyme inhibitors/receptor blockers) were involved (Levy et al., 2001; Rizzoni et al., 2003).

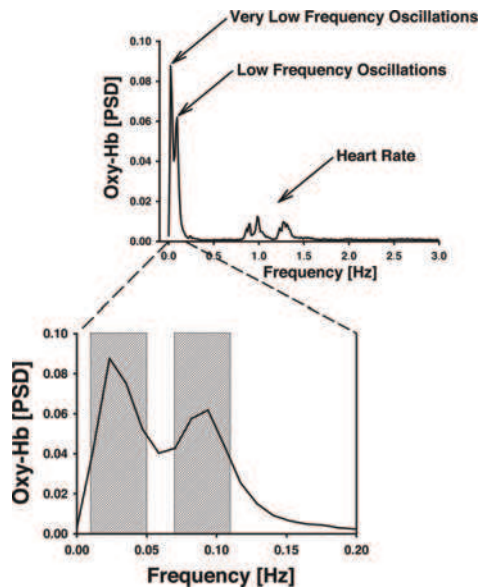


Figure 36 Normalized power spectral density (PSD) of oxyhemoglobin (Hb) in young subjects during rest. Spontaneous very low and low frequency oscillations were analyzed as mean in the spectral windows of 0.01-0.05 Hz, and 0.07-0.11 Hz, respectively.

The concentration of deoxyhemoglobin decreased, whereas the concentration of oxyhemoglobin increased significantly in young and elderly subjects during visual stimulation with the checkerboard (Figure 34, 35). There was no significant impact of age on oxy-, deoxy-, and total hemoglobin. Diagnosis and medication did not influence concentration changes.

Figure 36 shows the averaged normalized power spectral density for oxyhemoglobin in the visual cortex of young subjects during rest. Obviously, peaks were obtained for spontaneously very low and low frequency oscillations. As illustrated in Figure 37, almost the same pattern was observed for the VLFOs of deoxyhemoglobin in the young and elderly during rest. For LFOs during rest, peaks were found for oxyhemoglobin in the young subjects only, whereas power spectral density declined continuously in the elderly with an increasing frequency and, therefore, no LFO peak was observed. Stimulation led to a peak at 0.023 Hz in all chromophores and both age groups in accordance with a stimulation cycle of 35 s, corresponding to 0.028 Hz. The slight difference between peak and stimulation frequency was related to a limited spectral resolution of the power spectral density. A second peak was

detected again for the LFOs. To quantify spontaneous oscillations, means were calculated for a spectral window of 0.01-0.05 Hz for VLFOs, and of 0.07-0.11 Hz for LFOs, as concluded from the peaks locations (Figure 37).

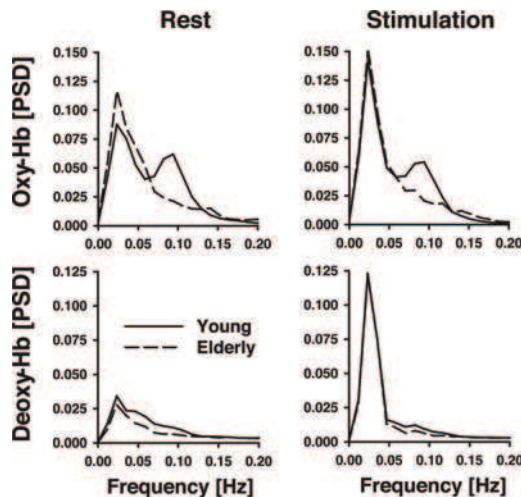


Figure 37 Normalized power spectral density (PSD) between 0 and 0.2 Hz in comparison between young and elderly subjects in the visual cortex during rest, and stimulation with a checkerboard. Thus, the frequency range includes spontaneous very low and low frequency oscillations and the stimulation frequency. Hb hemoglobin.

As illustrated in Figure 37 and 38, power spectral density of VLFOs and LFOs was generally stronger for oxyhemoglobin, compared with deoxyhemoglobin. Age influenced significantly the LFOs of oxy-, and deoxyhemoglobin. Mean power spectral density of the LFOs was higher in the young compared with the elderly subjects for both chromophores during rest and stimulation. Stimulation had generally no impact on the LFOs. The interaction between age and stimulation was generally not significant. Neither hypertension, nor medication (angiotensin-converting enzyme inhibitors/receptor blockers) influenced LFOs.

Further, stimulation influenced significantly the VLFOs of all chromophores (Figure 38). Visual stimulation was performed with a frequency of 0.028 Hz. Accordingly, we hypothesized that mean power spectral density in the VLFO range was generally higher during stimulation compared with the resting condition. Post hoc analysis revealed a significant effect for all chromophores except oxyhemoglobin in the elderly, when differences between rest and stimulation were compared for young and elderly subjects separately. Neither hypertension, nor medication (angiotensin-converting enzyme inhibitors/receptor blockers) had any significant impact on VLFOs.

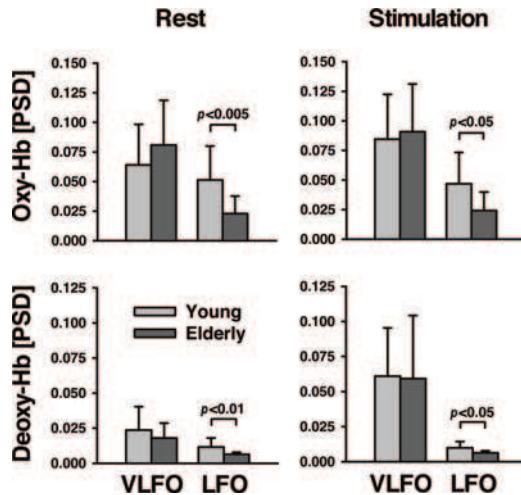


Figure 38 Normalized power spectral density (PSD) of spontaneous very low (VLFO) and low frequency oscillations (LFO) in comparison between young and elderly subjects in the visual cortex during rest and stimulation with a checkerboard. Note that stimulation frequency is contained in the VLFO range. Hb hemoglobin. Mean \pm SD. Significance values were tested with a 2-tailed unpaired Student's t-test.

We detected peaks of the power spectral density at around the same frequencies like other fNIRS or optical studies investigating spontaneous oscillations in the cortex (Elwell et al., 1999; Mayhew et al., 1996; Obrig et al., 2000a; Taga et al., 2000). Further, power spectral density of LFOs and VLFOs was much higher in oxy-, compared with deoxyhemoglobin, especially during rest, in accordance with previous reports (Obrig et al., 2000a). As illustrated in Figure 36, we detected also oscillations at \sim 0.25 Hz and several peaks between 0.8 and 1.4 Hz representing the influence of respiration, and heart beat on rCBF. Most strikingly, our results demonstrate that aging influences spontaneous slow oscillations in the cerebral microvasculature. LFOs (0.07-0.11 Hz) decreased for all chromophores during both, stimulation and rest, whereas VLFOs remained unaltered (0.01-0.05 Hz). Our data fit well with Hutchins' results (1996) showing that the amplitude of vasomotions in the cerebral arterioles of sedated rats decreased with aging. Several mechanisms might influence spontaneous oscillations. Vascular smooth muscle cells constitute, together with elastic laminae, the medial vessel layer (Lundberg & Crow, 1999). They are highly specialized as contractile cells controlling lumen diameter, and thereby regulating blood flow in response to nervous, hormonal, and local influences. Interestingly, the LFOs range corresponds well with the spontaneous activity recorded in microvascular smooth muscle cells (Golenhofen, 1970). Meyer et al. (1988) and Schmidt et al. (1992) concluded that this myogenic pacemaker mechanism causes vasomotion in terminal arterioles, and, hence, regulates capillary perfusion (Harrison et al., 2002). The intrinsic smooth muscle activity of resistance vessels was shown also for the skin at around 0.1 Hz with laser Doppler flowmetry (Kvandal et al., 2003; Kvernmo et al., 1998).

It is well known that aging leads to stiffening of the vascular wall by fibrosis (Lundberg & Crow, 1999). More precisely, the volume density of collagen increases, whereas that of elastin decreases. Collagen fibrils become organized into multi-branched bundles, whereas elastin fibers become disorganized, thinner, and often fragmented with age. Further, smooth muscle elements of vascular structures diminish (Hutchins et al., 1996). Hence, reduction of LFOs with aging as observed in our study may indicate a declining spontaneous activity in microvascular smooth muscle cells, presumably due to an increased stiffness. The vascular tonus might also be modulated by nervous influences. Sympathetic stimulation may alter LFOs in cerebral microvasculature as shown by laser Doppler flowmetry (Deriu et al., 1996). Moreover, it was suggested that VLFOs in the skin originate from neurogenic stimulation of resistance vessels (Kvandal et al., 2003; Kvernmo et al., 1998). In our study, VLFOs were generally independent of age. Intaglietta (1990) proposed that slow vasomotions (VLFOs) occur in larger vessels, whereas fast vasomotions (LFOs) originate from terminal arterioles. Neurogenic innervation was shown for larger cerebral vessels, whereas it is negligible in small ones (Farkas & Luiten, 2001; Ursino, 1991). Hence, our data might indicate that neurogenic stimulation is almost unaltered in aging.

Visual stimulation led to an increase of oxy-, total hemoglobin, and to a decrease of deoxyhemoglobin due to neurovascular coupling (Villringer & Dirnagl, 1995; Villringer & Chance, 1997). Amounts of concentration changes were in agreement with previous fNIRS studies (Heekeren et al., 1999; Obrig et al., 2000a; Schroeter et al., 2004a; Wobst et al., 2001; Wolf et al., 2002b). Although the hemodynamic response declines with aging in association cortices starting from roughly 50 years of age, it is said to decline in primary cortices after 65 years of age (Buckner et al., 2000; D'Esposito et al., 1999; Hock et al., 1995; Huettel et al., 2001; Mehagnoul-Schipper et al., 2002; Ross et al., 1997; Schroeter et al., 2003). Accordingly, we did not find age related differences for the mean hemodynamic response of oxy-, deoxy-, and total hemoglobin during visual stimulation. Taking together results of both approaches, spectral analysis and time line analysis of the functional hemodynamic response, one may conclude that the former method is much more sensitive to age related changes in the microvasculature than the latter one, and enables an earlier detection of such alterations.

Data suggest that fNIRS can detect spontaneous low frequency oscillations due to its high temporal sensitivity. Summarizing results, spontaneous low frequency oscillations decrease with aging in the microvasculature of the human visual cortex during both, rest and functional activation. Data might indicate a declining spontaneous activity in microvascular smooth muscle cells, in conjunction with an increased vessel stiffness.

2.7. Patient Studies

2.7.1. Brain Activation declines in Cerebral Microangiopathy during a Stroop Interference Task

Vascular dementia is the second most common type of dementia (Roman et al., 2002). The subcortical ischemic form (subcortical ischemic vascular dementia), which constitutes 36% to 67% of all vascular dementias, frequently causes cognitive impairment in elderly people. It is clinically homogenous, and results from small-vessel disease, or cerebral microangiopathy. Two main pathophysiological pathways are involved (Roman et al., 2002). In the first, critical stenosis and hypoperfusion of multiple medullary arterioles cause widespread incomplete infarction of deep (periventricular) white matter leading to leukoaraiosis with a clinical picture of Binswanger's disease (Figure 39). In the second, occlusion of the arteriolar lumen leads to the formation of lacunes resulting in a lacunar state (état lacunaire or état criblé). In practice, the two clinical pathways overlap, and lead to a variety of clinical symptoms and neuropsychological abnormalities, which are dominated by a dysexecutive syndrome (McPherson & Cummings, 1996). Several risk factors contribute to the development of cerebral microangiopathy, such as advanced age, smoking, hyperhomocysteinemia, hyperfibrinogenemia, and other conditions that can cause brain hypoperfusion (obstructive sleep apnoea, congestive heart failure, cardiac arrhythmias, and orthostatic hypotension) (Caplan, 1995; Roman et al., 2002). The most important risk factors are arterial hypertension and diabetes, which even reinforce each other (Corry & Tuck, 2000). Treatment is symptomatic and prevention requires control of treatable risk factors.

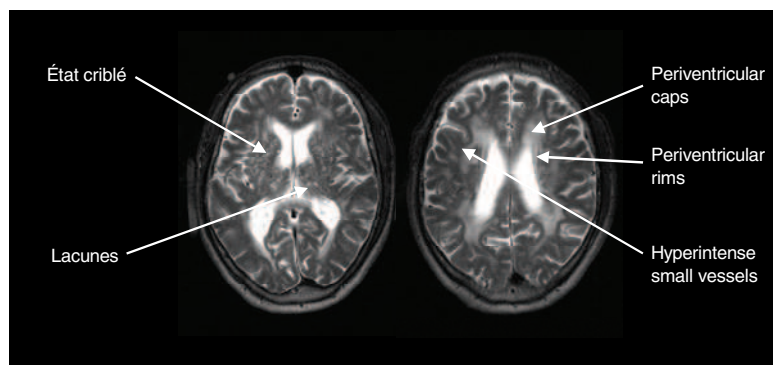


Figure 39 Structural changes in cerebral microangiopathy visualized with high-resolution MRI at 3.0 Tesla in T2-weighted sequence. Characteristic abnormalities are lacunar state of the basal ganglia and periventricular white matter disease (caps and rims, leukoaraiosis).

It is well known that vascular reactivity is reduced in the frontal lobe in correlation with severity of cerebral microangiopathy as shown for hyperventilation by fMRI (Hund-Georgiadis et al., 2002), and for hypercapnia by fNIRS (Terborg et al., 2000). Interestingly, neuropsychological deficits are correlated with functional imaging parameters (rCBF, regional metabolic rate of glucose) and atrophy, but not with structural white matter lesions in cerebral microangiopathy (Sabri et al., 1998, 1999). Thus, functional imaging might lead to a diagnosis of cerebral microangiopathy before morphological lesions occur.

Accordingly, we hypothesized that the hemodynamic response as elicited by Stroop interference is reduced particularly in the frontal lobe of patients suffering from cerebral microangiopathy. Further, we assumed that these reductions are correlated with behavioral deficits. fNIRS is particularly appropriate to examine brain function in elderly people and patients, because it is relatively insensitive to movement artifacts in comparison with other imaging methods, such as fMRI. Further, it is particularly sensitive to the microvasculature (Boushel et al., 2001; Liu et al., 1995a, 1995b). Therefore, changes in the concentration of oxy-, deoxy- and total hemoglobin were measured by fNIRS (NIRO-300 spectrometer, Hamamatsu Photonics K.K.) in the LPFC (F7/8, F3/4, FC3/4) during performance of an event-related Stroop task (Stroop, 1935; Zysset et al., 2001). Patients with cerebral microangiopathy were compared with healthy elderly controls (Schroeter et al., 2002a).

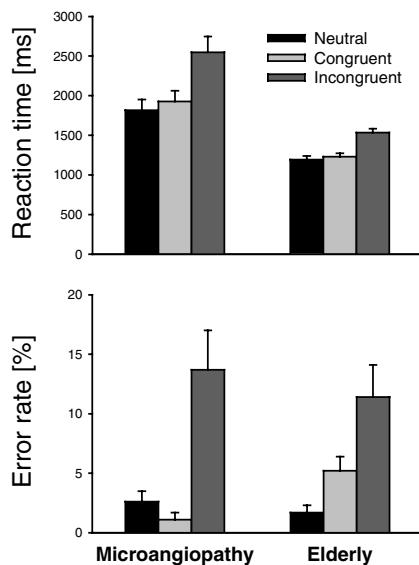


Figure 40 Reaction time and error rate in patients with cerebral microangiopathy and elderly controls during the color-word matching Stroop task.

Patients were treated in the Day Clinic of Cognitive Neurology of the University of Leipzig. They had previously been diagnosed with cerebral microangiopathy on the basis of anatomical MRI or computer tomography scans and a comprehensive clinical examination. Further, they were controlled for cerebral macroangiopathy and related lesions. Controls had no history of neurological or psychiatric disorders. Patients and controls suffered from additional medical diseases, mainly arterial hypertension, type II diabetes, and hypercholesterolemia. Accordingly, they received prominently angiotensin-converting enzyme inhibitors/angiotensin II receptor blockers, beta-adrenergic blockers, calcium channel blockers, diuretics, antidiabetic agents, statins, and inhibitors of thrombocytic aggregation.

As illustrated in Figure 40, patients showed generally longer reaction times than elderly controls. Further, patients and controls reacted slower during incongruent compared with congruent and neutral trials. Moreover, patients showed an higher interference effect, namely the difference between incongruent and neutral trials was larger. For error rate, patients and controls made more errors during the incongruent compared with the congruent and neutral condition, whereas there were no significant differences between both groups.

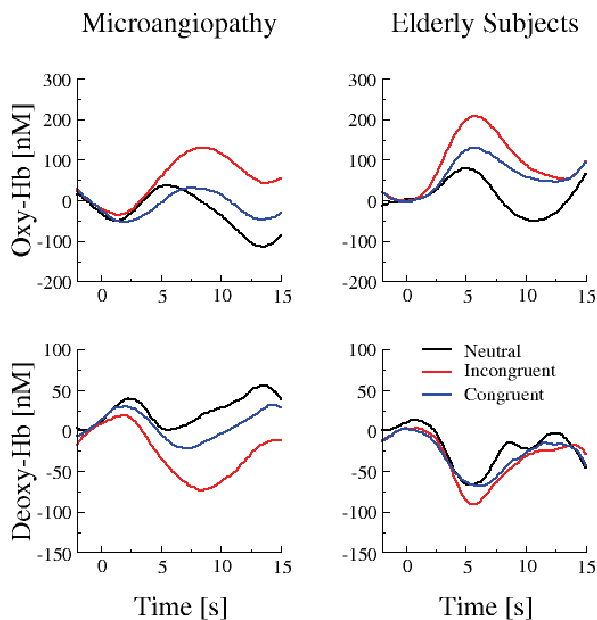


Figure 41 Changes of oxy- and deoxyhemoglobin in the left LPFC (FC3) during the Stroop task. The task is beginning at 0 s. Running averages over 2 s.

As illustrated in Figure 41, oxyhemoglobin increased more and deoxyhemoglobin decreased more during incongruent compared with neutral trials in the LPFC. Hence, incongruent trials led to a stronger hemodynamic response than neutral trials, indicating a higher brain activation due to interference in the LPFC. The hemodynamic response was reduced in the LPFC in cerebral microangiopathy compared with controls. Further, the vascular response occurred later in patients compared with controls. Summarizing results, and comparing it with primary (visual) cortices (see next chapter) our data support the assumption of a specific frontal deficit in cerebral microangiopathy as shown previously by fMRI (Hund-Georgiadis et al., 2002), and fNIRS (Terborg et al., 2000).

2.7.2. Spontaneous Slow Hemodynamic Oscillations are impaired in Cerebral Microangiopathy

Cerebral microangiopathy, or small-vessel disease is characterized by a degeneration of the cerebral microcirculation, which has a central role in its pathogenesis (Roman et al., 2002). Aging leads to a decrease in capillary density, thickening of the basement membrane, and microvascular fibrosis probably beginning as early as the fourth decade (Farkas & Luiten, 2001; Kalara, 1996; Marin, 1995; Shimokawa, 1999). Arterial hypertension may lead to microvascular alterations such as an increase in the wall-to-lumen ratio of precapillary resistance vessels (Levy et al., 2001). Accordingly, in cerebral microangiopathy, walls of the small penetrating arteries and arterioles are thickened and often hyalinized (Caplan, 1995). Fibrosis, loss of smooth muscle cells, and splitting of the internal elastic membrane can lead to increased vessel stiffness in cerebral microangiopathy (Tanoi et al., 2000). Consequently, vasomotor reactivity is reduced in cerebral microangiopathy as shown by PET (Roman et al., 2002), fNIRS, transcranial Doppler sonography (Terborg et al., 2000), and fMRI (Hund-Georgiadis et al., 2003). Moreover, damage to the blood-brain barrier, constituted by endothelial cells and astrocytes (Schroeter et al., 1999, 2001), may contribute to white-matter injury (Roman et al., 2002).

As discussed in chapter 2.6.3., it is well known, that spontaneous slow oscillations happen in cerebral hemodynamics and metabolism (Intaglietta, 1990; Mayhew et al., 1996; Obrig et al., 2000a). More specifically, LFOs occurring at around 0.1 Hz might be distinguished from VLFOs centered at about 0.04 Hz. Hudetz et al. (1998) discuss that spontaneous oscillations in cerebral hemodynamics may represent autoregulatory processes of rCBF, and may be of myogenic origin. Recently, we showed that aging leads to a specific reduction of LFOs in the cerebral microvasculature (Schroeter et al., 2004b). Interestingly, spectral analysis was more sensitive to age related microvascular alterations than time line analysis of the functional hemodynamic response in that study. As discussed above, cerebral microangiopathy accelerates development of vessel stiffness (Caplan, 1995; Roman et al., 2002; Tanoi et al., 2000). Hence, one may hypothesize that spontaneous oscillations further decline in cerebral microangiopathy (Bäzner et al., 1995). Accordingly, we investigated spontaneous oscillations during rest, and visual activation. We applied fNIRS (NIRO-300 spectrometer, Hamamatsu Photonics K.K., Japan), because it is particularly sensitive to the microvasculature (Boushel et al., 2001; Liu et al., 1995a, 1995b), and can measure changes in the concentration of oxy-, and deoxyhemoglobin and cytochrome-c-oxidase specifically, although it has a relatively low spatial resolution (Hoshi et al., 2003; Obrig & Villringer, 2003; Schroeter et al., 2002b; Strangman et al., 2002a; Villringer & Chance, 1997). For calculation, an age dependent differential pathlength factor was applied (Duncan et al., 1996). Optodes were placed at O1/2

of the international 10/20 system localized over the calcarine fissure (Homan et al., 1987; Steinmetz et al., 1989).

Imaging was performed at 3.0 T on a Bruker Medspec 30/100 system (Bruker Medical, Ettlingen, Germany). For staging cerebral microangiopathy a MRI-score was calculated on the basis of T2-weighted axial scans as proposed by Hund-Georgiadis et al. (2001). Criteria for scoring were the presence of lacunar infarctions and periventricular white matter lesions (Figure 39). The presence and severity were graded according to their extent and their uni- or bilateral distribution. The maximum theoretical score was 21 points and ranged in the patient group from 4 to 18 (mean 12.1 ± 4.5).

The neuropsychological battery assessed cognitive performance for attention, executive functions, and memory in the patient group. Alertness and divided attention was tested by the 'Testbatterie zur Aufmerksamkeitsprüfung' (TAP) (Zimmermann & Fimm, 1993). Impairment in executive functions was assessed by the 'behavioral assessment of the dysexecutive syndrome' (BADS) and a modified Stroop paradigm (Wolfram et al., 1986; Wilson et al., 1996). Memory functions were assessed by digit span and block span of the 'Wechsler Memory Scale' (WMS-R, Haerting et al., 2000) for short term, and by the verbal and visual memory quotient (WMS-R) and by the 'California Verbal Learning Test' (CVLT, Delis et al., 1987) for long term memory, respectively. A score (0 'unimpaired' to 3 'severely impaired') was calculated for each domain (attention, executive functions, learning and spans). Hence, the sum score ranged from 0 to 12 points. Mean scores for neuropsychological impairments were 0.75 ± 0.97 (attention), 1.17 ± 1.19 (executive function), 0.75 ± 1.22 (learning), 0.83 ± 0.84 (span), and 3.5 ± 3.4 for the sum score.

Such as in the previous experiment (chapter 2.6.3.), visual stimulation was performed with a full-field checkerboard. The resting condition consisted of a black screen. Each stimulation period lasted 18 s, known to elicit a maximal hemodynamic response (Panczel et al., 1999), and was preceded by a resting period of 17 s. Sixteen cycles were performed with a pause after eight cycles. Analysis in the frequency domain was performed as previously described (Schroeter et al., 2004b). Power spectral density was normalized for every subject to 1 (integral normalization) as proposed by Schroeter et al. (2004a). To exclude that additional medical diagnoses or medications biased our results, we re-analyzed data with medical diagnoses (hypertension, diabetes, hypercholesterolemia), and medications (angiotensin-converting enzyme inhibitors/angiotensin II receptor blockers, beta-adrenergic blockers, calcium channel blockers, statins) as covariates, because these factors might influence microcirculation (Bernardi et al., 1997; Harrison & Ohara, 1995; Levy et al., 2001; Meyer et

al., 2003; Scalia & Stalker, 2002; Stansberry et al., 1996). Cytochrome-c-oxidase as an intracellular enzyme was excluded from this analysis, as we did expect an impact on the vasculature only.

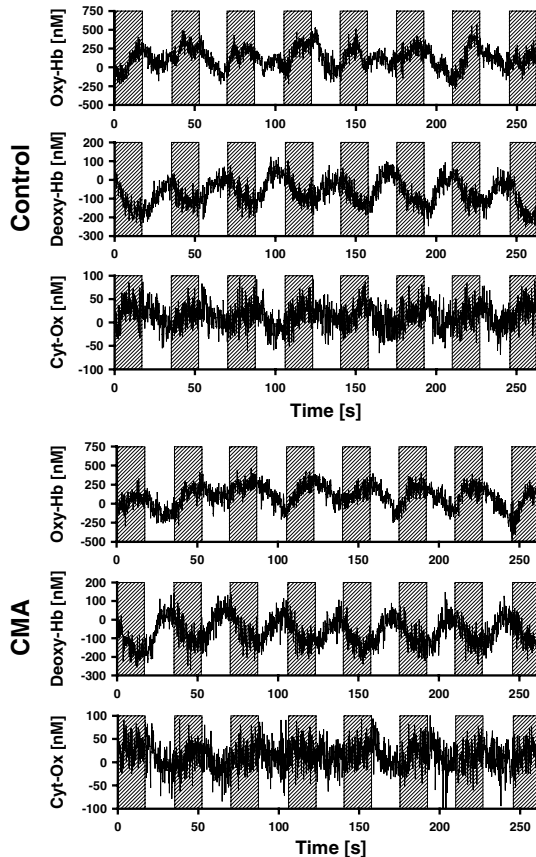


Figure 42 Concentration changes of oxy-, deoxy-hemoglobin (Hb) and the redox-state of the cytochrome-c-oxidase (Cyt-Ox) in the right visual cortex across controls and patients with cerebral microangiopathy (CMA) during the last eight blocks of stimulation with a checkerboard (marked by gray boxes).

The concentration of deoxyhemoglobin decreased, whereas the concentration of oxyhemoglobin and the redox state of cytochrome-c-oxidase increased in the visual cortex of patients and controls during stimulation with the checkerboard (Figure 42, 43) in agreement with previous fNIRS studies (Heekeren et al., 1999; Obrig et al., 2000b; Schroeter et al., 2004a, 2004b; Wobst et al., 2001; Wolf et al., 2002b). Hemodynamic responses due to visual stimulation did not significantly differ between patients and controls.

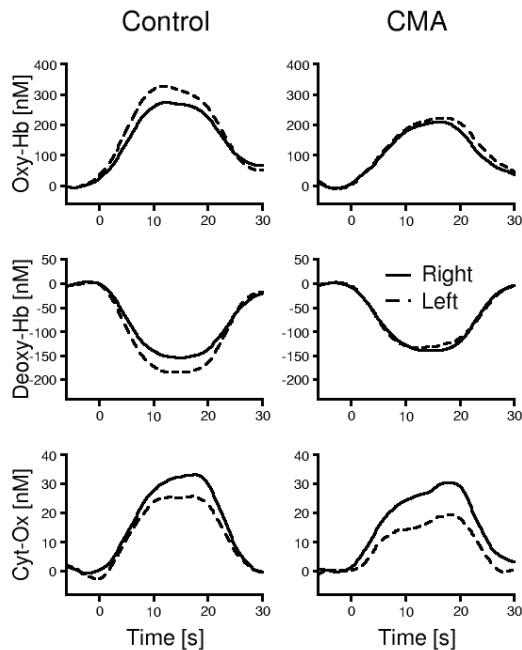


Figure 43 Epoch-related concentration changes of oxy-, deoxyhemoglobin (Hb) and the redox-state of the cytochrome-c-oxidase (Cyt-Ox) in the right and left visual cortex during stimulation with a checkerboard, averaged across all respective subjects. Stimulation lasted from 0 to 18 s. Running averages over 8 s.

When data were re-analyzed with diagnoses, and medications as covariates, angiotensin-converting enzyme inhibitors/angiotensin II receptor blockers significantly influenced concentration changes of oxy-, and deoxyhemoglobin. One might hypothesize a stronger vascular response in subjects receiving this medication than in drug-free subjects (Clozel et al., 1989; Levy et al., 2001), which was confirmed by post-hoc tests. If concentration changes elicited by visual stimulation were related to neuropsychological scores and the morphological MRI score, no significant results were obtained.

As illustrated in Figure 44, the peak for VLFOs at approximately 0.03 Hz was obtained for all parameters in patients and controls. Stimulation increased VLFOs of deoxyhemoglobin and cytochrome-c-oxidase significantly, because the stimulation cycle was contained in the VLFOs frequency range (Figure 45). For LFOs, peaks at around 0.09 Hz were found in controls for all parameters, whereas power spectral density declined continuously in the patient group with an increasing frequency and, therefore, no LFO peak was observed except for deoxyhemoglobin. As illustrated in Figures 44 and 45, power spectral density of VLFOs and LFOs was generally stronger for oxyhemoglobin, compared with deoxyhemoglobin, and cytochrome-c-oxidase.

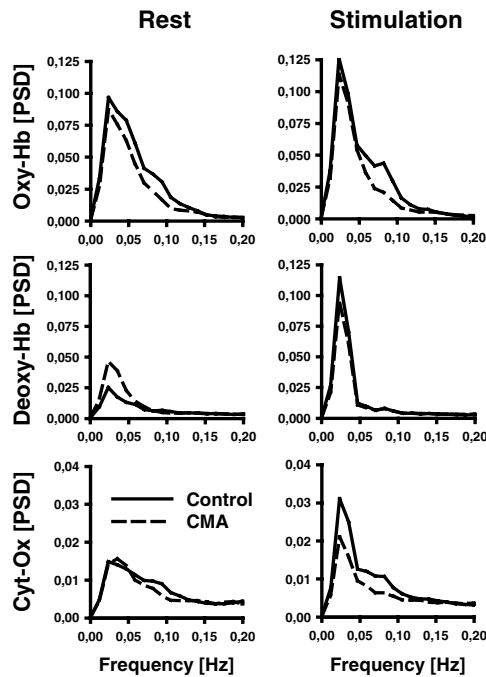


Figure 44 Normalized power spectral density (PSD) in comparison between patients with cerebral microangiopathy (CMA) and controls in the visual cortex during rest, and stimulation with a checkerboard. The frequency range includes spontaneous very low and low frequency oscillations, and the stimulation frequency. Hb hemoglobin, Cyt-Ox cytochrome-c-oxidase.

One might suppose that stimulation increases VLFOs, because the stimulation frequency was obviously contained in the VLFO band. As illustrated in Figure 45, post-hoc analysis revealed that, accordingly, VLFOs were significantly higher during stimulation than rest. There was a significant interaction between cerebral microangiopathy and stimulation for deoxyhemoglobin and a 'trend' for cytochrome-c-oxidase. Vascular reactivity is reduced in cerebral microangiopathy (Hund-Georgiadis et al., 2003; Terborg et al., 2000). Hence, with respect to interaction, one might expect a higher vascular reactivity and elevation of VLFOs due to stimulation in healthy controls compared with the patient group. This was indeed the case for deoxyhemoglobin, and cytochrome-c-oxidase.

Because LFOs decline with aging (Schroeter et al., 2004b), one may assume that cerebral microangiopathy leads to a further reduction. Analysis confirmed such an effect for the LFOs of oxyhemoglobin and cytochrome-c-oxidase (Figure 45). If the several medical diagnoses and medications were included in the analysis, the effect of cerebral microangiopathy disappeared. Rather, hypertension had a significant influence on LFOs of oxyhemoglobin. One may assume that LFOs are impaired by hypertension (Levy et al., 2001), which was confirmed by post hoc tests. For LFOs of deoxyhemoglobin, diabetes and statins had a

significant effect. One may assume that diabetes impairs LFOs of deoxyhemoglobin (Bernardi et al., 1997; Meyer et al., 2003; Stansberry et al., 1996), which was confirmed with post hoc tests. Although we hypothesized that statins increase LFOs of deoxyhemoglobin (Scalia & Stalker, 2002), post hoc tests revealed the opposite effect.

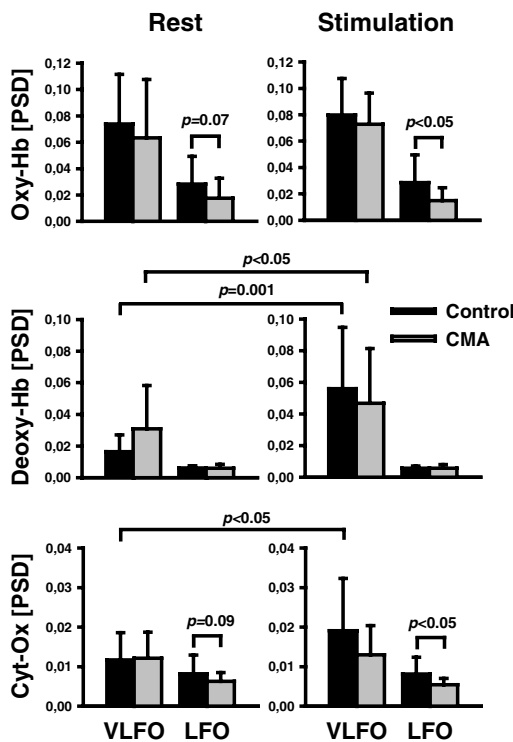


Figure 45 Normalized power spectral density (PSD) of low and very low frequency oscillations (LFO, VLFO) in the visual cortex during rest and visual stimulation in patients with cerebral microangiopathy (CMA) and controls. 1-tailed paired (rest vs. stimulation) and unpaired (patients vs. controls) Student's t-test.

A correlation analysis was performed relating results of the spectral analysis to the severity of cerebral microangiopathy and neuropsychological deficits. We hypothesized a negative correlation between power spectral analysis of the several hemodynamic parameters and the severity of cerebral microangiopathy as scored in MRI scans, which was confirmed only for VLFOs of oxyhemoglobin during stimulation, and VLFOs of cytochrome-c-oxidase during rest. There was no significant correlation between neuropsychological deficits and severity of cerebral microangiopathy as scored in MRI scans. Further, we supposed that neuropsychological deficits are negatively correlated with vascular reactivity, and hence, the difference of VLFOs between stimulation and rest. Indeed, mainly the subscores for executive dysfunction, learning, span, and the sum-score predicted the increase in the power spectral density due to stimulation for oxy- and deoxyhemoglobin. For LFOs, cerebral

microangiopathy impaired power spectral densities. Accordingly, one might suppose that neuropsychological deficits are negatively correlated with the LFOs of the several hemodynamic parameters, which was proved for executive dysfunction with deoxyhemoglobin during rest and stimulation, and for learning deficits with deoxyhemoglobin during rest.

Most strikingly, our results demonstrate that spontaneous slow hemodynamic oscillations are impaired in the cerebral microvasculature of patients with cerebral microangiopathy during both, stimulation and rest. These results agree with Bätzner et al. (1995) who reported generally reduced spontaneous low frequency oscillations in cerebral microangiopathy as assessed with transcranial Doppler monitoring. If additional diagnoses and medications were taken into account, the difference was related solely to arterial hypertension. Hence, data suggest that arterial hypertension decreases LFOs of oxyhemoglobin. Interestingly, the LFO range corresponds well with the spontaneous activity recorded in microvascular smooth muscle cells (Golenhofen, 1970). Meyer et al. (1988) and Schmidt et al. (1992) concluded that this myogenic pacemaker mechanism causes vasomotion in terminal arterioles, and regulates capillary perfusion (Harrison et al., 2002). Cerebral microangiopathy is related to loss of smooth muscle cells, and increased vessel stiffness (Caplan, 1995; Roman et al., 2002; Tanoi et al., 2000). Arterial hypertension, one risk factor of cerebral microangiopathy, also alters the structure and function of the microvasculature (Levy et al., 2001). It increases the wall-to-lumen ratio in precapillary resistance vessels, may enhance vasoconstriction and may impair vasodilator responses. Another mechanism, rarefaction of arterioles or capillaries, seems to be negligible in cerebral microvasculature. In summary, reduction of LFOs of oxyhemoglobin as observed in our study may indicate structural and functional alterations in the cerebral microvasculature in cerebral microangiopathy, mainly due to arterial hypertension. We detected significant effects of cerebral microangiopathy, and arterial hypertension on LFOs of oxyhemoglobin only, whereas LFOs of deoxyhemoglobin were unaltered. Oxyhemoglobin is mainly related to the arterial compartment whereas deoxyhemoglobin has to be attributed mainly to the venous part. As hypertension alters specifically precapillary resistance vessels (Levy et al., 2001), this compartment effect may obviously explain the different results for both chromophores.

Interestingly, our study indicates that antihypertensive drugs, namely angiotensin-converting enzyme inhibitors/angiotensin II receptor blockers, may improve the vascular response during functional stimulation. These results fit very well with literature reports. Brain microvessels contain components of the renin-angiotensin system (Brecher et al., 1978; Bunnemann et al., 1992) that is overactive in hypertension (Unger et al., 1988). Several

recent studies (reviewed in Levy et al., 2001) showed that angiotensin-converting enzyme inhibition or angiotensin II receptor blockers can reduce the media-to-lumen ratio of resistance vessels, and, hence, reverse the alterations due to hypertension. These drug effects on microvessel structure were even independent of the lowering of arterial blood pressure and of the renin-angiotensin system, which might explain the dissociation of the factors arterial hypertension and antihypertensive drugs in our study. Moreover, Clozel et al. (1989) demonstrated that angiotensin-converting enzyme inhibitors normalize the vascular reserve that is severely reduced in hypertension.

Our study additionally showed, that stimulation increases VLFOs of deoxyhemoglobin more in healthy controls than in the patient group. As the stimulation frequency is obtained in the VLFO range, data indicate that vascular reactivity as elicited by functional stimulation is reduced in cerebral microangiopathy in accordance with literature reports (Hund-Georgiadis et al., 2003; Roman et al., 2002; Terborg et al., 2000). A direct effect of cerebral microangiopathy, additional medical diagnoses, or drugs on proper VLFOs is unlikely, because the analysis revealed no significant effects of diagnosis on VLFOs, and no influences of the several covariates. Generally, slow vasomotions (VLFOs) occur in larger vessels that are rich in neurogenic innervation, whereas fast vasomotions (LFOs) originate from terminal arterioles, where neurogenic innervation is negligible (Farkas & Luiten, 2001; Intaglietta, 1990; Kvandal et al., 2003; Kvernmo et al., 1998; Ursino, 1991). Thus, our data indicate that neurogenic autoregulation is almost unaltered by cerebral microangiopathy, the additional medical diagnoses, and drugs.

Beside the aforementioned direct impairments in patients with cerebral microangiopathy, our study demonstrates impacts of diabetes and statins on the cerebral microvasculature. LFOs of deoxyhemoglobin are reduced in diabetes, and by statins. Interestingly, vasomotion at 0.1 Hz is reduced in patients suffering from diabetes, which was shown by laser Doppler flowmetry in microvessels of the finger (Meyer et al., 2003; Stansberry et al., 1996) and forearm skin microcirculation (Bernardi et al., 1997). Reduction in LFOs may be explained by thickening of the basement membrane, endothelial dysfunction, and, consequently loss of normal autoregulatory function in diabetes (Pallas & Larson, 1996). Data suggest that fNIRS may be applied to diagnose cerebral microvascular changes due to diabetes.

Unexpectedly, statins reduced LFOs of deoxyhemoglobin in our study, without any effect of hypercholesterolemia. Recent studies suggest that the vasoprotective effects of statins are, at least partially, independent of its cholesterol lowering actions (Scalia & Stalker, 2002). Statins exert additionally anti-inflammatory and immunomodulatory effects, and modulate

vascular remodeling even under normocholesterolemic conditions. Sterzer et al. (2001) showed that statins increase vasoreactivity as elicited by acetazolamide in subcortical small-vessel disease, which seems to contradict our results. However, they applied transcranial Doppler sonography to the middle cerebral artery, and examined consequently the macrovasculature. Together with our results one may assume that statins induce opposite changes in the micro- and macrovasculature. This compartment effect might also explain why we did not detect any effects of hypercholesterolemia, as it induces arteriosclerosis only in the macrovasculature (Harrison & Ohara, 1995). Significant effects of diabetes and statins were detected only for LFOs of deoxyhemoglobin leading to the assumption that they are related mainly to the venous compartment (see above).

Remarkably, impairments of LFOs and vascular reactivity in cerebral microangiopathy were tightly correlated with neuropsychological deficits in our study, in contrast to morphological severity of cerebral microangiopathy. The highest correlation coefficients were found for executive functions, which are known to be particularly impaired in cerebral microangiopathy (McPherson & Cummings, 1996; Roman et al., 2002). These results are in agreement with Hund-Georgiadis et al. (2002), who reported that morphological changes were not related to neuropsychological impairment in cerebral microangiopathy. Further, Sabri et al. (1998, 1999) showed that, in cerebral microangiopathy, neuropsychological deficits correlate with functional imaging parameters such as rCBF and glucose utilization during rest, but not with lacunar infarctions and deep white matter lesions. One may conclude that the latter ones are epiphenomena that may morphologically characterize cerebral microangiopathy but do not themselves indicate cognitive impairment. Dementia or neuropsychological deficits are reflected exclusively by functional imaging parameters that may be used for early diagnosis.

Summarizing results, the study shows that spontaneous low frequency oscillations, and vascular reactivity decrease in cerebral microangiopathy. Particularly, LFOs are impaired in contrast to VLFOs, which remain unaltered. Hence, cerebral microangiopathy accelerates microvascular changes due to aging and leads to impairment of autoregulation. Alterations have to be attributed mainly to arterial hypertension, and may be, at least partly, reversed by medical treatment such as angiotensin-converting enzyme inhibitors/angiotensin II receptor blockers. Results indicate that spectral analysis is much more sensitive to changes in the microvasculature due to aging or cerebral microangiopathy compared with time line analysis of the functional hemodynamic response, and, enables therefore an earlier detection of such alterations.

2.8. Towards Standard Analyses for Functional Near-Infrared Imaging

As discussed in the Introduction section and confirmed by the aforementioned experiments, fNIRS has several advantages in comparison with other imaging methods (Obrig et al., 2000b; Obrig & Villringer, 2003; Strangman et al., 2002a; Villringer & Chance, 1997). Namely, it is characterized by high flexibility, portability, low cost, biochemical specificity and easy application to patients and children. Therefore, it is useful to further establish fNIRS as a method for functional imaging. Almost all former fNIRS studies reported concentration changes of the chromophores, or used time line analysis approaches (Obrig & Villringer, 2003). For calculation they had to assume specific differential pathlength factors, which are highly variable (Essenpreis et al., 1993; Duncan et al., 1996; Zhao et al., 2002). In the last experiment (Schroeter et al., 2004a), we aimed at introducing a new standard tool to analyze fNIRS data that is almost independent of the assumed differential pathlength factors. fNIRS examines the hemodynamic response during brain activation like fMRI. Hence, we applied the general linear model, which is well established for fMRI data (Winer et al., 1991; Friston, 1994; Friston et al., 1995a, 1995b; Worsley & Friston, 1995).

In comparison to other imaging methods, optical approaches have an excellent temporal resolution (Pouratian et al., 2003; Villringer & Chance, 1997) that enables analysis in the frequency domain. Former fNIRS studies investigated spontaneous oscillations in cerebral oxygenation, differences of spectral power and phase between the several chromophores, and influences of functional stimulation and hypercapnia (Elwell et al., 1999; Obrig et al., 2000a; Taga et al., 2000). However, such spectral approaches have not yet been applied to spatially resolved optical imaging. Functional connectivities have been investigated by estimation of spectral parameters in several fMRI studies (Cordes et al. 2002; Müller et al., 2001, 2003). Sample coherence as a correlation coefficient in the frequency domain indicates whether two brain regions are activated with the same frequency. The hemodynamic response might be shifted temporally between the two regions. Accordingly, the phase shift represents the temporal displacement of the hemodynamic responses. Analysis results in maps, which give detailed information on brain regions belonging to a network structure. In addition they reveal the temporal behavior of the hemodynamic response. Such an approach was applied for visual stimulation by Müller et al. (2001, 2003) showing high coherence values and a delay of the BOLD signal for V5 compared to V1 during visual stimulation with moving colored stimuli. Since a few years spatially resolved optical imaging has been available (Obrig & Villringer, 2003). Hence, it might be challenging to explore the potential of spectral analysis for these imaging data.

In summary, the present study aimed at answering two questions. (i) Is it possible to apply the general linear model for analysis of optical imaging data? (ii) Can spectral analysis be employed to spatially distinguish between activated brain regions and to characterize the temporal behavior of the hemodynamic response? To investigate these questions, we used two visual tasks. We hypothesized that stimulation with a checkerboard activates the visual cortex (V1-V3), whereas stimulation with rotating 'L's additionally involves the motion area V5, which is more laterally located at the meeting point of the lateral occipital sulcus and the ascending limb of the inferior temporal sulcus (Bundo et al., 2000; Zeki et al., 1991; Zeki, 2003).

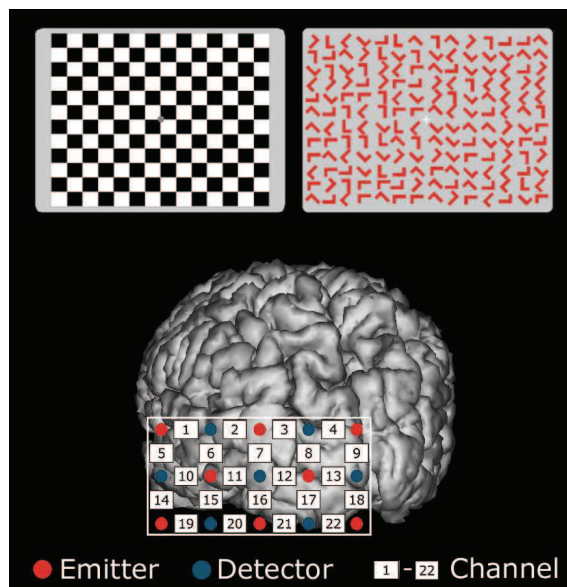


Figure 46 Location of the optode grid on the left back of the subject's head. The detector between channels 9/18 was placed exactly 10 % of the nasion-inion distance above the inion, in the midline of the subject's head. Thus, brain activation was measured in the left visual cortex. Further, both paradigms for visual stimulation are shown (checkerboard on the left, rotating 'L's on the right side).

A checkerboard paradigm (stimulation 18 s/rest 17 s), and an array of rotating red L-shapes (stimulation 18 s/rest 42 s) were used for stimulation (Figure 46). Changes in the concentration of oxy-, deoxy- and total hemoglobin were measured by an ETG-100 system (Hitachi Medical Corporation, Tokyo, Japan). Values were calculated according to Cope & Delpy (1988) as described in detail in Uludag et al. (2002), applying wavelength dependent differential pathlength factors (Essenpreis et al., 1993) and the spectra of the chromophores as reported by Wray et al. (1988). A sampling frequency of 10 Hz, and an emitter-detector spacing of 3 cm was applied. 22 channels were simultaneously measured at the left back of the subject's head covering an area of 12 x 6 cm (Figure 46). Hence, brain activation could

be measured in the occipitotemporal cortex and included the left visual cortex (V1-V3; corresponding to position O1 of the international 10/20 system) and brain regions processing moving stimuli (V5) (Homan et al., 1987; Steinmetz et al., 1989; Zeki, 2003).

Data processing was performed using the software package LIPSIA (Lohmann et al., 2001). A temporal highpass filter was used for baseline correction of the signal. The statistical evaluation was based on a least-squares estimation using the general linear model for serially autocorrelated observations (Friston, 1994; Friston et al., 1995a, 1995b; Worsley & Friston, 1995). The design matrix was generated with a box-car function. The model equation, including the observation data, the design matrix and the error term, was convolved with a Gaussian kernel of dispersion of 4 s full-width half-maximum. Hence, the function modeled the post-stimulus behavior of the hemodynamic response. The model includes an estimate of temporal autocorrelation. The effective degrees of freedom were estimated as described in Worsley & Friston (1995), and Seber (1977). Thereafter, visual stimulation was contrasted against the baseline condition (blank screen). For each subject, three contrast images (zmaps) were generated representing the different parameters (oxy-, deoxy-, and total hemoglobin). A group analysis based on the individual contrast images was performed for both paradigms separately. It consisted of a one-sample t-test across the contrast images of all subjects that indicated whether the observed difference between visual stimulation and baseline was significantly distinct from zero (Holmes & Friston, 1998). Finally, brain activation was compared between stimulation with the rotating 'L's and the checkerboard in a second-level analysis (paired t-test across the two contrast images of all subjects). The resulting zmaps were overlaid onto an anatomical reference image that was processed according to Schroeter et al. (2002b). Individual zmaps were generally not spatially normalized before averaging, because anatomical variability was regarded as minor compared with the spatial resolution of 3 cm.

Stimulation with the checkerboard paradigm: Spectral analysis was performed according to Müller et al. (2001, 2003). First, the center of activation was determined by analyzing the individual zmap of the deoxyhemoglobin matrix because changes of deoxyhemoglobin are most specific for brain activation (Obrig et al., 2000b; Schroeter et al., 2002b; Wobst et al., 2001). The pixel with the most negative z-value (see above) was defined as the activated pixel as concentration of deoxyhemoglobin decreases during activation (Villringer & Chance, 1997). Coherence and phase were analyzed for the stimulation frequency in relation to the activated pixel. The pixel with the lowest coherence to the activated pixel was defined as non-activated pixel. Generally, pixels were regarded coherent only if their coherence value exceeded 50 % (Obrig et al., 2000a). Accordingly, phase values were calculated for these

pixels only. Because the procedure described above leads to a coherence of 100 % and a phase delay of 0 s for the reference pixel, the phase differences represent the phase delay with respect to the reference pixel. Further, maps of power spectral density were calculated for the stimulation frequency. Power spectral density was normalized to 1 for every pixel and subject. Finally, resulting individual maps for coherence, phase, and power spectral density were averaged across subjects.

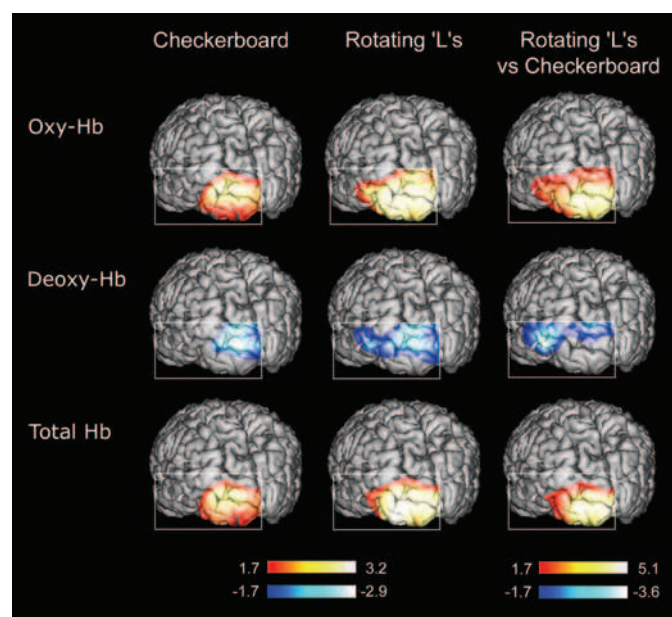


Figure 47 Averaged zmaps for visual stimulation overlaid onto an anatomical reference image: Stimulation vs. baseline during the checkerboard and rotating 'L's paradigm, and contrast between both paradigms. Zmaps are shown for oxy-, deoxy-, and total hemoglobin (Hb). Note that anatomical localization is not exact, and that scales are different. Z-values were thresholded at $z=1.7$, which corresponds to an alpha-level of 0.05.

Stimulation with the rotating 'L's paradigm: As for stimulation with the checkerboard, centers of activation were determined by analyzing the individual zmap of the deoxyhemoglobin matrix. Two pixels with highly negative z-values could be detected in almost all individual deoxyhemoglobin zmaps. The medial activated pixel was mostly colocalized with the individual minimal z-value during stimulation with the checkerboard. The second activated pixel was found laterally. Individual and averaged coherence and phase maps were

generated in relation to the medial activated pixel (deoxyhemoglobin) for the stimulation frequency. Further, individual and averaged maps of power spectral density were calculated for the same frequency after normalization to 1 for every pixel and subject.

A time line analysis was performed to validate results as obtained with the general linear model. For stimulation with the checkerboard, concentration changes of the parameters were analyzed in the activated and non-activated pixel as defined by the highest and lowest coherence with regard to the stimulation frequency. For stimulation with the rotating 'L's, concentration changes of the parameters were calculated for both, the medial and lateral activated pixels.

The analysis with the general linear model revealed positive z-values for oxy-, total hemoglobin, and negative z-values for deoxyhemoglobin, when visual stimulation during both paradigms was contrasted against the baseline condition (no stimulation) as a reference (Figure 47). The maximal hemodynamic response (deoxy-, total hemoglobin) was found in channel 13 during the checkerboard paradigm. The maximal hemodynamic response of oxyhemoglobin extended over channel 12 and 13. As illustrated in Figure 48, oxy-, and total hemoglobin increased, whereas deoxyhemoglobin decreased significantly in the pixel with the lowest z-value in the deoxyhemoglobin zmap during stimulation with the checkerboard. No significant concentration changes of the parameters were observed in the pixel with the lowest coherence with respect to the z-minimum of deoxyhemoglobin ('non-activated pixel'; Figure 48). Our results agree with recent fNIRS studies investigating the hemodynamic response during visual stimulation (Obrig et al., 2000a, 2000b; Wobst et al., 2001; Wolf et al., 2002b). It may be concluded that stimulation with the checkerboard activated specifically the visual cortex (presumably V1-V3) as channel 12 and 13 enclose position O1 of the international 10/20 system (Homan et al., 1987; Steinmetz et al., 1989).

Stimulation with the rotating 'L's additionally involves movement and color in comparison with the checkerboard paradigm. Thus, we hypothesized that activation maxima may shift laterally towards the occipitotemporal boundary zone, where the motion area V5 is localized (Bundo et al., 2000; Zeki et al., 1991; Zeki, 2003). The color area V4 might not be detected by fNIRS because it is localized ventromedially and depth penetration of fNIRS is limited (Germon et al., 1999). The z-maxima of oxy-, and total hemoglobin shifted slightly (Figure 47). For deoxyhemoglobin, two z-minima were obtained. One medial at the same channel as in the checkerboard paradigm (channel 13), the second laterally (channel 11). Generally, brain activation spread over a larger and particularly more laterally extending area than during stimulation with the checkerboard. Time line analysis was performed in the individually

determined medial and lateral minima of the deoxyhemoglobin zmap (Figure 48). A hemodynamic response occurred in both pixels during visual stimulation with a significant increase of oxy-, total hemoglobin, and decrease of deoxyhemoglobin, although it was lower in the lateral compared with the medial pixel. Interestingly, we found a post-stimulus undershoot of oxyhemoglobin, and an overshoot of deoxyhemoglobin for the second paradigm in accordance with previous fNIRS studies (Jasdzewski et al., 2003; Lindauer et al., 2001). Hence, the post-stimulus period should be modeled with the design function for fNIRS data like for fMRI data evaluation. The first paradigm did not show such a post-stimulus response, presumably because the intertrial interval was too short. The second-level analysis revealed that deoxyhemoglobin decreased more during the rotating 'L's than the checkerboard paradigm (Figure 47). For oxy-, and total hemoglobin, a higher activation was found as well during the rotating 'L's compared with the checkerboard paradigm.

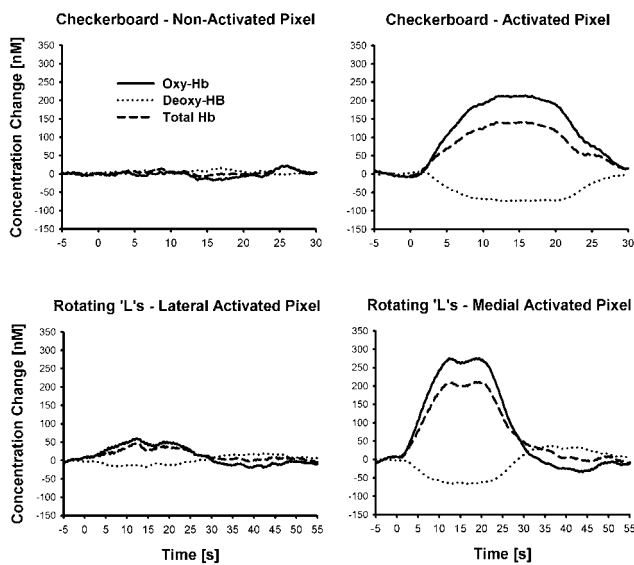


Figure 48 Changes in the concentration of oxy-, deoxy-, and total hemoglobin (Hb) during visual stimulation with a checkerboard and with the rotating 'L's. Stimulation lasted from 0 s to 18 s. Running averages over 2 s. Note that intertrial intervals were different for stimulation with the checkerboard (35 s) and rotating 'L's (60 s).

In summary, data analysis confirmed the hypothesis that a larger and particularly laterally extending brain area was activated during stimulation with moving colored stimuli. Zmaps of deoxyhemoglobin revealed two separated activation foci during stimulation with the rotating 'L's. The second-level analysis showed moreover a clearly higher brain activation in the occipitotemporal boundary zone during the rotating 'L's than during the checkerboard stimulation for that chromophore. Hence, fNIRS detected a second lateral activated brain region additionally to the primary and secondary visual cortex representing most probably the

motion area V5 (Bundo et al., 2000; Zeki et al., 1991; Zeki, 2003). Further, the hemodynamic response spread more dorsally from V1/2 as shown in the second-level analysis of deoxyhemoglobin, which might indicate additional activation in motion selective area V3A (Tootell et al., 1997; Zeki, 2003).

We believe that the analysis with the general linear model as performed in our study has a high impact for future fNIRS studies. Former imaging studies with fNIRS reported concentration changes of the chromophores, or used time line analysis approaches such as comparisons of concentration changes between conditions or to baseline (Obrig & Villringer, 2003). One group used correlation analysis with a hemodynamic response function to estimate concentration changes of the chromophores (Noguchi et al., 2002; Sato et al., 1999). Further, a previous functional optical imaging study in the rat introduced the general linear model to time line analysis (Berwick et al., 2002). We recently suggested (Schroeter et al., 2003) that fNIRS studies involving subjects of different age, or neuropsychiatric patients should be analyzed with statistical approaches that are almost independent of the assumed differential pathlength factors. We proposed to calculate effect sizes. Interestingly, as discussed in chapter 2.6.2., the differential pathlength factor does not only depend upon age and may vary between healthy and diseased populations (Duncan et al., 1996). It has moreover a high intra- (Zhao et al., 2002) and inter-subject variation (Essenpreis et al., 1993). Hence, one may generally criticize optical imaging studies because the assumed differential pathlength factor may vary intra-individually between the several pixels and inter-individually between subjects even of the same age. Imaging studies based on concentration changes are almost impossible with the commercially available imaging instruments, because differential pathlength factors are not measured for each pixel separately. Further, if concentration changes of the chromophores are calculated with the total differential pathlength factor, their magnitude is generally underestimated because the activated volume is smaller than the sampling volume, which is referred to as partial volume effect (Kohri et al., 2002; Uludag et al., 2002).

Thus, we propose extending approaches that are almost independent of differential pathlength factors¹ to all optical imaging studies. Analysis of fNIRS data with the general

¹ It has to be mentioned that the proposed approaches (effect sizes and the general linear model) do not correct for the wavelength dependence of the differential pathlength factor (Essenpreis et al., 1993; Kohl et al., 1998; Zhao et al., 2002). Although there is a considerable spread in absolute inter-individual magnitudes, the differential pathlength factor displays an extremely similar wavelength dependence in different subjects. Hence, the error is maximally 2 % (Essenpreis et al., 1993). Further, partial volume effects might differ between the several optode positions (Strangman et al., 2003), which is also not corrected for. This point has to be kept in mind particularly for optical studies comparing brain activation in widely separated brain regions. Both factors may lead to different signal-to-noise ratios at the several optode positions.

linear model enables such a statistics (Friston, 1994; Friston et al., 1995a, 1995b; Worsley & Friston, 1995). Firstly, correlation analysis as performed by comparing time lines with the modeled hemodynamic response function does not depend on absolute values. Further, statistics are calculated for every pixel separately, thereby the differential pathlength factors, which can be assumed constant over the time of the experiment in the respective pixel, does not influence the statistical map. Because of these crucial advantages we propose the general linear model (Winer et al., 1991) as implemented in several statistical programs (AFNI: Cox, 1996; FMRIB: Jezzard et al., 2001; LIPSIA: Lohmann et al., 2001; SPM-99: Wellcome Dept. of Cognitive Neurology, London, UK) as one possible standard statistical approach beside effect sizes to analyze functional optical imaging data.

Analysis with the general linear model is particularly feasible for deoxyhemoglobin. Its changes add linearly at least down to a stimulus duration of 6 s in contrast to oxy-/total hemoglobin and may be modeled as a linear transform system (Wobst et al., 2001). Second, it is highly correlated with the BOLD signal (Buxton et al., 1998; Mehagnoul-Schipper et al., 2002) in a linear manner (Chen et al., 2003; Punwani et al., 1998). However, one simultaneous fMRI/fNIRS study reported a higher correlation of the BOLD signal with oxy- than deoxyhemoglobin, presumably due to a higher contrast-to-noise ratio of oxyhemoglobin (Strangman et al., 2002b). Further, deoxyhemoglobin shows an inverse behavior compared with the BOLD signal, including the post-stimulus period (Jasdzewski et al., 2003; Lindauer et al., 2001, 2003). Hence, the same impulse response functions might be applied to deoxyhemoglobin as it was particularly shown for a modified Gamma function (Wobst et al., 2001). Our results support the assumptions that the general linear model is feasible especially for deoxyhemoglobin, and that its changes are most accurately related to brain activation as shown by previous fNIRS studies (Kleinschmidt et al., 1996; Obrig et al., 2000b; Schroeter et al., 2002b; Wobst et al., 2001). The activated area as revealed by deoxyhemoglobin was most focused compared with the other parameters in both paradigms. Further, two activation foci could be distinguished in a paradigm with moving colored stimuli for that chromophore. Finally, the second-level analysis detected the activation focus in the presumed motion area V5 solely for deoxyhemoglobin.

In the second part, we explored whether spatially resolved analysis in the frequency domain can be applied to optical imaging data. As discussed above, approaches that are independent of the differential pathlength factor have to be preferred for fNIRS data. Accordingly, we normalized power spectral density and applied coherence analysis that is per se independent of absolute values and, consequently, almost independent of the assumed differential pathlength factors. The power spectral density maps of

deoxyhemoglobin for the respective stimulation frequency revealed focal maxima (Figure 49). Stimulation with the checkerboard showed one maximum. Two clearly separated foci were detected during stimulation with the rotating 'L's paradigm. Coherence values were highest for the channel over the primary visual cortex (13) in both paradigms. For the rotating 'L's paradigm the area with high coherence values spread over a larger area and more laterally than during stimulation with the checkerboard. However, the coherence map did not exhibit two separated coherence peaks, rather a plateau sloping at the edges. Phase maps demonstrated laterally a phase delay of deoxyhemoglobin for stimulation with the rotating 'L's, whereas no spatial differences were found for phase during the checkerboard paradigm.

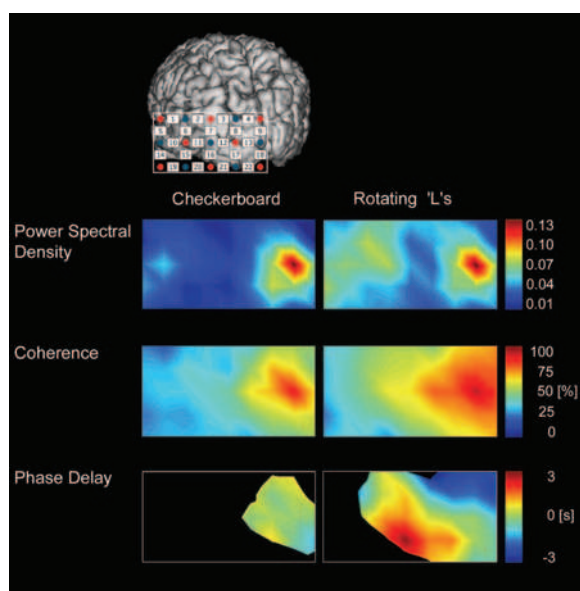


Figure 49 Averaged power spectral density-, coherence-, and phase-maps for visual stimulation with the checkerboard and rotating 'L's paradigm. Analysis was performed for the respective stimulation frequency in concentration changes of deoxyhemoglobin. Power spectral density was normalized to 1 for every subject and channel before averaging across subjects. Coherence and phase delay were calculated in relation to the medial activation focus. Phase delay is shown for a coherence above 50 % only.

In summary, our results indicate that the spectral analysis detected the same functional network like the zmaps. Spatial resolution is defined by the potential to distinguish separated activation foci. Accordingly, zmaps and power spectral density maps of deoxyhemoglobin revealed two activation foci during stimulation with the rotating 'L's. Thus, spatial resolution was higher for these approaches compared with coherence analysis, presumably because artifacts in the reference pixel might have confounded coherence values for the other pixels. Phase maps indicate that concentration of deoxyhemoglobin changed later in the lateral activated pixels compared with the medial ones. Although it is known that the latency of the hemodynamic response may vary between areas, we assume that different latencies in

visual areas reflect the underlying network structure. These results fit well with a fMRI study applying the same paradigm (Müller et al., 2001) that reported high coherence values and a delay of the BOLD signal for V5 compared to V1. Visual paradigms as applied in our study differed concerning the ratio between length of stimulation and baseline. Stimulation and baseline had the same duration during the checkerboard paradigm, whereas baseline was longer than stimulation for the rotating 'L's paradigm. Thus, data indicate that spectral analysis might be employed to paradigms where stimulation and baseline period have unequal length in agreement with fMRI studies (Müller et al., 2003).

By analyzing two visual paradigms the present study shows that the general linear model and spatially resolved spectral analysis can be used as standard statistical approaches for optical imaging data, particularly because they are almost independent of the assumed differential pathlength factors. The method can now be used to explore an entire new range of cognitive neuroscience paradigms and questions.

3. Embedding Optical Imaging into Cognitive Neuroscience

3.1. Previous Optical Studies in Cognitive Neuroscience

The chapter aims at placing our experiments into the field of other studies reported in the literature. First of all, we answered all questions that had been raised in chapter 2.1. Hence, we contributed important issues to establishing optical approaches in cognitive neuroscience. The first (multimodal imaging) experiment outlined a framework to understand neurovascular coupling. Further, it revealed that optical imaging is sensitive to cortical areas. The following studies showed that optical imaging can be used for cognitive experiments with event-related designs, and that randomized designs with short intertrial intervals are advantageous. Thereafter, we demonstrated that optical imaging is easily applicable in studies with children, elderly people, and patients. The last of our experiments yielded standard analyses for optical imaging.

To review previous optical cognitive studies by other groups we conducted a search in Medline and Current Contents with the following strategy: ((near and infrared) or optical) and brain and (language or cognition or cognitive or attention or memory or executive). The search was limited to the period from 1990 to February 2005 as no studies were reported before 1990. Studies investigating primary cortices were excluded, as we were interested in cognitive studies only. Further, we searched for fNIRS studies investigating brain function generally (search strategy: ((near and infrared and spectroscopy) or (diffuse and optical and imaging)) and (brain or cerebral); Medline, time period 1990-2004). Results of the search are presented in Figure 50, and Tables 1-6. Obviously, the number of optical studies increased over time. In 2004, 103 "general brain studies" were published, 17 of them were concerned with cognitive processes.

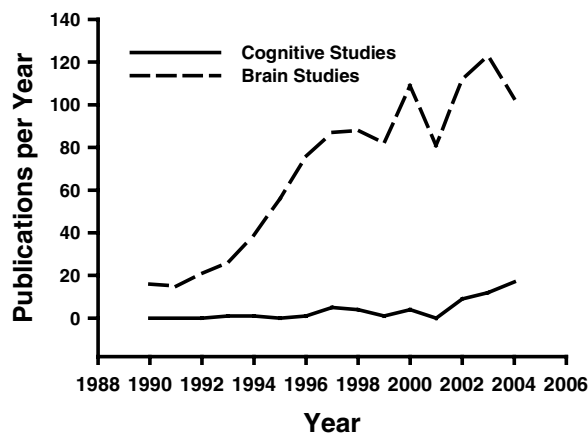


Figure 50 Optical studies investigating cognition or the brain generally, published between 1990 and 2004 (results of a search in Medline and Current Contents).

Table 1 Executive Functions

Author	Paradigm	Subjects	Oxy-Hb	Deoxy-Hb	Analysis	System (channels)	Region
Fallgatter & Strik 1998*	Wisconsin card sorting test; block design	10 adults	increase	no change	ANOVA	CritikonTM 2020 (2)	Fp1/F3 and Fp2/F4 frontal
Hoshi et al. 2000	backward digit span task; block design	8 adults	increase	not reported	t-test	64 channel system	
Schroeter et al. 2002b	Stroop task; event-related; ITI 12 s	14 adults	increase; interference significant in prefrontal cortex	decrease; interference significant in prefrontal cortex	ANOVA, t-test, correlation; fitting of a Gaussian function	NIRO-300 (6x2)	frontoparietal (10/20 system)
Herrmann et al. 2003b*	verbal-fluency task; block design	14 adults	increase	decrease	ANOVA	NIRO-300 (2)	frontal (between Fp1/2, F3/4 and F7/8)
Hoshi et al. 2003	n-back task, random generation task; block design	12 adults	increase	not reported	t-test	OMM-2000 Shimadzu (20)	prefrontal
Nioka & Sasaki 2003	Stroop task, influence of caffeine; block design	10 adults	increase; caffeine decreased oxy-Hb	decrease	ANOVA, t-test, correlation	HEO-200 (1)	left prefrontal cortex
Schroeter et al. 2003	Stroop task; event-related; ITI 12 s	14 young, and 14 elderly adults	increase; interference significant in prefrontal cortex; total Hb and Hb difference reduced with aging	decrease; interference significant in prefrontal cortex	ANOVA, t-test, correlation, effect size	NIRO-300 (5x2)	frontoparietal (10/20 system)
Watanabe et al. 2003	design fluency task, verbal fluency task; block design	10 adults	increase	no change	ANOVA, t-test	Hitachi ETG-100 (24)	frontal
Kameyama et al. 2004	word fluency task; block design	39 adults	increases larger in males than females, and in young than in middle-aged	not reported	ANOVA	Hitachi ETG-100 (48)	frontotemporal (10/20 system)
Schroeter et al. 2004c	Stroop task; event-related; randomized ITI 2, 4, 6, 12 s	17 adults	increase; amplitude decreased with 2 s ITI	decrease; interference effect increased with shorter ITI	ANOVA, t-test, correlation	NIRO-300 (2)	frontal (F3/4)

Hb hemoglobin; ITI intertrial interval; * statistics insufficient, i. e. due to no post-hoc tests, comparison of absolute values and not relative changes, or correlation coefficients without significance (p -) values.

Table 2 Language

Author	Paradigm	Subjects	Oxy-Hb	Deoxy-Hb	Analysis	System (channels)	Region
Fallgatter et al. 1998*	reading task; block design	10 adults	no change	increase	ANOVA	CritikonTM 2020 (2)	Fp1/F3 and Fp2/F4
Sato et al. 1999	speech recognition; block design	7 adults	increase in left superior temporal cortex	decrease in left superior temporal cortex	after baseline correction correlation with box car function; r-maps; ANOVA, Fisher's PLSD	Hitachi ETG-100 (44)	temporo-frontoparietal
Kennan et al. 2002b	language task (judgment of sentence accuracy); block design	6 adults	increase in total Hb particularly on left side			Hitachi ETG-100 (48)	frontolateral
Minagawa-Kawai et al. 2002	short and long vowel categories; block design	9 adults	increase of total Hb; oxy- and deoxy-Hb not reported		ANOVA, Fisher's PLSD	Hitachi ETG-100 (24)	bitemporoparietofrontal; controlled by MRI
Noguchi et al. 2002	syntactic and semantic decision task; event-related design; randomized ITI 20-28 s	8 adults	increase particularly during the syntactic decision task	not significant	after baseline correction correlation with basis function; r-maps; ANOVA	Hitachi ETG-100 (44)	temporo-frontoparietal
Quaresima et al. 2002*	translation and language switching; block design	8 adults	increase	decrease	ANOVA	Oxymon (12)	left lateral frontal lobe (10/20 system)
Cannestra et al. 2003	covert visual object naming task (Boston naming test); block design	8 adults	increase	decrease, more localized than oxy-Hb	t-test	full spectrum system (2)	precentral and inferior frontal gyrus; controlled by MRI
Horovitz & Gore 2004*	semantic processing task; event-related; ITI not specified	6 adults	increase of total Hb in Broca's and Wernicke's area; correlation with ERPs (N400)		correlation with design (gamma) function	Hitachi ETG-100 (24)	left frontotemporal
Minagawa-Kawai et al. 2004	short and long vowel contrast, phonemic contrast; block design	7 adults	increase of total Hb; oxy- and deoxy-Hb not reported		ANOVA, Fisher's PLSD	Hitachi ETG-100 (24)	bitemporoparietofrontal; controlled by MRI

ERP event related potential; Hb hemoglobin; ITI intertrial interval; * statistics insufficient, i. e. due to no post-hoc tests, comparison of absolute values and not relative changes, or correlation coefficients without significance (p -) values.

In the introduction section we discussed several advantages of optical imaging in comparison with other imaging techniques (Figure 4). Interestingly, recent studies mirror these theoretically deduced advantages. Optical imaging studies were conducted with paradigms investigating, in adults, executive functions (10), language (9), and other cognitive domains (14) (Tables 1-3). Six

studies examined cognitive neurodevelopment (Table 4). Moreover, 17 studies investigated cognition in psychiatric, and 2 in neurological patients (Table 5 and 6, respectively). In total, 58 cognitive studies have applied optical imaging approaches until now.

A few of the optical studies used paradigms that afford a high robustness to movements making application of fMRI almost impossible. The tasks included object permanence (Baird et al., 2002), trail making (Weber et al., 2004), mirror drawing (Okada et al., 1994, 1996) as well as delayed visual feedback where one arm had been moved (Shimada et al., 2004, 2005). Moreover, optical imaging was combined with other imaging techniques such as ERPs (Horowitz & Gore, 2004; Kennan et al., 2004a), or PET (Hock et al., 1997), which is a main advantage of the method compared with fMRI.

Table 3 Others

Author	Paradigm	Subjects	Oxy-Hb	Deoxy-Hb	Analysis	System (channels)	Region
Villringer et al. 1993*	calculation task; block design	10 adults	increase	decrease	no statistics	NIRO-500 (1)	left frontal
Fallgatter & Strik 1997*	continuous performance test; block design	10 adults	no stimulation dependent change in concentration	higher increase on left compared with right side	ANOVA, t-test	CritikonTM 2020 (2)	Fp1/F3 and Fp2/F4
Hock et al. 1997	calculation task; block design	12 young, and 17 elderly adults	increase; lower in the elderly	decrease	t-test, correlation	NIRO-500 (1)	left frontal (Fp1)
Hoshi & Tamura 1997*	calculation task; block design	8 adults	increase	decrease	no statistics	2 OM-100A, Shimadzu (2)	prefrontal
Kennan et al. 2002a*	oddball auditory paradigm; event-related; average ITI of 19 s	5 adults	increase of total Hb and P300 (ERP)		fit of design (χ^2) function; no statistics beside mean \pm SD ANOVA	Hitachi ETG-100 (24)	left hemisphere
Herrmann et al. 2003a*	emotional tasks (pictures of facial affect, international affective picture system); block design	14 adults	increase left prefrontal	no change		NIRO-300 (2)	frontal (between Fp1/2, F3/4 and F7/8)
Kwee & Nakada 2003*	picture completion and arrangement, matrix reasoning; block design	60 adults (age range 20-90 years)	changes in hemoglobin oxygen relative saturation with aging	declined	not specified	Invos 4100 (2)	frontal
Izzetoglu et al. 2004	warship commander task; block design	8 adults	(oxy-Hb – deoxy-Hb) correlated with load		ANOVA, correlation	16 channel system	frontal
Okamoto et al. 2004b	apple peeling; block design	12 adults	prefrontal increase beside elevations in premotor cortex, motor cortex, and supplementary motor area	slight changes	ANOVA	OMM-2000, Shimadzu (up to 34)	bitemporo-parietofrontal; controlled by MRI
Shimada et al. 2004	delayed visual feedback of the moving hand in a reaching task; block design	12 adults	decrease; stronger during delay condition	no change	t-test, correlation	OMM-1080S, Shimadzu (24)	frontal (10/20 system)
Shimada et al. 2005	delayed visual feedback of the moving hand; block design	12 adults	increase	decrease	general linear model, correlation with box car function	OMM-1080S, Shimadzu (48)	parietal (10/20 system)
Tanida et al. 2004	calculation task; block design	16 adults	increase	decrease	t test, correlation	NIRO-300 (2)	Fp1/2
Toichi et al. 2004	attention tasks (letter cancellation, continuous performance test); tasks for higher cognition (word generation/remembering [free recall], Raven's colored progressive matrices); block design	10 Japanese and 10 American adults	increase	decrease (attention tasks) or increase (tasks for higher cognition)	ANOVA, Fisher's PLSD	NIRO-300 (2)	prefrontal (between Fp1/2 and F3/4)
Suzuki et al. 2005*	Rating line drawings on semantic differential scales; block design	8 adults	increase	not reported	ANOVA, Ryan's test	Hitachi ETG-100 (24)	bifrontoparieto-temporal; localization of optodes was transformed into Talairach system

ERP event related potential; Hb hemoglobin; ITI intertrial interval; * statistics insufficient, i. e. due to no post-hoc tests, comparison of absolute values and not relative changes, or correlation coefficients without significance (p -) values.

As discussed extensively in the Introduction section, optical imaging is particularly suited for neurodevelopmental studies, and psychiatric and neurological patients due to its robustness to movements. Obviously, neonates, children and acutely ill patients might not inhibit movements for a long time. The most remarkable optical imaging study on development examined object permanence (Baird et al., 2002). Although it is characterized by methodological limitations (no control area, where brain activation did not change between the time before and after object permanence), it gives a hint to the most exciting fields for application of optical imaging in the future. Moreover, studies with psychiatric patients who might not stand the confined environment of fMRI experiments show that patients with anxiety disorders, such as panic disorder, and with posttraumatic stress disorder are accessible to imaging studies (Akiyoshi et al., 2003; Matsuo et al., 2003a; 2003b). Further, although not conducted till now, studies with patients suffering from acute mania or schizophrenia might come into the realm of possibility.

Some cognitive studies reported changes in the redox-state of the cytochrome-c-oxidase. Although measuring the redox-state of the cytochrome-c-oxidase is controversial (Hekeeren et al., 1999; Uludag et al., 2002, 2004), and most cognitive studies could not detect task-specific effects (Schroeter et al., 2002b, 2004d), one of our previous studies showed that changes of cytochrome-c-oxidase as elicited by Stroop interference increase specifically in the aging prefrontal and parietal cortex in contrast to oxy- and deoxyhemoglobin (Schroeter et al., 2003). These results fit well with studies that reported age dependent changes in the activity and protein content of cytochrome-c-oxidase (Cottrell et al., 2001; Ojaimi et al., 1999a, 1999b). Data suggest that imaging of cytochrome-c-oxidase might open a new window to brain function, particularly because changes of this enzyme can provide more direct information about neuronal activity than hemoglobin changes (Hekeeren et al., 1999; Jöbsis et al., 1977). However, as discussed in the Introduction, full-spectrum approaches have to be applied and methodological problems have to be solved.

Table 4 Development

Author	Paradigm	Subjects	Oxy-Hb	Deoxy-Hb	Analysis	System (channels)	Region
Baird et al. 2002*	object permanence; event-related; ITI not specified	12 infants (5-12 months of age)	increase after object permanence in comparison with time before	no change	ANOVA	4 channel system	frontal (F3/4 of the 10/20 system)
Hoshi & Chen 2002*	anticipation, pleasant and unpleasant emotions; block design	16 children (4-6 years)	decrease during unpleasant emotion	not analyzed	t-test	2 HEO-200, Omron; portable (2)	Fp1 and Fp2
Pena et al. 2003	infant-directed speech; block design	12 neonates	increases of total Hb higher in left than right hemisphere			Hitachi ETG-100 (24)	temporofrontoparietal (10/20 system)
Schroeter et al. 2004d	Stroop task; event-related; ITI 12 s	14 young adults; 23 school children (7-13 years)	increase; interference effect increases with development	decrease; interference effect increases with development	ANOVA, t-test, correlation	NIRO-300 (3x2)	prefrontal (10/20 system)
Tsujimoto et al. 2004	item-recognition task; event-related; ITI 25 s	7 young adults; 16 preschool children (5-6 years)	load dependent prefrontal increases; in children higher and more extended	decrease, although not significant	t-test	Hitachi ETG-100 (24)	frontal (10/20 system)
Weber et al. 2004	trail-making test; block design	8 healthy school children (10-13 years)	increase on both sides	increase on left side	Wilcoxon	NIRO-300 (2)	frontal cortex; Fp1/F3 and Fp2/F4

Hb hemoglobin; ITI intertrial interval; * statistics insufficient, i. e. due to no post-hoc tests, comparison of absolute values and not relative changes, or correlation coefficients without significance (p -values).

Most previous optical cognitive studies used block designs. Recently, several studies showed that event-related designs can also be applied, preferably with randomized approaches (Baird et al., 2002; Horowitz & Gore, 2004; Kennan et al., 2004a; Noguchi et al., 2002; Schroeter et al., 2002a, 2002b, 2003, 2004c, 2004d; Tsujimoto et al., 2004). Moreover, due to high temporal sensitivity of the method, brain activation even during single trials can be investigated as shown by Schroeter et al. (2002b).

Table 5 Psychiatry

Author	Paradigm	Subjects	Oxy-Hb	Deoxy-Hb	Analysis	System (channels)	Region
Okada et al. 1994	mirror drawing task; block design	38 patients with schizophrenia; 38 controls	increase; in schizophrenia inconsistent	decrease; in schizophrenia inconsistent	X ² -test, median test using nonparametric one-way analysis, general linear models, t-test	2 channel system (Shimadzu) (2)	prefrontal
Okada et al. 1996	mirror drawing task; block design	36 patients with depression; 36 controls	increase	decrease	Mann-Whitney test, X ² -test, ANOVA, t-test	2 channel system	prefrontal
Fallgatter et al. 1997*	verbal fluency test; block design	10 patients with AD; 10 controls	increase on left compared with right side in controls only	decrease during letter-compared with category-based fluency	ANOVA	CritikonTM 2020 (2)	Fp1/F3 and Fp2/F4
Hock et al. 1997	verbal fluency task; block design	19 patients with AD; 19 controls	in parietal areas increase in controls higher than decrease in AD	decrease (not significant)	t-test	2 NIRO-500 (2)	P3, Fp1
Eschweiler et al. 2000	arithmetic, drawing tasks; block design	12 patients with depression	total Hb: increase; absence of TMS stimulation site before TMS predicted clinical response to TMS	of task-related increase at the TMS stimulation site before TMS predicted clinical response to TMS	ANOVA, correlation	4 channel system	frontal (F3/4, Fp1/2)
Fallgatter & Strik 2000*	continuous performance test; block design	9 patients with schizophrenia; 10 controls	no stimulation dependent change	higher increase on left side in controls compared with patients	ANOVA	2 CritikonTM 2020 (4)	Fp1/F3 and Fp2/F4
Matsuo et al. 2000	verbal fluency task; block design	9 patients with MD; 10 controls	increase in controls; no change in MD	decrease in controls; no change in MD	ANOVA, t-test	HEO-200 (1)	frontal (Fp1/F3)
Matsuo et al. 2002	verbal fluency task; block design	14 patients with MD; 11 with bipolar disorder; 21 controls	increase in controls; significantly less in patients	decrease in controls	ANOVA, t-test	HEO-200 (1)	frontal (Fp1/F3)
Akiyoshi et al. 2003	neutral, anxiety-relevant or anxiety-irrelevant but emotionally relevant stimuli (international affective picture system); block design	23 patients with panic disorder without depression, 31 controls	left frontal oxy-Hb in controls higher during anxiety-relevant or anxiety-irrelevant but emotionally relevant stimuli; smaller difference in patients	not reported	ANOVA, least significant difference test	NIRO-300 (2)	Fp1/F3 and Fp2/F4
Matsuo et al. 2003a	trauma-related stimuli; block design	8 subjects with PTSD, 26 subjects after trauma without PTSD, 12 controls	increase in all groups	decrease only in PTSD	ANOVA, Dunnett's t-test, t-test, correlation	Hitachi ETG-100 (24)	prefrontal
Matsuo et al. 2003b	verbal fluency task; block design	8 subjects with PTSD, 26 controls	Increase; smaller in PTSD	decrease	ANOVA, t-test, correlation	Hitachi ETG-100 (24)	frontal
Herrmann et al. 2004	verbal fluency task; block design	9 patients with MD, 9 controls	increase; reduced in MD	decrease; reduced in MD	ANOVA, t-test	NIRO-300 (2)	frontal (between Fp1/2, F3/4 and F7/8)
Matsuo et al. 2004	verbal fluency task (word repetition task as control); block design	9 patients with bipolar disorder, currently in remission, 9 controls	increase; reduced in patients	no change	ANOVA, t-test	Hitachi ETG-100 (24)	frontal
Shinba et al. 2004	random number generation task; block design	13 patients with schizophrenia; 10 controls	increase; smaller in schizophrenia	decrease; smaller in schizophrenia	ANOVA, Duncan test, correlation	NIRO-300 (2)	frontal (approximately Fp1/F7 and Fp2/F8)
Suto et al. 2004	word fluency task; block design	10 patients with MD, 13 patients with schizophrenia, 16 controls	increase; smaller in MD/schizophrenia than controls	decrease, not statistically analyzed	ANOVA, Scheffe multiple comparison, t-tests	Hitachi ETG-100 (48)	frontal, temporo-parietal (10/20 system)
Watanabe & Kato 2004	verbal fluency test and letter number span test; block design	62 patients with schizophrenia, 31 controls	increase; smaller increase in schizophrenia during verbal fluency; atypical antipsychotics led to a larger increase during letter number span compared with typical ones	decrease; smaller in schizophrenia	ANOVA, t-test, correlation	HEO-200 (1)	frontal (Fp1/3)
Schroeter et al. 2002a	Stroop task; event-related; ITI 12 s	8 patients with cerebral microangiopathy, 14 controls	increase, reduced in microangiopathy; interference significant in prefrontal cortex	decrease, reduced in microangiopathy; interference significant in prefrontal cortex	ANOVA, t-test	NIRO-300 (3x2)	frontal (10/20 system)

AD Alzheimer's disease; Hb hemoglobin; ITI intertrial interval; MD major depression; PTSD posttraumatic stress disorder; TMS transcranial magnetic stimulation; * statistics insufficient, i. e. due to no post-hoc tests, comparison of absolute values and not relative changes, or correlation coefficients without significance (*p*-values).

Generally, one has to state that some of the previous cognitive optical imaging studies lack sufficient statistics (Baird et al., 2002; Fallgatter & Strik, 1997, 1998, 2000; Fallgatter et al., 1997, 1998; Hermann et al., 2003a, 2003b; Horovitz & Gore, 2004; Hoshi & Chen, 2002; Hoshi & Tamura, 1997; Kennan et al., 2002a; Kwee & Nakada, 2003; Quaresima et al., 2002; Suzuki et al., 2005; Villringer et al., 1993). For instance, authors did not calculate post-hoc tests, or just reported correlation coefficients without significance values. Although most studies did not measure differential pathlength factors, some of them reported and compared absolute concentration values of the chromophores only. Instead, relative changes can be measured with that method only.

Former optical imaging studies used time line analysis approaches such as comparisons of concentration changes between conditions or to baseline. Only some groups used correlation analysis with a hemodynamic response function to estimate concentration changes of the chromophores (Horovitz & Gore, 2004; Kennan et al., 2002a; Noguchi et al., 2002; Sato et al., 1999; Schroeter et al., 2002b; Shimada et al., 2005; Watanabe et al., 1998), or calculation of effect sizes (Schroeter et al., 2003, 2004c), which are independent of the assumed differential pathlength factors (Schroeter et al., 2004a).

If ones takes into account that skin-cortex distance varies strongly across the human head (see Figure 10; Okamoto et al., 2004a), and that depth penetration of fNIRS is limited (Germon et al., 1999), one may hypothesize that even not all superficial cortical areas can be measured with the usual source-detector separation of 3-4 cm. Particularly the superior parietal lobules may be missed, which is supported by one of our own studies (see chapter 2.5.1.; Schroeter et al., 2002b). Namely, we could not detect the stronger brain activation due to interference along the intraparietal sulcus, which had been reported in a previous fMRI study with the same task (Zysset et al., 2001). Contrary, Hock et al. (1997) detected in their study changes in brain activation in the parietal lobe due to Alzheimer's disease. Further, we showed that changes of cytochrome-c-oxidase as elicited by Stroop interference increase specifically in the aging prefrontal and parietal cortex (Schroeter et al., 2003).

Table 6 Neurology

Author	Paradigm	Subjects	Oxy-Hb	Deoxy-Hb	Analysis	System (channels)	Region
Sakatani et al. 1998	speech tasks, such as confrontational naming; block design	10 post-stroke aphasia patients; 6 post-stroke nonaphasic patients; 13 controls	increase in all groups	slight decrease in controls/nonaphasics; increase in aphasics	ANOVA, Student-Newman-Keuls test	NIRO-500 (1)	Fp2
Watanabe et al. 1998	word-generation task; block design	11 healthy adults; 6 patients with epilepsy	increase in total Hb particularly on left side		correlation with design (square pulse) function, laterality index	Hitachi ETG-100 (24)	frontotemporal

Hb hemoglobin.

In summary, our studies contribute several aspects to the integration of optical imaging into cognitive neuroscience, and cognitive neuropsychiatry.

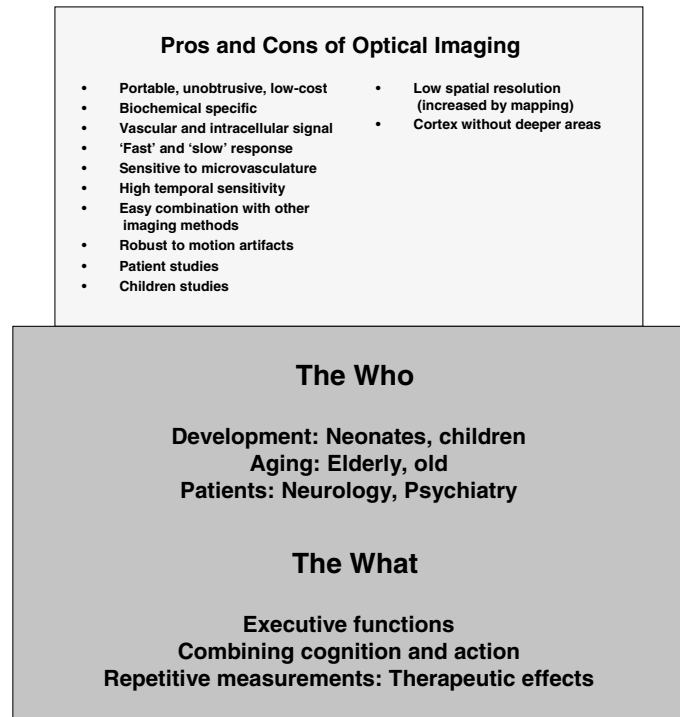


Figure 51 Prospects for optical imaging in cognitive neuroscience.

3.2. Prospects for Optical Imaging in Cognitive Neuroscience

After summarizing the findings of our studies and embedding it into the context of literature reports, we want to discuss the prospects for optical imaging in cognitive neuroscience, and cognitive neuropsychiatry in the last chapter. As raised in the Introduction section, cognitive neuroscience aims at understanding the relationship between mind and brain by attributing mental functions to brain structures (Gazzaniga, 2004). Cognitive neuropsychiatry links neuropsychiatric symptoms as disturbances of cognitive processes with brain structures (Halligan & David, 2001). In chapter 1.2.2. we discussed the several advantages of optical imaging in comparison with other imaging techniques that have led to pioneering and exciting results in the last decade. Obviously, as optical imaging can tolerate extensive movements and is unobtrusive, it is especially well suited

for cognitive neuropsychiatry that is per se concerned with psychiatric and neurological patients (Figure 51). Furthermore, we propose that optical imaging is generally suited for studies on development (neonates and children), and aging (elderly and old people). Moreover, the method should be applied when paradigms are investigated that involve movement, for instance executive functions, and studies involving cognition and action. Although it has not been conducted until now, therapeutic effects might be examined, because brain monitoring can be performed for extended periods.

In the future, functional optical studies might provide more direct information about neural activity beside changes in hemoglobin oxygenation by measuring the ‘fast’ optical signal and changes of cytochrome-c-oxidase (Gratton et al., 2003; Wong-Riley, 1989). Moreover, brain activation may be investigated in freely moving subjects (Vaithianathan et al., 2004).

Regarding methodological issues positioning of optodes according to the international 10/20 system is sufficient, because spatial resolution of current optical instruments is limited. Recent studies debated whether oxy- or deoxyhemoglobin is more reliable as an indicator for brain activation. Our studies support together with previous reports the second notion (Kleinschmidt et al., 1996; Obrig et al., 2000b; Schroeter et al., 2002b; 2004a; Wobst et al., 2001). As discussed before, the differential pathlength factor has a high variability (Duncan et al., 1996; Essenpreis et al., 1993; Zhao et al., 2002). Hence, we propose several statistical standard approaches for optical imaging, which are independent of this factor (general linear model, effect sizes, normalized power spectral density).

4. References

- Adleman NE, Menon V, Blasey CM, White CD, Warsofsky IS, Glover GH, Reiss AL (2002) A developmental fMRI study of the Stroop color-word task. *Neuroimage* 16: 61-75.
- Akiyoshi J, Hieda K, Aoki Y, Nagayama H (2003) Frontal brain hypoactivity as a biological substrate of anxiety in patients with panic disorders. *Neuropsychobiology* 47: 165-170.
- Anderson CM & Nedergaard M (2003) Astrocyte-mediated control of cerebral microcirculation. *Trends Neurosci* 26: 340-344.
- Aubert A & Costalat R (2002) A model of the coupling between brain electrical activity, metabolism, and hemodynamics: Application to the interpretation of functional neuroimaging. *Neuroimage* 17: 1162-1181.
- Bäzner H, Konietzko M, Daffertshofer M, Hennerici MG (1995) Modification of low-frequency spontaneous oscillations in blood flow velocity in large- and small-artery disease. *J Neuroimag* 5: 212-218.
- Baird AA, Kagan J, Gaudette T, Walz KA, Herschlag N, Boas DA (2002) Frontal lobe activation during object permanence: Data from near-infrared spectroscopy. *Neuroimage* 16: 1120-1126.
- Banich MT, Milham MP, Atchley R, Cohen NJ, Webb A, Wszalek T, Kramer AF, Liang ZP, Wright A, Shenker J, Magin R (2000) fMRI studies of Stroop tasks reveal unique roles of anterior and posterior brain systems in attentional selection. *J Cogn Neurosci* 12: 988-1000.
- Barch DM, Braver TS, Akbudak E, Conturo T, Ollinger J, Snyder A (2001) Anterior cingulate cortex and response conflict: Effects of response modality and processing domain. *Cereb Cortex* 11: 837-848.
- Barfod C, Akgören N, Fabricius M, Dirnagl U, Lauritzen M (1997) Laser-Doppler measurements of concentration and velocity of moving blood cells in rat cerebral circulation. *Acta Physiol Scand* 160: 123-132.
- Bernardi L, Rossi M, Leuzzi S, Mevio E, Fornasari G, Calciati A, Orlandi C, Fratino P (1997) Reduction of 0.1 Hz microcirculatory fluctuations as evidence of sympathetic dysfunction in insulin-dependent diabetes. *Cardiovasc Res* 34: 185-191.
- Berwick J, Martin C, Martindale J, Jones M, Johnston D, Zheng Y, Redgrave P, Mayhew J (2002) Hemodynamic response in the unanesthetized rat: Intrinsic optical imaging and spectroscopy of the barrel cortex. *J Cereb Blood Flow Metab* 22: 670-679.
- Bluestone AY, Abdoulaev G, Schmitz CH, Barbour RL, Hielscher AH (2001) Three-dimensional optical tomography of hemodynamics in the human head. *Optics Express* 9: 272-286.
- Boas DA, Gaudette T, Strangman G, Cheng X, Marota JJA, Mandeville JB (2001) The accuracy of near infrared spectroscopy and imaging during focal changes in cerebral hemodynamics. *Neuroimage* 13: 76-90.
- Boas DA, Dale AM, Franceschini MA (2004) Diffuse optical imaging of brain activation: Approaches to optimizing image sensitivity, resolution, and accuracy. *Neuroimage* 23: S275-S288.
- Booth JR, Burman DD, Meyer JR, Lei Z, Trommer BL, Davenport ND, Li W, Parrish TB, Gitelman DR, Mesulam MM (2003) Neural development of selective attention and response inhibition. *Neuroimage* 20: 737-751.
- Boushel R, Langberg H, Olesen J, Gonzales-Alonzo J, Bülow J, Kjaer M (2001) Monitoring tissue oxygen availability with near-infrared spectroscopy (NIRS) in health and disease. *Scand J Med Sci Sports* 11: 213-222.
- Brecher P, Tercyak A, Gavras H, Chobanian AV (1978) Peptidyl dipeptidase in rabbit brain microvessels. *Biochimica et Biophysica Acta* 526: 537-546.
- Buchheim K, Obrig H, von Pannwitz W, Müller A, Heekeren H, Villringer A, Meierkord H (2004) Decrease in haemoglobin oxygenation during absence seizures in adult humans. *Neurosci Lett* 354: 119-122.
- Buckner RL, Snyder AZ, Sanders AL, Raichle ME, Morris JC (2000) Functional brain imaging of young, nondemented, and demented older adults. *J Cogn Neurosci* 12(6; suppl 2): 24-34.

- Bundo M, Kaneoke Y, Inao S, Yoshida J, Nakamura A, Kakigi R (2000) Human visual motion areas determined individually by magnetoencephalography and 3D magnetic resonance imaging. *Hum Brain Mapp* 11: 33-45.
- Bunge SA, Dudukovic NM, Thomason ME, Vaidya CJ, Gabrieli JDE (2002) Immature frontal lobe contributions to cognitive control in children: Evidence from fMRI. *Neuron* 33: 301-311.
- Bunemann B, Fuxe K, Ganten D (1992) The brain renin-angiotensin system: Localization and general significance. *J Cardiovasc Pharmacol* 19 (suppl 6): S51-S62.
- Burock MA, Buckner RL, Woldorff MG, Rosen BR, Dale AM (1998) Randomized event-related experimental designs allow for extremely rapid presentation rates using functional MRI. *Neuroreport* 9: 3735-3739.
- Buxton RB, Wong EC, Frank LR (1998) Dynamics of blood flow and oxygenation changes during brain activation: The balloon model. *Magn Reson Med* 39: 855-864.
- Buxton RB, Wong EC, Frank LR (1999) The post-stimulus undershoot of the functional MRI signal. In: Moonen CTW, Bandettini PA (Eds.) *Functional MRI*. Springer, Berlin, Germany, pp. 253-262.
- Cannestra AF, Bookheimer SY, Pouratian N, O'Farrell A, Sicotte N, Martin NA, Becker D, Rubino G, Toga AW (2000) Temporal and topographical characterization of language cortices using intraoperative optical intrinsic signals. *Neuroimage* 12: 41-54.
- Cannestra AF, Pouratian N, Bookheimer SY, Martin NA, Becker DP, Toga AW (2001) Temporal spatial differences observed by functional MRI and human intraoperative optical imaging. *Cereb Cortex* 11: 773-782.
- Cannestra AF, Wartenburger I, Obrig H, Villringer A, Toga AW (2003) Functional assessment of Broca's area using near infrared spectroscopy in humans. *Neuroreport* 14: 1961-1965.
- Caplan LR (1995) Binswanger's disease – revisited. *Neurology* 45: 626-633.
- Carter CS, Mintun M, Cohen JD (1995) Interference and facilitation effects during selective attention: An $H_2^{15}O$ PET study of Stroop task performance. *Neuroimage* 2: 264-272.
- Carter CS, MacDonald AM, Botvinick M, Ross LL, Stenger VA, Noll D, Cohen JD (2000) Parsing executive processes: Strategic vs. evaluative functions of the anterior cingulate cortex. *Proc Natl Acad Sci U.S.A.* 97: 1944-1948.
- Casey BJ, Trainor RJ, Orendi JL, Schubert AB, Nystrom LE, Giedd JN, Castellanos FX, Haxby JV, Noll DC, Cohen JD, Forman SD, Dahl RE, Rapoport JL (1997) A developmental functional MRI study of prefrontal activation during performance of a go-no-go task. *J Cog Neurosci* 9: 835-847.
- Chen Y, Tailor DR, Intes X, Chance B (2003) Correlation between near-infrared spectroscopy and magnetic resonance imaging of rat brain oxygenation modulation. *Phys Med Biol* 48: 417-427.
- Churchland PS & Sejnowski TJ (1988) Perspectives on cognitive neuroscience. *Science* 242: 741-745.
- Clozel JP, Kuhn H, Hefti F (1989) Effects of cilazapril on the cerebral circulation in spontaneously hypertensive rats. *Hypertension* 14: 645-651.
- Cohen J (1988) *Statistical power analysis for the behavioral sciences*, 2nd ed. Lawrence Erlbaum Associates, Hillsdale, NJ.
- Colantuoni A, Bertuglia S, Intaglietta M (1994) Microvascular vasomotion - origin of laser Doppler flux motion. *Int J Microcirc Clin Exp* 14: 151-158.
- Comalli PE, Wapner S, Werner H (1962) Interference effects of Stroop color-word test in childhood, adulthood and aging. *J Genet Psychol* 100: 47-53.
- Cooper CE, Cope M, Quaresima V, Ferrari M, Nemoto E, Springett R, Matcher S, Amess P, Penrice J, Tyszczyk L, Wyatt J, Delpy DT (1997) Measurement of cytochrome oxidase redox state by near infrared spectroscopy. *Adv Exp Med Biol* 413: 63-73.
- Cooper CE & Springett R (1997) Measurement of cytochrome oxidase and mitochondrial energetics by near-infrared spectroscopy. *Philos Trans R Soc Lond B Biol Sci* 352: 669-676.
- Cope M, Delpy DT, Reynolds EOR, Wray S, Wyatt J, van der Zee P (1987) Methods of quantitating cerebral near infrared spectroscopy data. *Adv Exp Med Biol* 222: 183-189.

- Cope M & Delpy DT (1988) System for long-term measurement of cerebral blood and tissue oxygenation on newborn infants by near infrared transillumination. *Med Biol Eng Comput* 26: 289-294.
- Cope M, van der Zee P, Essenpreis M, Arridge SR, Delpy DT (1991) Data analysis methods for near infrared spectroscopy of tissue: problems in determining the relative cytochrome aa3 concentration. *SPIE* 1431: 251-262.
- Cordes D, Haughton V, Carew JD, Arfanakis K, Maravilla K (2002) Hierarchical clustering to measure connectivity in fMRI resting-state data. *Magn Reson Imaging* 20: 305-317.
- Corry DB, Tuck ML (2000) Protection from vascular risk in diabetic hypertension. *Current Hypertension Reports* 2: 154-159.
- Cottrell DA, Blakely EL, Johnson MA, Ince PG, Borthwick GM, Turnbull DM (2001) Cytochrome c oxidase deficient cells accumulate in the hippocampus and choroid plexus with age. *Neurobiol Aging* 22: 265-272.
- Cox RW (1996) AFNI – software for analysis and visualization of functional magnetic resonance neuroimages. *Comp Biomed Res* 29: 162-173.
- Coyle S, Ward T, Markham C, McDarby G (2004) On the suitability of near-infrared (NIR) systems for next-generation brain-computer interfaces. *Physiol Meas* 25: 815-822.
- Dale AM (1999) Optimal experimental design for event-related fMRI. *Hum Brain Mapp* 8: 109-114.
- Daniel DB, Pelotte M, Lewis J (2000) Lack of sex differences on the Stroop color-word test across three age groups. *Percept. Mot Skills* 90: 483-484.
- David AS & Halligan PW (2000) Cognitive neuropsychiatry: potential for progress. *J Neuropsychiat Clin Neurosci* 12: 506-510.
- De Brabander JM, Kramers RJK, Uylings HBM (1998) Layer-specific dendritic regression of pyramidal cells with ageing in the human prefrontal cortex. *Eur J Neurosci* 10: 1261-1269.
- Delis DC, Kramer JH, Kaplan E, Obler BA (1987) The California verbal learning test: Adult version. Psychological Corporation, San Antonio, USA.
- Deriu F, Roatta S, Grassi C, Urcioli R, Micieli G, Passatore M (1996) Sympathetically-induced changes in microvascular cerebral blood flow and in the morphology of its low-frequency waves. *J Auton Nerv Syst* 59: 66-74.
- DeSoto MC, Fabiani M, Geary DC, Gratton G (2001) When in doubt, do it both ways: brain evidence of the simultaneous activation of conflicting motor responses in a spatial Stroop task. *J Cogn Neurosci* 13: 523-536.
- D'Esposito M, Zarahn E, Aguirre GK, Rypma B (1999) The effect of normal aging on the coupling of neural activity to the bold hemodynamic response. *Neuroimage* 10: 6-14.
- D'Esposito M, Deouell LY, Gazzaley A (2003) Alterations in the BOLD fMRI signal with ageing and disease: A challenge for neuroimaging. *Nat Rev Neurosci* 4: 863-872.
- Duncan A, Meek JH, Clemence M, Elwell CE, Tyszczuk L, Cope M, Delpy DT (1995) Optical pathlength measurements on adult head, calf and forearm and the head of the newborn infant using phase resolved optical spectroscopy. *Phys Med Biol* 40: 295-304.
- Duncan A, Meek JH, Clemence M, Elwell CE, Fallon P, Tyszczuk L, Cope M, Delpy DT (1996) Measurement of cranial optical path length as a function of age using phase resolved near infrared spectroscopy. *Pediatr Res* 39: 889-894.
- Durston S, Thomas KM, Yang YH, Ulug AM, Zimmerman RD, Casey BJ (2002) A neural basis for the development of inhibitory control. *Develop Sci* 5: F9-F16.
- Eda H, Oda I, Ito Y, Wada Y, Oikawa Y, Tsunazawa Y, Takada M, Tsuchiya Y, Yamashita Y, Oda M, Sassaroli A, Yamada Y, Tamura M (1999) Multichannel time-resolved optical tomography imaging system. *Rev Scien Instr* 70: 3595-3602.
- Elwell CE (1995) A practical users guide to near infrared spectroscopy. Hamamatsu Photonics KK.
- Elwell CE, Springett R, Hillman E, Delpy DT (1999) Oscillations in cerebral haemodynamics. Implications for functional studies. In: Eke A, Delpy DT (Eds.) *Oxygen transport to tissue XXI*. Kluwer Academic/Plenum Publishers, New York, pp. 57-65.

- Eschweiler GW, Wegerer C, Schlotter W, Spandl C, Stevens A, Bartels M, Buchkremer G (2000) Left prefrontal activation predicts therapeutic effects of repetitive transcranial magnetic stimulation (rTMS) in major depression. *Psychiatry Res: Neuroimaging* 99: 161–172.
- Essenpreis M, Elwell CE, Cope M, van der Zee P, Arridge SR, Delpy DT (1993) Spectral dependence of temporal point spread functions in human tissues. *Appl Optics* 32: 418-424.
- Fabiani M, Ho J, Stinard A, Gratton G (2003) Multiple visual memory phenomena in a memory search task. *Psychophysiology* 40: 472-485.
- Fabbri F, Henry ME, Renshaw PF, Nadgir S, Ehrenberg BL, Franceschini MA, Fantini S (2003) Bilateral near-infrared monitoring of the cerebral concentration and oxygen-saturation of hemoglobin during right unilateral electro-convulsive therapy. *Brain Res* 992: 193-204.
- Fallgatter AJ, Roesler M, Sitzmann L, Heidrich A, Mueller TJ, Strik WK (1997) Loss of functional hemispheric asymmetry in Alzheimer's dementia assessed with near-infrared spectroscopy. *Cognit Brain Res* 6: 67-72.
- Fallgatter AJ & Strik WK (1997) Right frontal activation during the continuous performance test assessed with near-infrared spectroscopy in healthy subjects. *Neurosci Lett* 223: 89-92.
- Fallgatter AJ, Muller TJ, Strik WK (1998) Prefrontal hypooxygenation during language processing assessed with near-infrared spectroscopy. *Neuropsychobiology* 37(4): 215-218.
- Fallgatter AJ & Strik WK (1998) Frontal brain activation during the Wisconsin card sorting test assessed with two-channel near-infrared spectroscopy. *Eur Arch Psych Clin Neurosci* 248: 245-249.
- Fallgatter AJ & Strik WK (2000) Reduced frontal functional asymmetry in schizophrenia during a cued continuous performance test assessed with near-infrared spectroscopy. *Schizophr Bull* 26: 913-919.
- Fan J, Flombaum JI, McCandliss BD, Thomas KM, Posner MI (2003) Cognitive and brain consequences of conflict. *Neuroimage* 18: 42-57.
- Farkas E & Luiten PGM (2001) Cerebral microvascular pathology in aging and Alzheimer's disease. *Prog Neurobiol* 64: 575-611.
- Fischer B, Biscaldi M, Gezeck S (1997) On the development of voluntary and reflexive components in human saccade generation. *Brain Res* 754: 285-297.
- Fladby T, Bryhn G, Halvorsen O, Rose I, Wahlund M, Wiig P, Wetterberg L (2004) Olfactory response in the temporal cortex of the elderly measured with near-infrared spectroscopy: A preliminary feasibility study. *J Cereb Blood Flow Metab* 24: 677-680.
- Fox PT, Raichle ME, Mintun MA, Dence C (1988) Nonoxidative glucose consumption during focal physiologic neural activity. *Science* 241: 462-464.
- Frackowiak RSJ, Toga AW, Mazziotta JC (2002) *Brain mapping: The methods*. 2nd edition, Academic Press, San Diego.
- Frahm J, Bruhn H, Merboldt KD, Hänicke W (1992) Dynamic MR imaging of human brain oxygenation during rest and photic stimulation. *J Magn Reson Imaging* 2: 501-505.
- Frahm J, Krüger G, Merboldt KD, Kleinschmidt A (1996) Dynamic uncoupling and recoupling of perfusion and oxidative metabolism during focal brain activation in man. *Magn Reson Med* 35: 143-148.
- Franceschini MA & Boas DA (2004) Noninvasive measurement of neuronal activity with near-infrared optical imaging. *Neuroimage* 21: 372-386.
- Friston KJ (1994) Statistical parametric mapping. In: Thatcher RW, Hallet M, Zeffiro T, John ER, Huerta M (Eds.) *Functional Neuroimaging*. Academic Press, San Diego, pp. 79-93.
- Friston KJ, Holmes AP, Worsley KJ, Poline JP, Frith CD, Frackowiak RSJ (1995a) Statistical parametric maps in functional imaging: A general linear approach. *Hum Brain Mapp* 2: 189-210.
- Friston KJ, Holmes AP, Poline JB, Grasby BJ, Williams CR, Frackowiak RSJ, Turner R (1995b) Analysis of fMRI time-series revisited. *Neuroimage* 2: 45-53.
- Gaillard WD, Grandin CB, Xu B (2001) Developmental aspects of pediatric fMRI: Considerations for image acquisition, analysis, and interpretation. *Neuroimage* 13: 239-249.

- Gazzaniga MS (2004) *The cognitive neurosciences III*. Bradford book, MIT Press, Cambridge, MA, London, UK.
- George MS, Ketter TA, Parekh PI, Rosinsky N, Ring H, Casey BJ, Trimble MR, Horwitz B, Herscovitch P, Post RM (1994) Regional brain activity when selecting a response despite interference: An H₂¹⁵O study of the Stroop and an emotional Stroop. *Hum Brain Mapp* 1: 194-209.
- Germon TJ, Evans PD, Barnett NJ, Wall P, Manara AR, Nelson RJ (1999) Cerebral near infrared spectroscopy: Emitter-detector separation must be increased. *Br J Anaesth* 82: 831-837.
- Giedd JN, Blumenthal J, Jeffries NO, Castellanos FX, Liu H, Zijdenbos A, Paus T, Evans AC, Rapoport JL (1999) Brain development during childhood and adolescence: A longitudinal MRI study. *Nat Neurosci* 2: 861-863.
- Golenhofen K (1970) Slow rhythms in smooth muscle. In: Bühlbring E, Brading AF, Jones AW, Tomita T (Eds.) *Smooth muscle*. Edward Arnold Ltd., London, England, pp. 316-342.
- Gratton G, Corballis PM, Cho E, Fabiani M, Hood DC (1995a) Shades of gray matter: Noninvasive optical images of human brain responses during visual stimulation. *Psychophysiology* 32: 505-509.
- Gratton G, Fabiani M, Friedman D, Franceschini MA, Fantini S, Corballis P, Gratton E (1995b) Rapid changes of optical parameters in the human brain during a tapping task. *J Cogn Neurosci* 7: 446-456.
- Gratton G (1997) Attention and probability effects in the human occipital cortex: An optical imaging study. *Neuroreport* 8: 1749-1753.
- Gratton G, Fabiani M, Corballis PM, Hood DC, Goodman-Wood MR, Hirsch J, Kim K, Friedman D, Gratton E (1997) Fast and localized event-related optical signals (EROS) in the human occipital cortex: Comparisons with the visual evoked potential and fMRI. *Neuroimage* 6: 168-180.
- Gratton G, Fabiani M, Goodman-Wood MR, Desoto MC (1998) Memory-driven processing in human medial occipital cortex: An event-related optical signal (EROS) study. *Psychophysiology* 35: 348-351.
- Gratton G, Sarno A, Maclin E, Corballis PM, Fabiani M (2000) Toward noninvasive 3-D imaging of the time course of cortical activity: Investigation of the depth of the event-related optical signal. *Neuroimage* 11: 491-504.
- Gratton G & Fabiani M (2001) Shedding light on brain function: The event-related optical signal. *Trends Cogn Sci* 5: 357-363.
- Gratton G, Goodman-Wood MR, Fabiani M. (2001) Comparison of neuronal and hemodynamic measures of the brain response to visual stimulation: An optical imaging study. *Hum Brain Mapp* 13: 13-25.
- Gratton G & Fabiani M (2003) The event-related optical signal (EROS) in visual cortex: Replicability, consistency, localization, and resolution. *Psychophysiology* 40: 561-571.
- Gratton G, Fabiani M, Elbert T, Rockstroh B (2003) Seeing right through you: Applications of optical imaging to the study of the human brain. *Psychophysiology* 40: 487-491.
- Haerting C, Markowitsch HJ, Neufeld H, Calabrese P, Deisinger K, Kessler J (2000) WMS-R: Deutsche Adaptation der revidierten Fassung der Wechsler Memory Scale [German version of the revised version of the Wechsler Memory Scale]. Hans Huber, Bern, Switzerland.
- Haginoya K, Munakata M, Kato R, Yokoyama H, Ishizuka M, Iinuma K (2002) Ictal cerebral haemodynamics of childhood epilepsy measured with near-infrared spectrophotometry. *Brain* 125: 1960-1971.
- Halligan PW & David AS (2001) Cognitive neuropsychiatry: Towards a scientific psychopathology. *Nature Rev Neurosci* 2: 209-215.
- Harner PF & Sannit T (1974) *A review of the international ten-twenty system of electrode placement*. Astro-Med, Inc, West Warwick, RI.
- Harrison DG & Ohara Y (1995) Physiologic consequences of increased vascular oxidant stresses in hypercholesterolemia and atherosclerosis: Implications for impaired vasomotion. *American J Cardiol* 75: 75B-81B.
- Harrison RV, Harel N, Panesar J, Mount RJ (2002) Blood capillary distribution correlates with hemodynamic-based functional imaging in cerebral cortex. *Cereb Cortex* 12: 225-233.

- Heekeren HR, Kohl M, Obrig H, Wenzel R, von Pannwitz W, Matcher SJ, Dirnagl U, Cooper CE, Villringer A (1999) Noninvasive assessment of changes in cytochrome-c oxidase oxidation in human subjects during visual stimulation. *J Cereb Blood Flow Metab* 19: 592-603.
- Herrmann MJ, Ehlis AC, Fallgatter AJ (2003a) Prefrontal activation through task requirements of emotional induction measured with NIRS. *Biol Psychol* 64: 255-263.
- Herrmann MJ, Ehlis AC, Fallgatter AJ (2003b) Frontal activation during a verbal-fluency task as measured by near-infrared spectroscopy. *Brain Res Bull* 61: 51-56.
- Herrmann MJ, Ehlis AC, Fallgatter AJ (2004) Bilaterally reduced frontal activation during a verbal fluency task in depressed patients as measured by near-infrared spectroscopy. *J Neuropsychiatr Clin Neurosci* 16: 170-175.
- Herwig U, Satrapi P, Schönfeldt-Lecuona C (2003) Using the international 10-20 EEG system for positioning of transcranial magnetic stimulation. *Brain Topogr* 16: 95-99.
- Hielscher AH, Bluestone AY, Abdoulaev GS, Klose AD, Lasker J, Stewart M, Netz U, Beuthan J (2002) Near-infrared diffuse optical tomography. *Dis Markers* 18: 313-337.
- Hirth C, Obrig H, Villringer K, Thiel A, Bernarding J, Mühlnickel W, Flor H, Dirnagl U, Villringer A (1996) Non-invasive functional mapping of the human motor cortex using near-infrared spectroscopy. *Neuroreport* 7: 1977-1981.
- Hock C, Müller-Spahn F, Schuh-Hofer S, Hofmann M, Dirnagl U, Villringer A (1995) Age dependency of changes in cerebral hemoglobin oxygenation during brain activation: A near-infrared spectroscopy study. *J Cereb Blood Flow Metab* 15: 1103-1108.
- Hock C, Villringer K, Müller-Spahn F, Wenzel R, Heekeren H, Schuh-Hofer S, Hofmann M, Minoshima S, Schwaiger M, Dirnagl U, Villringer A (1997) Decrease in parietal cerebral hemoglobin oxygenation during performance of a verbal fluency task in patients with Alzheimer's disease monitored by means of near-infrared spectroscopy (NIRS) - correlation with simultaneous rCBF-PET measurements. *Brain Res* 755: 293-303.
- Hoge RD, Atkinson J, Gill B, Crelier GR, Marrett S, Pike GB (1999a) Stimulus-dependent BOLD and perfusion dynamics in human V1. *Neuroimage* 9: 573-585.
- Hoge RD, Atkinson J, Gill B, Crelier GR, Marrett S, Pike GB (1999b) Investigation of BOLD signal dependence on cerebral blood flow and oxygen consumption: The deoxyhemoglobin dilution model. *Magn Reson Med* 42: 849-863.
- Holmes AP & Friston KJ (1998) Generalisability, random effects and population inference. *Neuroimage* 7: 754.
- Homan RW, Herman J, Purdy P (1987) Cerebral location of international 10-20 system electrode placement. *Electroencephalogr Clin Neurophysiol* 66: 376-382.
- Horowitz SG & Gore JC (2004) Simultaneous event-related potential and near-infrared spectroscopic studies of semantic processing. *Hum Brain Mapp* 22: 110-115.
- Hoshi Y & Tamura M (1997) Near-infrared optical detection of sequential brain activation in the prefrontal cortex during mental tasks. *Neuroimage* 5: 292-297.
- Hoshi Y, Oda I, Wada Y, Ito Y, Yamashita Y, Oda M, Ohta K, Yamada Y, Tamura M (2000) Visuospatial imagery is a fruitful strategy for the digit span backward task: A study with near-infrared optical tomography. *Cognit Brain Res* 9: 339-342.
- Hoshi Y & Chen SJC (2002) Regional cerebral blood flow changes associated with emotions in children. *Pediatr Neurol* 27: 275-281.
- Hoshi Y (2003) Functional near-infrared optical imaging: Utility and limitations in human brain mapping. *Psychophysiology* 40: 511-520.
- Hoshi Y, Tsou BH, Billock VA, Tanosaki M, Iguchi Y, Shimada M, Shinba T, Yamada Y, Oda I (2003) Spatiotemporal characteristics of hemodynamic changes in the human lateral prefrontal cortex during working memory tasks. *Neuroimage* 20: 1493-1504.
- Hudetz AG, Biswal BB, Shen H, Lauer KK, Kampine JP (1998) Spontaneous fluctuations in cerebral oxygen supply. In: Hudetz AG & Bruley DF (Eds.) *Oxygen transport to tissue XX*. Plenum Press, New York, pp. 551-559.

- Huettel SA, Singerman JD, McCarthy G (2001) The effects of aging upon the hemodynamic response measured by functional MRI. *Neuroimage* 13: 161-175.
- Hund-Georgiadis M, Norris DG, Guthke T, von Cramon DY (2001) Characterization of cerebral small vessel disease by proton spectroscopy and morphological magnetic resonance. *Cerebrovasc Diseases* 12: 82-90.
- Hund-Georgiadis M, Ballaschke O, Scheid R, Norris DG, von Cramon DY (2002) Characterization of cerebral microangiopathy using 3 Tesla MRI: Correlation with neurological impairment and vascular risk factors. *J Magnetic Reson Imaging* 15: 1-7.
- Hund-Georgiadis M, Zysset S, Naganawa S, Norris DG, von Cramon DY (2003) Determination of cerebrovascular reactivity by means of fMRI signal changes in cerebral microangiopathy: a correlation with morphological abnormalities. *Cerebrovasc Dis* 16:158-65.
- Hutchins PM, Lynch CD, Cooney PT, Curseen KA (1996) The microcirculation in experimental hypertension and aging. *Cardiovasc Res* 32: 772-780.
- Intaglietta M (1990) Vasomotion and flowmotion: Physiological mechanisms and clinical evidence. *Vasc Med Rev* 1: 101-112.
- Irikura K, Maynard KI, Moskowitz MA (1994) Importance of nitric oxide synthase inhibition to the attenuated vascular responses induced by topical L-nitroarginine during vibrissal stimulation. *J Cereb Blood Flow Metab* 14: 45-48.
- Ito Y, Kennan RP, Watanabe E, Koizumi H (2000) Assessment of heating effects in skin during continuous wave near infrared spectroscopy. *J Biomed Opt* 5: 383-390.
- Izzetoglu K, Bunce S, Onaral B, Pourrezaei K, Chance B (2004) Functional optical brain imaging using near-infrared during cognitive tasks. *Int J Hum-Comput Interact* 17: 211-227.
- Jasdzewski G, Strangman G, Wagner J, Kwong KK, Poldrack RA, Boas DA (2003) Differences in the hemodynamic response to event-related motor and visual paradigms as measured by near-infrared spectroscopy. *Neuroimage* 20: 479-488.
- Jezzard P, Matthews P, Smith S (2001) *Functional MRI: An Introduction to Methods*. Oxford University Press, Oxford, England.
- Jöbsis FF (1977) Noninvasive infrared monitoring of cerebral and myocardial sufficiency and circulatory parameters. *Science* 198: 1264-1267.
- Jöbsis FF, Keizer JH, LaManna JC, Rosenthal M (1977) Reflectance spectrophotometry of cytochrome aa3 in vivo. *J Appl Physiol* 43: 858-872.
- Jones RA (1999) Origin of the signal undershoot in BOLD studies of the visual cortex. *NMR Biomed* 12: 299-308.
- Kalaria RN (1996) Cerebral vessels in ageing and Alzheimer's disease. *Pharmacol Therapeut* 72: 193-214.
- Kameyama M, Fukuda M, Uehara T, Mikuni M (2004) Sex and age dependencies of cerebral blood volume changes during cognitive activation: A multichannel near-infrared spectroscopy study. *Neuroimage* 22: 1715-1721.
- Kawahata N, Daitoh N, Shirai F, Hara S (1997) Reduction in mean cerebral blood flow measurements using ^{99m}Tc-ECD SPECT during normal aging. *Kaku Igaku* 34: 909-916.
- Kennan RP, Horovitz SG, Maki A, Yamashita Y, Koizumi H, Gore JC (2002a) Simultaneous recording of event-related auditory oddball response using transcranial near infrared optical topography and surface EEG. *Neuroimage* 16: 587-592.
- Kennan RP, Kim D, Maki A, Koizumi H, Constable RT (2002b) Non-invasive assessment of language lateralization by transcranial near infrared optical topography and functional MRI. *Hum Brain Mapp* 16: 183-189.
- Kida I, Yamamoto T, Tamura M (1996) Interpretation of BOLD MRI signals in rat brain using simultaneously measured near-infrared spectrophotometric information. *NMR Biomed* 9: 333-338.
- Kleinschmidt A, Obrig H, Requardt M, Merboldt KD, Dirnagl U, Villringer A, Frahm J (1996) Simultaneous recording of cerebral blood oxygenation changes during human brain activation by magnetic resonance imaging and near-infrared spectroscopy. *J Cereb Blood Flow Metab* 16: 817-826.

- Klingberg T, Forssberg H, Westerberg H (2002) Increased brain activity in frontal and parietal cortex underlies the development of visuospatial working memory capacity during childhood. *J Cog Neurosci* 14: 1-10.
- Kohl M, Nolte C, Heekeren HR, Horst S, Scholz U, Obrig H, Villringer A (1998) Determination of the wavelength dependence of the differential pathlength factor from near-infrared pulse signals. *Phys Med Biol* 43: 1771-1782.
- Kohri S, Hoshi Y, Tamura M, Kato C, Kuge Y, Tamaki N (2002) Quantitative evaluation of the relative contribution ratio of cerebral tissue to near-infrared signals in the adult human head: A preliminary study. *Physiol Meas* 23: 301-312.
- Kruggel F & von Cramon DY (1999) Modeling the hemodynamic response in single-trial functional MRI experiments. *Magn Reson Med* 42: 787-797.
- Kvandal P, Stefanovska A, Veber M, Kvernmo HD, Kirkeboen KA (2003) Regulation of human cutaneous circulation evaluated by laser Doppler flowmetry, iontophoresis, and spectral analysis: Importance of nitric oxide and prostaglandines. *Microvasc Res* 65: 160-171.
- Kvernmo HD, Stefanovska A, Bracic M, Kirkeboen KA, Kvernebo K (1998) Spectral analysis of the laser Doppler perfusion signal in human skin before and after exercise. *Microvasc Res* 56: 173-182.
- Kwee IL & Nakada T (2003) Dorsolateral prefrontal lobe activation declines significantly with age - functional NIRS study. *J Neurol* 250: 525-529.
- Kwon H, Reiss AL, Menon V (2002) Neural basis of protracted developmental changes in visuo-spatial working memory. *Proc Natl Acad Sci U.S.A.* 99: 13336-13341.
- Kwong KK, Belliveau JW, Chesler DA, Goldberg IE, Weisskoff RM, Poncelet BP, Kennedy DN, Hoppel BE, Cohen MS, Turner R, Cheng HM, Brady TJ, Rosen BR (1992) Dynamic magnetic resonance imaging of human brain activity during primary sensory stimulation. *Proc Natl Acad Sci USA* 89: 5675-5679.
- LaManna JC, Sick TJ, Pikarsky SM, Rosenthal M (1987) Detection of an oxidizable fraction of cytochrome oxidase in intact rat brain. *Am J Physiol* 253: C477-83.
- Lee JH, Garwood M, Menon R, Adriany G, Andersen P, Truwit CL, Ugurbil K (1995) High contrast and fast three-dimensional magnetic resonance imaging at high fields. *Magn Reson Med* 34: 308-312.
- Lee SP, Duong TQ, Yang G, Iadecola C, Kim SG (2001) Relative changes of cerebral arterial and venous blood volumes during increased cerebral blood flow: Implications for BOLD fMRI. *Magn Reson Med* 45: 791-800.
- Leung HC, Skudlarski P, Gatenby JC, Peterson BS, Gore JC (2000) An event-related functional MRI study of the Stroop color word interference task. *Cereb Cortex* 10: 552-560.
- Levin HS, Culhane KA, Hartmann J, Evankovich K, Mattson AJ (1991) Developmental changes in performance on tests of purported frontal lobe functioning. *Dev Neuropsychol* 7: 377-395.
- Levy BI, Ambrosio G, Pries AR, Struijker-Boudier HAJ (2001) Microcirculation in hypertension - A new target for treatment? *Circulation* 104: 735-740.
- Lindauer U, Rojl G, Leithner C, Kühl M, Gold L, Gethmann J, Kohl-Bareis M, Villringer A, Dirnagl U (2001) No evidence for early decrease in blood oxygenation in rat whisker cortex in response to functional activation. *Neuroimage* 13: 988-1001.
- Lindauer U, Gethmann J, Kühl M, Kohl-Bareis M, Dirnagl U (2003) Neuronal activity-induced changes of local cerebral microvascular blood oxygenation in the rat: Effect of systemic hyperoxia or hypoxia. *Brain Res* 975: 135-140.
- Liu H, Boas DA, Zhang Y, Yodh AG, Chance B (1995a) Determination of optical properties and blood oxygenation in tissue using continuous NIR light. *Phys Med Biol* 40: 1983-1993.
- Liu H, Chance B, Hielscher AH, Jacques SL, Tittel FK (1995b) Influence of blood vessels on the measurement of hemoglobin oxygenation as determined by time-resolved reflectance spectroscopy. *Med Phys* 22: 1209-1217.
- Lockwood AH, LaManna JC, Snyder S, Rosenthal M (1984) Effects of acetazolamide and electrical stimulation on cerebral oxidative metabolism as indicated by the cytochrome oxidase redox state. *Brain Res* 308: 9-14.

- Logothetis NK, Pauls J, Augath M, Trinath T, Oeltermann A (2001) Neurophysiological investigation of the basis of the fMRI signal. *Nature* 412: 150-157.
- Lohmann G, Müller K, Bosch V, Mentzel H, Hessler S, Chen L, von Cramon DY (2001) Lipsia - A new software system for the evaluation of functional magnetic resonance images of the human brain. *Comput Med Imaging Graph* 25: 449-457.
- Lu HZ, Golay X, Pekar JJ, van Zijl PCM (2003) Functional magnetic resonance imaging based on changes in vascular space occupancy. *Magn Reson Med* 50: 263-274.
- Lu HZ, Golay X, Pekar JJ, van Zijl PCM (2004) Sustained poststimulus elevation in cerebral oxygen utilization after vascular recovery. *J Cereb Blood Flow Metab* 24: 764-770.
- Luna B, Thulborn KR, Munoz DP, Merriam EP, Garver KE, Minshew NJ, Keshavan MS, Genovese CR, Eddy WF, Sweeney JA (2001) Maturation of widely distributed brain function subserves cognitive development. *Neuroimage* 13: 786-793.
- Lundberg MS & Crow MT (1999) Age-related changes in the signaling and function of vascular smooth muscle cells. *Exp Gerontol* 34: 549-557.
- Ma J, Ayata C, Huang PL, Fishman MC, Moskowitz MA (1996) Regional cerebral blood flow response to vibrissal stimulation in mice lacking type I NOS gene expression. *Am J Physiol* 270: H1085-H1090.
- Mackert BM, Wubbeler G, Leistner S, Uludag K, Obrig H, Villringer A, Trahms L, Curio G (2004) Neurovascular coupling analyzed non-invasively in the human brain. *Neuroreport* 15: 63-66.
- Maclin EL, Low KA, Sable JJ, Fabiani M, Gratton G (2004) The event-related optical signal to electrical stimulation of the median nerve. *Neuroimage* 21: 1798-1804.
- MacLeod CM (1991) Half a century of research on the Stroop effect: An integrative review. *Psychol Bull* 109: 163-203.
- Malonek D & Grinvald A (1996) Interactions between electrical activity and cortical microcirculation revealed by imaging spectroscopy: Implications for functional brain mapping. *Science* 272: 551-554.
- Mandeville JB, Marota JJA, Kosofsky BE, Keltner JR, Weissleder R, Rosen BR, Weisskoff RM (1998) Dynamic functional imaging of relative cerebral blood volume during rat forepaw stimulation. *Magn Reson Med* 39: 615-624.
- Mandeville JB, Marota JJA, Ayata C, Zaharchuk G, Moskowitz MA, Rosen BR, Weisskoff RM (1999) Evidence of a cerebrovascular postarteriole windkessel with delayed compliance. *J Cereb Blood Flow Metab* 19: 679-689.
- Marin J (1995) Age-related changes in vascular responses: A review. *Mech Ageing Dev* 79: 71-114.
- Martin AJ, Friston KJ, Colebatch JG, Frackowiak RSJ (1991) Decreases in regional cerebral blood flow with normal aging. *J Cereb Blood Flow Metab* 11: 684-689.
- Matsuo K, Kato T, Fukuda M, Kato N (2000) Alteration of hemoglobin oxygenation in the frontal region in elderly depressed patients as measured by near-infrared spectroscopy. *J Neuropsychiatry Clin Neurosci* 12: 465-471.
- Matsuo K, Kato N, Kato T (2002) Decreased cerebral haemodynamic response to cognitive and physiological tasks in mood disorders as shown by near-infrared spectroscopy. *Psychol Med* 32: 1029-1037.
- Matsuo K, Kato T, Taneichi K, Matsumoto A, Ohtani T, Hamamoto T, Yamasue H, Sakano Y, Sasaki T, Sadamatsu M, Iwanami A, Asukai N, Kato N (2003a) Activation of the prefrontal cortex to trauma-related stimuli measured by near-infrared spectroscopy in posttraumatic stress disorder due to terrorism. *Psychophysiology* 40: 492-500.
- Matsuo K, Taneichi K, Matsumoto A, Ohtani T, Yamasue H, Sakano Y, Sasaki T, Sadamatsu M, Kasai K, Iwanami A, Asukai N, Kato N, Kato T (2003b) Hypoactivation of the prefrontal cortex during verbal fluency test in PTSD: A near-infrared spectroscopy study. *Psychiatry Research: Neuroimaging* 124(1): 1-10.
- Matsuo K, Watanabe A, Onodera Y, Kato N, Kato T (2004) Prefrontal hemodynamic response to verbal-fluency task and hyperventilation in bipolar disorder measured by multi-channel near-infrared spectroscopy. *J Affect Disord* 82: 85-92.

- Mayhew JE, Askew S, Zheng Y, Porrill J, Westby WM, Redgrave P, Rector DM, Harper RM (1996) Cerebral vasomotion: A 0.1-Hz oscillation in reflected light imaging of neural activity. *Neuroimage* 4: 183-193.
- Mayhew J, Zheng Y, Hou Y, Vuksanovic B, Berwick J, Askew S, Coffey P (1999) Spectroscopic analysis of changes in remitted illumination: The response to increased neural activity in brain. *Neuroimage* 10: 304-326.
- Mayhew J, Johnston D, Berwick J, Jones M, Coffey P, Zheng Y (2000) Spectroscopic analysis of neural activity in brain: Increased oxygen consumption following activation of barrel cortex. *Neuroimage* 12: 664-675.
- Mchedlishvili G (1986) Arterial behavior and blood circulation in the brain. Plenum Press, New York.
- Mchedlishvili G & Varazashvili M (1987) Hematocrit in cerebral capillaries and veins under control and ischemic conditions. *J Cereb Blood Flow Metab* 7: 739-744.
- McPherson SE & Cummings JL (1996) Neuropsychological aspects of vascular dementia. *Brain Cogn* 31: 269-282.
- Meek JH, Firbank M, Elwell CE, Atkinson J, Braddick O, Wyatt JS (1998) Regional hemodynamic responses to visual stimulation in awake infants. *Pediatr Res* 43: 840-843.
- Mehagnoul-Schipper DJ, van der Kallen BF, Colier WN, van der Sluijs MC, van Erning LJ, Thijssen HO, Oeseburg B, Hoefnagels WH, Jansen RW (2002) Simultaneous measurements of cerebral oxygenation changes during brain activation by near-infrared spectroscopy and functional magnetic resonance imaging in healthy young and elderly subjects. *Hum Brain Mapp* 16: 14-23.
- Meltzer CC, Cantwell MN, Greer PJ, Ben-Eliezer D, Smith G, Frank G, Kaye WH, Houck PR, Price JC (2000) Does cerebral blood flow decline in healthy aging? A PET study with partial-volume correction. *J Nucl Med* 41: 1842-1848.
- Meyer JU, Borgström P, Lindblom L, Intaglietta M (1988) Vasomotion patterns in skeletal muscle arterioles during changes in arterial pressure. *Microvasc Res* 35: 193-203.
- Meyer MF, Rose CJ, Hülsmann JO, Schatz H, Pfohl M (2003) Impaired 0.1-Hz vasomotion assessed by laser Doppler anemometry as an early index of peripheral sympathetic neuropathy in diabetes. *Microvasc Res* 65: 88-95.
- Miezin FM, Maccotta L, Ollinger JM, Petersen SE, Buckner RL (2000) Characterizing the hemodynamic response: Effects of presentation rate, sampling procedure, and the possibility of ordering brain activity based on relative timing. *Neuroimage* 11: 735-759.
- Mildner T, Norris DG, Schwarzbauer C, Wiggins CJ (2001) A qualitative test of the balloon model for BOLD-based MR signal changes at 3T. *Magn Reson Med* 46: 891-899.
- Milham MP, Erickson KI, Banich MT, Kramer AF, Webb A, Wszalek T, Cohen NJ (2002) Attentional control in the aging brain: Insights from an fMRI study of the Stroop task. *Brain Cogn* 49: 277-296.
- Minagawa-Kawai Y, Mori K, Furuya I, Hayashi R, Sato Y (2002) Assessing cerebral representations of short and long vowel categories by NIRS. *Neuroreport* 13: 581-584.
- Minagawa-Kawai Y, Mori K, Sato Y, Koizumi T (2004) Differential cortical responses in second language learners to different vowel contrasts. *Neuroreport* 15: 899-903.
- Miyai I, Tanabe HC, Sase I, Eda H, Oda I, Konishi I, Tsunazawa Y, Suzuki T, Yanagida T, Kubota K (2001) Cortical mapping of gait in humans: A near-infrared spectroscopic topography study. *Neuroimage*. 14: 1186-1192.
- Miyai I, Yagura H, Oda I, Konishi I, Eda H, Suzuki T, Kubota K (2002) Premotor cortex is involved in restoration of gait in stroke. *Ann Neurol* 52: 188-194.
- Miyai I, Yagura H, Hatakenaka M, Oda I, Konishi I, Kubota K (2003) Longitudinal optical imaging study for locomotor recovery after stroke. *Stroke* 34: 2866-2870.
- Monsell S, Taylor TJ, Murphy K (2001) Naming the color of a word: Is it responses or task sets that compete? *Mem Cogn* 29: 137-151.
- Moosmann M, Ritter P, Krastel I, Brink A, Thees S, Blankenburg F, Taskin B, Obrig H, Villringer A (2003) Correlates of alpha rhythm in functional magnetic resonance imaging and near infrared spectroscopy. *Neuroimage* 20: 145-158.

- Morren G, Wolf U, Lemmerling P, Wolf M, Choi JH, Gratton E, De Lathauwer L, Van Huffel S (2004) Detection of fast neuronal signals in the motor cortex from functional near infrared spectroscopy measurements using independent component analysis. *Med Biol Eng Comput* 42: 92-99.
- Müller K, Lohmann G, Bosch V, von Cramon DY (2001) On multivariate spectral analysis of fMRI time series. *Neuroimage* 14: 347-356.
- Müller K, Mildner T, Lohmann G, von Cramon DY (2003) Investigating the stimulus-dependent temporal dynamics of the BOLD signal using spectral methods. *J Magn Reson Imaging* 17: 375-382.
- Munoz DP, Broughton J, Goldring J, Armstrong I (1998) Age-related performance of human subjects on saccadic eye movement tasks. *Exp Brain Res* 217: 1-10.
- Nakano S, Asada T, Matsuda H, Uno M, Takasaki M (2000) Effects of healthy aging on the regional cerebral blood flow measurements using ^{99m}Tc -ECD SPECT assessed with statistical parametric mapping. *Nippon Ronen Igakkai Zasshi* 37: 49-55.
- Nedergaard M, Ransom B, Goldman SA (2003) New roles for astrocytes: Redefining the functional architecture of the brain. *Trends Neurosci* 26: 523-530.
- Niioka T & Sasaki M (2003) Individual cerebral hemodynamic response to caffeine was related to performance on a newly developed Stroop color-word task. *Opt Rev* 10: 607-608.
- Noguchi Y, Takeuchi T, Sakai KL (2002) Lateralized activation in the inferior frontal cortex during syntactic processing: Event-related optical topography study. *Hum Brain Mapp* 17: 89-99.
- Noguchi Y, Watanabe E, Sakai KL (2003) An event-related optical topography study of cortical activation induced by single-pulse transcranial magnetic stimulation. *Neuroimage* 19: 156-162.
- Norris DG (2000) Reduced power multi-slice MDEFT imaging. *J Magn Reson Imaging* 11: 445-451.
- Obrig H & Villringer A (1997) Near-infrared spectroscopy in functional activation studies. Can NIRS demonstrate cortical activation? In: Villringer A, Dirnagl U (Eds.) *Optical imaging of brain function and metabolism II*. Plenum Press, New York, pp. 113-127.
- Obrig H, Neufang M, Wenzel R, Kohl M, Steinbrink J, Einhäupl K, Villringer A (2000a) Spontaneous low frequency oscillations of cerebral hemodynamics and metabolism in human adults. *Neuroimage* 12: 623-639.
- Obrig H, Wenzel R, Kohl M, Horst S, Wobst P, Steinbrink J, Thomas F, Villringer A (2000b) Near-infrared spectroscopy: Does it function in functional activation studies of the adult brain? *Int J Psychophysiol* 35: 125-142.
- Obrig H, Israel H, Kohl-Bareis M, Uludag K, Wenzel R, Müller B, Arnold G, Villringer A (2002) Habituation of the visually evoked potential and its vascular response: Implications for neurovascular coupling in the healthy adult. *Neuroimage* 17: 1-18.
- Obrig H & Villringer A (2003) Beyond the visible – imaging the human brain with light. *J Cereb Blood Flow Metab* 23: 1-18.
- Ogawa S, Tank DW, Menon R, Ellermann JM, Kim SG, Merkle H, Ugurbil K (1992) Intrinsic signal changes accompanying sensory stimulation: Functional brain mapping with magnetic resonance imaging. *Proc Natl Acad Sci USA* 89: 5951-5955.
- Ogawa S, Menon RS, Tank DW, Kim SG, Merkle H, Ellermann JM, Ugurbil K (1993) Functional brain mapping by blood oxygenation level-dependent contrast magnetic resonance imaging: a comparison of signal characteristics with a biophysical model. *Biophys J* 64: 803-812.
- Ojaimi J, Masters CL, McLean C, Opeskin K, McKelvie P, Byrne E (1999a) Irregular distribution of cytochrome c oxidase protein subunits in aging and Alzheimer's disease. *Ann Neurol* 46: 656-660.
- Ojaimi J, Masters CL, Opeskin K, McKelvie P, Byrne E (1999b) Mitochondrial respiratory chain activity in the human brain as a function of age. *Mech Ageing Dev* 111: 39-47.
- Okada F, Tokumitsu Y, Hoshi Y, Tamura M (1994) Impaired interhemispheric integration in brain oxygenation and hemodynamics in schizophrenia. *Eur Arch Psychiatry Clin Neurosci* 244: 17-25.
- Okada F, Takahashi N, Tokumitsu Y (1996) Dominance of the 'nondominant' hemisphere in depression. *J Affect Disord* 37: 13-21.

- Okamoto M, Dan H, Sakamoto K, Takeo K, Shimizu K, Kohno S, Oda I, Isobe S, Suzuki T, Kohyama K, Dan I (2004a) Three-dimensional probabilistic anatomical cranio-cerebral correlation via the international 10-20 system oriented for transcranial functional brain mapping. *Neuroimage* 21: 99-111.
- Okamoto M, Dan H, Shimizu K, Takeo K, Amita T, Oda I, Konishi I, Sakamoto K, Isobe S, Suzuki T, Kohyama K, Dan I (2004b) Multimodal assessment of cortical activation during apple peeling by NIRS and fMRI. *Neuroimage* 21: 1275-1288.
- Pallas F & Larson DF (1996) Cerebral blood flow in the diabetic patient. *Perfusion* 11: 363-370.
- Panczel G, Daffertshofer M, Ries S, Spiegel D, Hennerici M (1999) Age and stimulus dependency of visually evoked cerebral blood flow responses. *Stroke* 30: 619-623.
- Pena M, Maki A, Kovacic D, Dehaene-Lambertz G, Koizumi H, Bouquet F, Mehler J (2003) Sounds and silence: An optical topography study of language recognition at birth. *Proc Natl Acad Sci USA* 100: 11702-11705.
- Pollmann S, Dove A, von Cramon DY, Wiggins CJ (1998) Use of short intertrial intervals in single-trial experiments: A 3T fMRI-study. *Neuroimage* 8: 327-339.
- Pollmann S, Dove A, von Cramon DY, Wiggins CJ (2000) Event-related fMRI: comparison of conditions with varying BOLD overlap. *Hum Brain Mapp* 9: 26-37.
- Pouratian N, Bookheimer SY, O'Farrell AM, Sicotte NL, Cannestra AF, Becker D, Toga AW (2000) Optical imaging of bilingual cortical representations. *J Neurosurg* 93: 676-681.
- Pouratian N, Sicotte N, Rex D, Martin NA, Becker D, Cannestra AF, Toga AW (2002) Spatial/temporal correlation of BOLD and optical intrinsic signals in humans. *Magnetic Reson Med* 47: 766-776.
- Pouratian N, Sheth SA, Martin NA, Toga AW (2003) Shedding light on brain mapping: Advances in human optical imaging. *Trends Neurosci* 26: 277-282.
- Punwani S, Cooper CE, Clemence M, Penrice J, Amess P, Thornton J, Ordidge RJ (1997) Correlation between absolute deoxyhaemoglobin [dHb] measured by near infrared spectroscopy (NIRS) and absolute R2' as determined by magnetic resonance imaging (MRI). *Adv Exp Med Biol* 413: 129-137.
- Punwani S, Ordidge RJ, Cooper CE, Amess P, Clemence M (1998) MRI measurements of cerebral deoxyhaemoglobin concentration [dHb] – correlation with near infrared spectroscopy (NIRS). *NMR Biomed* 11: 281-289.
- Quaresima V, Ferrari M, van der Sluijs MCP, Menssen J, Colier WNJM (2002) Lateral frontal cortex oxygenation changes during translation and language switching revealed by non-invasive near-infrared multi-point measurements. *Brain Res Bull* 59: 235-243.
- Raz N, Gunning FM, Head D, Dupuis JH, McQuain J, Briggs SD, Loken WJ, Thornton AE, Acker JD (1997) Selective aging of the human cerebral cortex observed in vivo: Differential vulnerability of the prefrontal gray matter. *Cereb Cortex* 7: 268-282.
- Rinne T, Gratton G, Fabiani M, Cowan N, Maclin E, Stinard A, Sinkkonen J, Alho K, Naatanen R (1999) Scalp-recorded optical signals make sound processing in the auditory cortex visible. *Neuroimage* 10: 620-624.
- Rivkin MJ (2000) Developmental neuroimaging of children using magnetic resonance techniques. *Ment Retard Dev Disabil Res Rev* 6: 68-80.
- Rizzoni D, Porteri E, Boari GEM, De Ciuceis C, Sleiman I, Muiesan ML, Castellano M, Miclini M, Agabiti-Rosei E (2003) Prognostic significance of small-artery structure in hypertension. *Circulation* 108: 2230-2235.
- Roman GC, Erkinjuntti T, Wallin A, Pantoni L, Chui HC (2002) Subcortical ischaemic vascular dementia. *Lancet Neurol* 1: 426-436.
- Ross MH, Yurgelun-Todd DA, Renshaw PF, Maas LC, Mendelson JH, Mello NK, Cohen BM, Levin JM (1997) Age-related reduction in functional MRI response to photic stimulation. *Neurology* 48: 173-176.
- Roy C & Sherrington C (1890) On the regulation of the blood-supply of the brain. *J Physiol* 11: 85-108.
- Rubia K, Overmeyer S, Taylor E, Brammer M, Williams SCR, Simmons A, Andrew C, Bullmore ET (2000) Functional frontalisation with age: mapping neurodevelopmental trajectories with fMRI. *Neurosci Biobehav Rev* 24: 13-19.

- Ruff CC, Woodward TS, Laurens KR, Liddle PF (2001) The role of the anterior cingulate cortex in conflict processing: Evidence from reverse Stroop interference. *Neuroimage* 14: 1150-1158.
- Sabri O, Hellwig D, Schreckenberger M, Cremerius U, Schneider R, Kaiser HJ, Doherty C, Mull M, Ringelstein EB, Buell U (1998) Correlation of neuropsychological, morphological and functional (regional cerebral blood flow and glucose utilization) findings in cerebral microangiopathy. *J Nucl Med* 39: 147-54.
- Sabri O, Ringelstein EB, Hellwig D, Schneider R, Schreckenberger M, Kaiser HJ, Mull M, Buell U (1999) Neuropsychological impairment correlates with hypoperfusion and hypometabolism but not with severity of white matter lesions on MRI in patients with cerebral microangiopathy. *Stroke* 30: 556-66.
- Sakatani K, Xie YX, Lichty W, Li SW, Zuo HC (1998) Language-activated cerebral blood oxygenation and hemodynamic changes of the left prefrontal cortex in poststroke aphasic patients - a near-infrared spectroscopy study. *Stroke* 29: 1299-1304.
- Sakatani K, Katayama Y, Yamamoto T, Suzuki S (1999) Changes in cerebral blood oxygenation of the frontal lobe induced by direct electrical stimulation of thalamus and globus pallidus: a near infrared spectroscopy study. *J Neurol Neurosurg Psychiatry* 67: 769-773.
- Sato H, Takeuchi T, Sakai KL (1999) Temporal cortex activation during speech recognition: An optical topography study. *Cognition* 73: B55-B66.
- Scalia R & Stalker TJ (2002) Microcirculation as a target for the anti-inflammatory properties of statins. *Microcirculation* 9: 431-442.
- Schiller PH (1966) Developmental study of color-word interference. *J Exp Psychol* 72: 105-108.
- Schmidt JA, Intaglietta M, Borgström P (1992) Periodic hemodynamics in skeletal muscle during local arterial pressure reduction. *J Appl Physiol* 73: 1077-1083.
- Schroeter ML (1998) The antioxidative system of the blood-brain barrier – influences of astrocytes and hypoxia/reoxygenation. MD Thesis, With Honors (summa cum laude), Humboldt-University Berlin. Available on the internet: <http://dochostr.rz.hu-berlin.de/dissertationen>
- Schroeter ML, Mertsch K, Giese H, Müller S, Sporbert A, Hickel B, Blasig IE (1999) Astrocytes enhance radical defence in capillary endothelial cells constituting the blood-brain barrier. *FEBS Lett* 449: 241-244.
- Schroeter ML, Müller S, Lindenau J, Wiesner B, Hanisch UK, Wolf G, Blasig IE (2001) Astrocytes induce manganese superoxide dismutase in brain capillary endothelial cells. *Neuroreport* 12: 2513-2517.
- Schroeter ML, Kruggel F, von Cramon DY (2002a) The hemodynamic response is reduced in microangiopathy during performance of a Stroop-task and visual stimulation. *Aktuel Neurol* 29 (suppl): S90.
- Schroeter ML, Zysset S, Kupka T, Kruggel F, von Cramon DY (2002b) Near-infrared spectroscopy can detect brain activity during a color-word matching Stroop task in an event-related design. *Hum Brain Mapp* 17: 61-71.
- Schroeter ML, Zysset S, Kruggel F, von Cramon DY (2003) Age-dependency of the hemodynamic response as measured by functional near-infrared spectroscopy. *Neuroimage* 19: 555-564.
- Schroeter ML, Bücheler MM, Müller K, Uludag K, Obrig H, Lohmann G, Tittgemeyer M, Villringer A, von Cramon DY (2004a) Towards a standard analysis for functional near-infrared imaging. *Neuroimage* 21: 283-290.
- Schroeter ML, Schmiedel O, von Cramon DY (2004b) Spontaneous low frequency oscillations decline in the aging brain. *J Cereb Blood Flow Metab* 24: 1183-1191.
- Schroeter ML, Zysset S, von Cramon DY (2004c) Shortening intertrial intervals in event-related cognitive studies with near-infrared spectroscopy. *Neuroimage* 22: 341-346.
- Schroeter ML, Zysset S, Wahl MM, von Cramon DY (2004d) Prefrontal activation due to Stroop interference increases during development - an event-related fNIRS study. *Neuroimage* 23: 1317-1325.
- Seber GAF (1977) *Linear Regression Analysis*. Wiley, New York.

- Seiyama A, Seki J, Tanabe HC, Sase I, Takatsuki A, Miyauchi S, Eda H, Hayashi S, Imaruoka T, Iwakura T, Yanagida T (2004) Circulatory basis of fMRI signals: relationship between changes in the hemodynamic parameters and BOLD signal intensity. *Neuroimage* 21: 1204-1214.
- Shimada S, Hiraki K, Matsuda G, Oda I (2004) Decrease in prefrontal hemoglobin oxygenation during reaching tasks with delayed visual feedback: A near-infrared spectroscopy study. *Cognit Brain Res* 20: 480-490.
- Shimada S, Hiraki K, Oda I (2005) The parietal role in the sense of self-ownership with temporal discrepancy between visual and proprioceptive feedbacks. *Neuroimage* 24: 1225-1232.
- Shimokawa H (1999) Endothelial dysfunction: A novel therapeutic target. Primary endothelial dysfunction: Atherosclerosis. *J Moll Cell Cardiol* 31: 23-37.
- Shinba T, Nagano M, Kariya N, Ogawa K, Shinozaki T, Shimosato S, Hoshi Y (2004) Near-infrared spectroscopy analysis of frontal lobe dysfunction in schizophrenia. *Biol Psychiatry* 55: 154-164.
- Siegel GJ, Agranoff BW, Albers RW, Fisher SK, Uhler MD (Eds.) (1999) *Basic Neurochemistry: Molecular, Cellular and Medical Aspects*. Lippincott Williams & Wilkins, Philadelphia.
- Siegel AM, Culver JP, Mandeville JB, Boas DA (2003) Temporal comparison of functional brain imaging with diffuse optical tomography and fMRI during rat forepaw stimulation. *Phys Med Biol* 48: 1391-1403.
- Slosman DO, Chicherio C, Ludwig C, Genton L, de Ribaupierre S, Hans D, Pichard C, Mayer E, Annoni JM, de Ribaupierre A (2001) ¹³³Xe SPECT cerebral blood flow study in a healthy population: Determination of T-scores. *J Nucl Med* 42: 864-870.
- Sowell ER, Thompson PM, Holmes CJ, Jernigan TL, Toga AW (1999) In vivo evidence for post-adolescent brain maturation in frontal and striatal regions. *Nat Neurosci* 2: 859-861.
- Sowell ER, Thompson PM, Tessner KD, Toga AW (2001) Mapping continued brain growth and gray matter density reduction in dorsal frontal cortex: Inverse relationships during postadolescent brain maturation. *J Neurosci* 21: 8819-8829.
- Stansberry KB, Shapiro SA, Hill MA, McNitt PM, Meyer MD, Vinik AI (1996) Impaired peripheral vasomotion in diabetes. *Diabetes Care* 19: 715-21.
- Steinbrink J, Kohl M, Obrig H, Curio G, Syre F, Thomas F, Wabnitz H, Rinneberg H, Villringer A (2000) Somatosensory evoked fast optical intensity changes detected non-invasively in the adult human head. *Neurosci Lett* 291: 105-108.
- Steinmetz H, Fürst G, Meyer BU (1989) Craniocerebral topography within the international 10-20 system. *Electroencephalogr Clin Neurophysiol* 72: 499-506.
- Stepnoski RA, LaPorta A, Raccaia-Behling F, Blonder GE, Slusher RE, Kleinfeld D (1991) Noninvasive detection of changes in membrane potential in cultured neurons by light scattering. *Proc Natl Acad Sci USA* 88: 9382-9386.
- Stern MD (1975) In vivo evaluation of microcirculation by coherent light scattering. *Nature* 254: 56-58.
- Sterzer P, Meintzschel F, Rösler A, Lanfermann H, Steinmetz H, Sitzer M (2001) Pravastatin improves cerebral vasomotor reactivity in patients with subcortical small-vessel disease. *Stroke* 32: 2817-2820.
- Strangman G, Boas DA, Sutton JP (2002a) Non-invasive neuroimaging using near-infrared light. *Biol Psychiat* 52: 679-693.
- Strangman G, Culver JP, Thompson JH, Boas DA (2002b) A quantitative comparison of simultaneous BOLD fMRI and NIRS recordings during functional brain activation. *Neuroimage* 17: 719-731.
- Strangman G, Franceschini MA, Boas DA (2003) Factors affecting the accuracy of near-infrared spectroscopy concentration calculations for focal changes in oxygenation parameters. *Neuroimage* 18: 865-879.
- Steinmetz H, Fürst G, Meyer BU. 1989. Craniocerebral topography within the international 10-20 system. *Electroenc Clin Neurophysiol* 72: 499-506.
- Stroop J (1935) Studies of interference in serial verbal reactions. *J Exp Psychol* 18: 643-662.
- Suarez E, Viegas MD, Adjouadi M, Barreto A (2000) Relating induced changes in EEG signals to orientation of visual stimuli using the ESI-256 machine. *Biomed Sci Instrum* 36: 33-38.

- Suto T, Fukuda M, Ito M, Uehara T, Mikuni M (2004) Multichannel near-infrared spectroscopy in depression and schizophrenia: Cognitive brain activation study. *Biol Psychiatry* 55: 501-511.
- Suzuki M, Miyai I, Ono T, Oda I, Konishi I, Kochiyama T, Kubota K (2004) Prefrontal and premotor cortices are involved in adapting walking and running speed on the treadmill: An optical imaging study. *Neuroimage* 23: 1020-1026.
- Suzuki M, Gyoba J, Sakuta Y (2005) Multichannel NIRS analysis of brain activity during semantic differential rating of drawing stimuli containing different affective polarities. *Neurosci Letters* 375: 53-58.
- Syre F, Obrig H, Steinbrink J, Kohl M, Wenzel R, Villringer A (2003) Are VEP correlated fast optical signals detectable in the human adult by non-invasive nearinfrared spectroscopy (NIRS)? *Adv Exp Med Biol* 530: 421-431.
- Taga G, Konishi Y, Maki A, Tachibana T, Fujiwara M, Koizumi H (2000) Spontaneous oscillation of oxy- and deoxy-hemoglobin changes with a phase difference throughout the occipital cortex of newborn infants observed using non-invasive optical topography. *Neurosci Lett* 282: 101-104.
- Taga G, Asakawa K, Maki A, Konishi Y, Koizumi H (2003) Brain imaging in awake infants by near-infrared optical topography. *Proc Natl Acad Sci USA* 100: 10722-10727.
- Tamm L, Menon V, Reiss AL (2002) Maturation of brain function associated with response inhibition. *J Am Acad Child Adolesc Psychiatr* 41: 1231-1238.
- Tanida M, Sakatani K, Takano R, Tagai K (2004) Relation between asymmetry of prefrontal cortex activities and the autonomic nervous system during a mental arithmetic task: Near infrared spectroscopy study. *Neurosci Lett* 369: 69-74.
- Tanoi Y, Okeda R, Budka H (2000) Binswanger's encephalopathy: Serial sections and morphometry of the cerebral arteries. *Acta Neuropathol* 100: 347-355.
- Tanosaki M, Hoshi Y, Iguchi Y, Oikawa Y, Oda I, Oda M (2001) Variation of temporal characteristics in human cerebral hemodynamic responses to electric median nerve stimulation: A near-infrared spectroscopic study. *Neurosci Lett* 316: 75-78.
- Tanosaki M, Sato C, Shimada M, Iguchi Y, Hoshi Y (2003) Effect of stimulus frequency on human cerebral hemodynamic responses to electric median nerve stimulation: A near-infrared spectroscopic study. *Neurosci Lett* 352: 1-4.
- Taylor SF, Kornblum S, Lauber EJ, Minoshima S, Koeppe RA (1997) Isolation of specific interference processing in the Stroop task: PET activation studies. *Neuroimage* 6: 81-92.
- Terborg C, Gora F, Weiller C, Rother J (2000) Reduced vasomotor reactivity in cerebral microangiopathy: a study with near-infrared spectroscopy and transcranial Doppler sonography. *Stroke* 31: 924-929.
- Thevenaz P, Blu T, Unser M (2000) Image Interpolation and resampling. In: Bankman IN (Ed.) *Handbook of Medical Image Processing and Analysis*. Academic Press, San Diego, pp. 393-420.
- Tisserand DJ, Pruessner JC, Arigita EJS, van Boxtel MPJ, Evans AC, Jolles J, Uylings HBM (2002) Regional frontal cortical volumes decrease differentially in aging: An fMRI study to compare volumetric approaches and voxel based morphometry. *Neuroimage* 17: 657-669.
- Toichi M, Findling RL, Kubota Y, Calabrese JR, Wiznitzer M, McNamara NK, Yamamoto K (2004) Hemodynamic differences in the activation of the prefrontal cortex: attention vs. higher cognitive processing. *Neuropsychologia* 42: 698-706.
- Toronov V, Webb A, Choi JH, Wolf M, Michalos A, Gratton E, Hueber D (2001a) Investigation of human brain hemodynamics by simultaneous near-infrared spectroscopy and functional magnetic resonance imaging. *Med Phys* 28: 521-527.
- Toronov V, Webb A, Choi JH, Wolf M, Safonova L, Wolf U, Gratton E (2001b) Study of local cerebral hemodynamics by frequency-domain near-infrared spectroscopy and correlation with simultaneously acquired functional magnetic resonance imaging. *Optics Express* 9: 417-427.
- Toronov V, Walker S, Gupta R, Choi JH, Gratton E, Hueber D, Webb A (2003) The roles of changes in deoxyhemoglobin concentration and regional cerebral blood volume in the fMRI BOLD signal. *Neuroimage* 19: 1521-1531.

- Totaro R, Barattelli G, Quaresima V, Carolei A, Ferrari M (1998) Evaluation of potential factors affecting the measurement of cerebrovascular reactivity by near-infrared spectroscopy. *Clin Sci (Colch)* 95: 497-504.
- Tootell RBH, Mendola JD, Hadjikhani NK, Ledden PJ, Liu AK, Reppas JB, Sereno MI, Dale AM (1997) Functional analysis of V3A and related areas in human visual cortex. *J Neurosci* 17: 7060-7078.
- Treisman A & Fearnley S (1969) The Stroop test: selective attention to colours and words. *Nature* 222: 437-439.
- Tsuji M, Duplessis A, Taylor G, Crocker R, Volpe JJ (1998) Near infrared spectroscopy detects cerebral ischemia during hypotension in piglets. *Pediatr Res* 44: 591-595.
- Tsujimoto S, Yamamoto T, Kawaguchi H, Koizumi H, Sawaguchi T (2004) Prefrontal cortical activation associated with working memory in adults and preschool children: An event-related optical topography study. *Cereb Cortex* 14: 703-712.
- Ugurbil K, Garwood M, Ellermann J, Hendrich K, Hinke R, Hu X, Kim SG, Menon R, Merkle H, Ogawa S, Salmi R (1993) Imaging at high magnetic fields: Initial experiences at 4T. *Magn Reson Quart* 9: 259-277.
- Uludag K, Kohl M, Steinbrink J, Obrig H, Villringer A (2002) Crosstalk in the Lambert-Beer calculation for near-infrared wavelengths estimated by Monte Carlo simulations. *J Biomed Optics* 7: 51-59.
- Uludag K, Steinbrink J, Kohl-Bareis M, Wenzel R, Villringer A, Obrig H (2004) Cytochrome-c-oxidase redox changes during visual stimulation measured by near-infrared spectroscopy cannot be explained by a mere cross talk artefact. *Neuroimage* 22: 109-119.
- Unger T, Badoer E, Ganten D, Lang RE, Rettig R (1988) Brain angiotensin: Pathways and pharmacology. *Circulation* 77(suppl I): 1-40.
- Ursino M (1991) Mechanisms of cerebral blood flow regulation. *Crit Rev Biomed Eng* 18: 255-288.
- Vaithianathan T, Tullis IDC, Everdell N, Leung T, Gibson A (2004) Design of a portable near infrared system for topographic imaging of the brain in babies. *Review of Scientific Instruments* 75: 3276-3283.
- Verhaeghen P & De Meersman LD (1998) Aging and the Stroop effect: A meta-analysis. *Psychol Aging* 13: 120-126.
- Villringer A, Planck J, Hock C, Schleinkofer L, Dirnagl U (1993) Near infrared spectroscopy (NIRS) - a new tool to study hemodynamic changes during activation of brain function in human adults. *Neurosci Lett* 154: 101-104.
- Villringer A & Dirnagl U (1995) Coupling of brain activity and cerebral blood flow: Basis of functional neuroimaging. *Cerebrovasc Brain Metab Rev* 7: 240-276.
- Villringer A & Chance B (1997) Non-invasive optical spectroscopy and imaging of human brain function. *Trends Neurosci* 20: 435-442.
- Villringer K, Minoshima S, Hock C, Obrig H, Ziegler S, Dirnagl U, Schwaiger M, Villringer A (1997) Assessment of local brain activation. A simultaneous PET and near-infrared spectroscopy study. *Adv Exp Med Biol* 413: 149-153.
- Watanabe E, Maki A, Kawaguchi F, Takashiro K, Yamashita Y, Koizumi H, Mayanagi Y (1998) Non-invasive assessment of language dominance with near-infrared spectroscopic mapping. *Neurosci Lett* 256: 49-52.
- Watanabe A, Matsuo K, Kato N, Kato T (2003) Cerebrovascular response to cognitive tasks and hyperventilation measured by multi-channel near-infrared spectroscopy. *J Neuropsychiatry Clin Neurosci* 15(4): 442-449.
- Watanabe A & Kato T (2004) Cerebrovascular response to cognitive tasks in patients with schizophrenia measured by near-infrared spectroscopy. *Schizophr Bull* 30: 435-444.
- Weber P, Lutschg J, Fahnenstich H (2004) Attention-induced frontal brain activation measured by near-infrared spectroscopy. *Pediatr Neurol* 31: 96-100.
- Weisskoff RM (1999) Basic theoretical models of BOLD signal change. In: Moonen CTW, Bandettini PA (Eds.) *Functional MRI*. Springer, Berlin, Germany, pp. 115-124.

- Wenzel R, Wobst P, Heekeren HH, Kwong KK, Brandt SA, Kohl M, Obrig H, Dirnagl U, Villringer A (2000) Saccadic suppression induces focal hypooxygenation in the occipital cortex. *J Cereb Blood Flow Metab* 20: 1103-1110.
- Williams R, Ponesse JS, Schachar RJ, Logan GD, Tannock R (1999) Development of inhibitory control across the life span. *Dev Psychol* 35: 205-13.
- Wilson B, Alderman N, Burgess PW, Emslie H, Evans JJ (1996) Behavioral assessment of the dysexecutive syndrome. Thames Valley Test company, Bury St. Edmunds, England.
- Winer BJ, Brown DR, Michels KM (1991) Statistical principles in experimental design. 3rd ed., McGraw Hill, New York.
- Wobst P, Wenzel R, Kohl M, Obrig H, Villringer A (2001) Linear aspects of changes in deoxygenated hemoglobin concentration and cytochrome oxidase oxidation during brain activation. *Neuroimage* 13: 520-530.
- Wolf M, Wolf U, Choi JH, Gupta R, Safonova LP, Paunescu LA, Michalos A, Gratton E (2002a) Functional frequency-domain near-infrared spectroscopy detects fast neuronal signal in the motor cortex. *Neuroimage* 17: 1868-1875.
- Wolf M, Wolf U, Toronov V, Michalos A, Paunescu LA, Choi JH, Gratton E (2002b) Different time evolution of oxy- and deoxyhemoglobin concentration changes in the visual and motor cortices during functional stimulation: A near-infrared spectroscopy study. *Neuroimage* 16: 704-712.
- Wolf M, Wolf U, Choi JH, Toronov V, Paunescu LA, Michalos A, Gratton E (2003) Fast cerebral functional signal in the 100-ms range detected in the visual cortex by frequency-domain near-infrared spectrophotometry. *Psychophysiology* 40: 521-528.
- Wolfram H, Neumann J, Wiczorek V (1986) Psychologische Leistungstests in der Neurologie und Psychiatrie [Psychological performance test for neurology and psychiatry]. Thieme, Leipzig, Germany.
- Wong-Riley MTT (1989) Cytochrome oxidase: An endogenous metabolic marker for neuronal activity. *Trends Neurosci* 12: 94-101.
- Wong-Riley MTT, Nie F, Hevner RF, Liu S (1998) Brain cytochrome oxidase: functional significance and bigenomic regulation in the CNS. In: Gonzalez-Lima F (Ed.) *Cytochrome oxidase in neuronal metabolism and Alzheimer's disease*. Plenum Press, New York, pp. 1-53.
- Worsley KJ, Friston KJ (1995) Analysis of fMRI time-series revisited - again. *Neuroimage* 2: 173-181.
- Wray S, Cope M, Delpy DT, Wyatt JS, Reynolds EO (1988) Characterization of the near infrared absorption spectra of cytochrome aa3 and haemoglobin for the non-invasive monitoring of cerebral oxygenation. *Biochim Biophys Acta* 933: 184-192.
- Zaramella P, Freato F, Amigoni A, Salvadori S, Marangoni P, Suppiej A, Schiavo B, Chiandetti L (2001) Brain auditory activation measured by near-infrared spectroscopy (NIRS) in neonates. *Pediatr Res* 49: 213-219.
- Zeki S (2003) Improbable areas in the visual brain. *Trends Neurosci* 26: 23-26.
- Zeki S, Watson JDG, Lueck CJ, Friston KJ, Kennard C, Frackowiak RSJ (1991) A direct demonstration of functional specialization in human visual cortex. *J Neurosci* 11: 641-649.
- Zhao H, Tanikawa Y, Gao F, Onodera Y, Sassaroli A, Tanaka K, Yamada Y (2002) Maps of optical differential pathlength factor of human adult forehead, somatosensory motor and occipital regions at multi-wavelengths in NIR. *Phys Med Biol* 47: 2075-2093.
- Zimmermann P, Fimm B (1993) Testbatterie zur Aufmerksamkeitsprüfung (TAP) [Test battery for the assessment of attention]. Psytest, Würselen, Germany.
- Zysset S, Müller K, Lohmann G, von Cramon DY (2001) Color-word matching Stroop task: separating interference and response conflict. *Neuroimage* 13: 29-36.

5. Appendix

Optische Bildgebung in der kognitiven Neurowissenschaft - Zusammenfassung

1. Einleitung

In den letzten Jahren wurden verschiedene Verfahren entwickelt, mit deren Hilfe eine neurale Aktivierung im Gehirn untersucht werden kann. Einerseits können elektrophysiologische Verfahren, wie z. B. die Magnetenzephalographie (MEG) und die Elektroenzephalographie (EEG) inklusive der Messung ereigniskorrelierter Potentiale (EKP), die neurale Aktivierung direkt messen. Entsprechend haben sie eine hohe zeitliche Auflösung, während ihre räumliche Auflösung jedoch begrenzt ist. Andererseits nutzen indirekte Verfahren das Prinzip der neurovaskulären Kopplung, welches von einer überproportionalen Steigerung des regionalen zerebralen Blutflusses im Verhältnis zur Erhöhung des Sauerstoff- und Glukoseverbrauches ausgeht. Diese indirekten Verfahren messen Veränderungen des zerebralen Blutflusses, des zerebralen Blutvolumens bzw. der Blutoxygenierung. Sie umfassen die Positronenemissionstomographie (PET), die Single-Positronenemissionscomputertomographie (SPECT) sowie die weitverbreitete funktionelle Magnetresonanztomographie (fMRT). Während die PET und SPECT den Zerfall radioaktiver Isotope nutzen, basiert die fMRT auf der Messung der Blutoxygenierung mittels des blood oxygenation level dependent (BOLD-) Kontrastes.

Seit der Erstbeschreibung durch Jöbsis im Jahre 1977 ist die Methode der optischen Bildgebung bzw. funktionellen Nahinfrarot-Spektroskopie (fNIRS) bekannt. Sie nutzt die Tatsache, daß Licht im Nahinfrarotbereich die Schädelkalotte durchdringen kann und daß oxygeniertes und deoxygeniertes Hämoglobin sowie das Atmungskettenenzym Cytochromoxidase durch spezifische Absorptionsspektren in diesem Bereich des Lichtes gekennzeichnet sind. Insofern können, bei Messung mit mehreren Wellenlängen, Änderungen dieser sogenannten Chromophoren bestimmt werden. Da die optische Bildgebung hiermit für die Blutoxygenierung sensitiv ist, ordnet sie sich in die indirekten Verfahren ein. Für sämtliche indirekte Verfahren ist charakteristisch, daß ihre zeitliche Auflösung aufgrund der Trägheit der neurovaskulären Kopplung begrenzt ist. Die räumliche Auflösung ist hingegen, besonders bei der fMRT, gut.

Die Vorteile der optischen Bildgebung (fNIRS) liegen in der leichten Anwendbarkeit, der biochemischen Spezifität (definierte biochemische Substanzen können detektiert werden), den geringen Kosten, der hohen zeitlichen Auflösung (ms) und der leichten Kombinierbarkeit

mit anderen (im besonderen elektrophysiologischen) Verfahren. Durch die Untersuchung der Blutoxygenierung und der Cytochromoxidase können gleichzeitig vaskuläre-extrazelluläre und intrazelluläre Parameter erfaßt werden. Die relativ geringe Empfindlichkeit gegenüber Bewegungsartefakten und die geringe Inanspruchnahme der Probanden durch die Methode lassen sie besonders für Studien zur Entwicklung kognitiver Funktionen, zur Untersuchung von Alterungsprozessen und für Patientenstudien geeignet erscheinen. Bezüglich der Nachteile ist zu erwähnen, daß die räumliche Auflösung beschränkt (cm) und die Eindringtiefe auf den äußeren Kortex begrenzt ist. Insofern sind Aktivierungen in medianen kortikalen Arealen nicht detektierbar.

In den letzten Jahren wurde die optische Bildgebung bevorzugt zur Untersuchung der Gehirnaktivierung während Stimulation von primären kortikalen (motorischen bzw. visuellen) Arealen eingesetzt. Hiermit wurde die Methode validiert und die Physiologie der neurovaskulären Kopplung untersucht. Kognitive Studien konzentrierten sich auf exekutive Funktionen bzw. Sprachaufgaben. Bisher wurden im wesentlichen Block-Designs angewendet, ereigniskorrelierte Studien fanden sich hingegen kaum.

Entsprechend den Vorteilen der Methode zielten die am Max-Planck-Institut für Kognitions- und Neurowissenschaften in den Jahren von 2000 bis 2005 durchgeführten Experimente auf die Beantwortung der folgenden Fragen:

- Welche Gehirnareale können mit der optischen Bildgebung untersucht werden? Was ist das typische Muster bzgl. der Chromophore während einer kortikalen Stimulation? Können die fMRT und fNIRS simultan eingesetzt werden?
- Können ereigniskorrelierte Stimulationsdesigns während kognitiver fNIRS-Studien eingesetzt werden? Können die Abstände zwischen den einzelnen Versuchsdurchläufen (Trials) optimiert werden?
- Sind kognitive ereigniskorrelierte fNIRS-Studien mit Kindern, älteren Probanden und Patienten möglich?
- Welche statistischen Verfahren sind als Standardverfahren für die optische Bildgebung geeignet?

2. Experimente

Die zur Beantwortung der aufgeworfenen Fragen durchgeführten Experimente sollen nunmehr zusammengefaßt werden. Das erste Experiment untersuchte die Gehirnaktivierung im visuellen Kortex während einer Stimulation mit roten sich um die eigene Achse drehenden Ls. Parallel wurde die hämodynamische Antwort mit fNIRS und fMRT gemessen. Um den sogenannten Poststimulus-Undershoot des BOLD-Signales mit zu erfassen, wurde ein langer Abstand (ca. 60 s) zwischen den einzelnen Versuchsdurchläufen gewählt.

Während bzw. kurz nach der Stimulation stiegen die Konzentrationen von oxygeniertem Hämoglobin, Gesamthämoglobin, der Redox-Status der Cytochromoxidase und das BOLD-Signal an, während die Konzentration von deoxygeniertem Hämoglobin abfiel. Während des Poststimulus-Undershoot fand sich ein inverses Muster, das oxygenierte Hämoglobin und das BOLD-Signal fielen ab, währenddessen die Konzentration des deoxygenierten Hämoglobins anstieg. Das Gesamthämoglobin und die Cytochromoxidase veränderten sich hingegen nicht signifikant.

Hiermit zeigten die Veränderungen direkt nach Stimulationsbeginn das typische durch einen Anstieg der Blutoxygenierung bedingte Muster an. Die Veränderungen während des Poststimulus-Undershoot wiesen auf einen prolongierten Sauerstoffverbrauch hin. Von den Chromophoren war das deoxygenierte Hämoglobin am engsten mit dem BOLD-Signal korreliert, was mit der Auslösung des BOLD-Signales durch das paramagnetische deoxygenierte Hämoglobin erklärt werden kann. Die Eindringtiefe des nahinfraroten Lichtes betrug in unserer Studie ca. 1,5 cm, was mit der Detektierbarkeit von Gehirnaktivierungen in den äußeren kortikalen Arealen korreliert. Im Resultat konnten die ersten Fragen beantwortet werden. Parallele Experimente mit der fNIRS und fMRT sind möglich und können zu neuen Erkenntnissen bezüglich der neurovaskulären Kopplung führen.

Die folgenden Experimente untersuchten die Möglichkeit ereigniskorrelierter Stimulationsdesigns während kognitiver fNIRS-Studien. Als Paradigma wurde die Farb-Wort-Interferenz-Aufgabe nach Stroop angewendet, da das erstmalig 1935 von Stroop beschriebene Phänomen der Farb-Wort-Interferenz ein stabiles Paradigma darstellt und bereits in verschiedenen fMRT-Studien zuverlässig zu lateralen (frontoparietalen) kortikalen Aktivierungen geführt hatte. Während der Stroop-Aufgabe wird den Probanden ein farbiges Wort, welches ebenfalls eine Farbe bedeutet, präsentiert. Sollen die Probanden die Bedeutung des Wortes benennen indem sie es lesen, treten keine Schwierigkeiten auf. Soll jedoch die Farbe des Wortes benannt werden, tritt bei nicht übereinstimmender

Wortbedeutung eine zeitliche Verzögerung und höhere Fehlerrate auf. Dieses Phänomen wird als Stroop-Interferenz bezeichnet.

Das Paradigma erzeugte auch in unseren Experimenten eine stabile Interferenz bezüglich der Fehlerrate und der Reaktionszeiten (gemessen als Differenz zwischen inkongruenter und neutraler Bedingung). Im lateralen frontalen Kortex zeigten sich stärkere Aktivierungen während der inkongruenten im Vergleich mit der neutralen Bedingung der Stroop-Aufgabe, was eine Bedeutung frontolateraler Areale für die Bewältigung der Interferenz anzeigt. Zur Analyse wurde an jeden einzelnen Durchlauf eine Gauß-Funktion angepaßt. Bei der Beschreibung mit den Parametern Höhe der hämodynamischen Antwort, Breite und Lag (Verzögerung) derselben stellte sich heraus, daß das deoxygenierte Hämoglobin während der inkongruenten Bedingung im Verhältnis zum oxygenierten Hämoglobin im zeitlichen Verlauf verzögert war. Dieses Phänomen führten wir auf einen durch die Interferenz bedingten erhöhten Sauerstoffverbrauch zurück.

Nachdem gezeigt werden konnte, daß ereigniskorrelierte Stimulationsdesigns sehr wohl für die optische Bildgebung angewendet werden können, zielte das folgende Experiment auf eine Optimierung der Intervalle zwischen den experimentellen Durchläufen. Wie bereits im vorherigen Experiment wurde die Farb-Wort-Interferenz-Aufgabe nach Stroop in einem ereigniskorrelierten Stimulationsdesign herangezogen. Die Intertrialintervalle wurden von 12 s, über 6 und 4 s bis zu 2 s variiert.

Für jedes Intertrialintervall wurde eine signifikante behaviorale Stroop-Interferenz gefunden. Die hämodynamische Antwort war größer während inkongruenter Durchläufe verglichen mit neutralen Durchläufen für 12 s, 6 s und 2 s. Ein Intertrialintervall von 4 s ergab keinen signifikanten Unterschied. Interessanterweise war für ebendieses Intertrialintervall auch die Effektstärke der behavioralen Interferenz von allen Intertrialintervallen am geringsten, was eine optimale Performanz der Probanden vermuten läßt. Offensichtlich benötigten die Probanden nur eine geringe zusätzliche Gehirnaktivierung, um die Stroop-Interferenz bewältigen zu können. Für die anderen Intertrialintervalle galt, daß die Effektstärke der hämodynamischen Antwort mit Verringerung der Länge des Intertrialintervalls zunahm. Daraus kann abgeleitet werden, daß in kognitiven Studien eine Verkürzung der Intertrialintervalle grundsätzlich zu einer Verbesserung des Signal-Rausch-Verhältnisses führen kann.

Mit den zwei letztgenannten Studien konnte der zweite Fragekomplex beantwortet werden. Demnach sind ereigniskorrelierte kognitive fNIRS-Studien möglich. Prinzipiell scheint eine Verkürzung der Intertrialintervalle sinnvoll zu sein.

In den folgenden Experimenten sollte untersucht werden, ob kognitive ereigniskorrelierte fNIRS-Studien mit Kindern, älteren Probanden und Patienten möglich sind. Wiederum wurde aus den bereits genannten Gründen die Farb-Wort-Interferenz-Aufgabe nach Stroop eingesetzt.

Zuerst wurden Kinder mit einem Alter von 7-13 Jahren untersucht. Erneut zeigte sich ein signifikanter behavioraler Interferenz-Effekt. In Übereinstimmung mit der Literatur, die eine abnehmende Stroop-Interferenz mit der Entwicklung zum Erwachsenenalter berichtet, war der Interferenzeffekt bei den Kindern größer als bei den Erwachsenen. Bezüglich der Gehirnaktivierung zeigte sich, daß Kinder bevorzugt den linken lateralen präfrontalen Kortex aktivieren, was mit der verbalen Dimension der Stroop-Aufgabe korrespondiert.

Wenn die Kinder und Erwachsenen aus der vorherigen Studie zusammengefaßt wurden, ergab eine Regressionsanalyse, daß die durch die Interferenz hervorgerufene Gehirnaktivierung im dorsolateralen präfrontalen Kortex mit dem Alter zunahm. Diese Ergebnisse stimmen gut mit morphometrischen und histologischen Studien überein, die eine Reifung des dorsolateralen präfrontalen Kortex bis hinein ins Erwachsenenalter beschreiben. Interessanterweise zeigten die Kinder eine wesentlich höhere Variabilität der hämodynamischen Daten als die Erwachsenen, was bei Korrelation mit der behavioralen Performanz auf eine unterschiedlich weit fortgeschrittene kognitive Entwicklung bei den Kindern zurückgeführt werden kann.

Im Ergebnis ist die Anwendung der fNIRS für ereigniskorrelierte kognitive Studien bei Kindern sehr wohl möglich und als gegenüber Bewegungsartefakten relativ unempfindliches Verfahren als besonders geeignet einzustufen.

In der nächsten Studie wurde das kognitive Altern untersucht. Erneut wurde die Farb-Wort-Interferenz-Aufgabe nach Stroop in einem ereigniskorrelierten Design als Paradigma ausgewählt. Die Konzentrationsänderungen der Chromophore wurden in unseren Studien prinzipiell mittels des modifizierten Lambert-Beerschen Gesetzes berechnet. In dieses geht als Faktor der sogenannte differentielle Weglängenfaktor ein, der für Streuungseffekte korrigiert. Dieser Faktor ist in hohem Maße altersabhängig. Deshalb verwendeten wir in unserer Studie ein Analyseverfahren zur Berechnung des Signal-Rausch-Verhältnisses,

genauer Effektstärken, welche altersunabhängig sind, da hierbei der differentielle Weglängenfaktor entfällt.

Behavioral nahm der Interferenzeffekt mit dem Alter zu. Die Analyse mit Effektstärken zeigte jedoch, daß kein signifikanter Unterschied mehr zwischen den Reaktionszeiten beider Gruppen zu verzeichnen war. Dieses Ergebnis unterstützt sogenannte General-Slowing-Theorien des Alterns, welche Altersveränderungen mit einer generellen kognitiven Verlangsamung erklären.

Obwohl die älteren Probanden wie die jüngeren Probanden ein laterales präfrontales Netzwerk aktivierten, war die Aktivierung bei den älteren Probanden prinzipiell geringer und ein signifikanter Interferenzeffekt konnte nicht an allen gemessenen präfrontalen Positionen nachgewiesen werden. Die Analyse mittels Effektstärken ergab eine spezifische altersabhängige Reduktion der präfrontalen Aktivierung, mithin in assoziativen kortikalen Regionen. Im Gegensatz dazu waren die Effektstärken in primären (motorischen) Arealen gleich.

Diese Ergebnisse stimmen gut mit in der Literatur berichteten Studien überein, welche einen mit dem Alter reduzierten Blutfluß in zuerst assoziativen und später primären Kortexarealen sowie eine altersabhängige Abnahme des Volumens der präfrontalen grauen Substanz und eine Reduktion der Dendriten in der Schicht V in diesem Bereich beschreiben.

Zusammengefaßt kann von den Ergebnissen unserer Studie in Kombination mit den Literaturangaben auf eine Abnahme der hämodynamischen Antwort (und mithin der Gehirnaktivierung) ab dem 50. Lebensjahr in assoziativen Cortices und ab dem 65. Lebensjahr in primären Cortices geschlossen werden. Die optische Bildgebung scheint zur Untersuchung des kognitiven Alterns geeignet zu sein, wenn die Altersabhängigkeit des differentiellen Weglängenfaktors berücksichtigt wird.

Diese Ergebnisse konnten mit der nachfolgenden Studie unterstützt werden. Hierbei verglichen wir spontane hämodynamische Oszillationen bei jüngeren und älteren Erwachsenen während visueller Stimulation mit einem Schachbrettmuster und unter Ruhebedingungen.

Bezüglich der visuellen Stimulation waren die hämodynamischen Antworten bei beiden Altersgruppen vergleichbar. Bei Analyse der Zeitreihen mit einer Power-Spektrum-Analyse konnten die aus der Literatur bekannten langsamen und sehr langsamen Oszillationen

dargestellt werden. Für die Power-Spektrum-Analyse wurden die Daten vor dem Vergleich normalisiert, um wiederum eine von dem differentiellen Weglängenfaktor unabhängige Auswertung zu ermöglichen. Ein spezifischer Alterseffekt konnte für die langsamen spontanen Oszillationen detektiert werden, welche mit dem Alter abnahmen. Dieses Ergebnis stimmt gut mit histologischen und physiologischen Berichten überein, die eine Abnahme der vaskulären Reagibilität mit dem Alter beschreiben.

Die optische Bildgebung scheint aufgrund ihrer hohen zeitlichen Auflösung besonders für die Untersuchung von spontanen Oszillationen geeignet zu sein.

Im letzten Teil des dritten Fragekomplexes war die Eignung der fNIRS für Patientenstudien zu betrachten. Als Patientengruppe wählten wir Patienten mit einer zerebralen Mikroangiopathie bzw. subkortikalen vaskulären Enzephalopathie aus, da die Pathologie hierbei diffus über das gesamte Gehirn verteilt und somit die relativ geringe räumliche Auflösung der Methode von untergeordneter Bedeutung ist. Außerdem scheint die fNIRS aufgrund ihrer spezifischen Sensitivität für das mikrovaskuläre Kompartiment für diese Patientengruppe besonders geeignet zu sein.

Erneut wurde die Farb-Wort-Interferenz-Aufgabe nach Stroop in einem ereigniskorrelierten Design als Paradigma ausgewählt. Die Patienten reagierten generell langsamer als die Kontrollprobanden. Des weiteren war der behaviorale Interferenzeffekt bei den Patienten stärker ausgeprägt.

Bezüglich der hämodynamischen Antwort zeigten die Patienten im Vergleich mit den Kontrollprobanden eine geringere Stärke während der Stroop-Aufgabe. Außerdem war die hämodynamische Antwort bei den Patienten verzögert. Diese Ergebnisse korrespondieren gut mit Literaturangaben, welche eine reduzierte frontale Gefäßreagibilität bei Patienten mit zerebraler Mikroangiopathie berichteten.

In der folgenden Studie verglichen wir die spontanen hämodynamischen Oszillationen bei Patienten mit zerebraler Mikroangiopathie mit Kontrollprobanden wiederum während visueller Stimulation mit einem Schachbrettmuster und unter Ruhebedingungen. Dieses Experiment erschien insbesondere deshalb interessant, weil die Mikroangiopathie die kleinen Gefäße betrifft und diese gut mit der fNIRS erfaßt werden können.

Bezüglich der visuellen Stimulation waren die hämodynamischen Antworten in der Patienten- und der Kontrollgruppe vergleichbar. Bei der Analyse der Zeitreihen mit einer Power-

Spektrum-Analyse konnten erneut die aus der Literatur bekannten langsamen und sehr langsamen Oszillationen dargestellt werden. Für die Power-Spektrum-Analyse wurden die Daten vor dem Vergleich normalisiert, um eine von dem differentiellen Weglängenfaktor unabhängige Auswertung zu ermöglichen.

In der Patientengruppe zeigte sich wie bereits während des Alterns eine Abnahme der langsamen spontanen Oszillationen. Interessanterweise stellte sich in einer Analyse, die den Einfluß der vaskulären Risikofaktoren einbezog, heraus, daß diese Abnahme auf den Faktor arterielle Hypertonie zurückzuführen war. Weiterhin zeigte sich, daß Diabetes mellitus ebenfalls zu einer Reduktion der langsamen spontanen Oszillationen führte. Diese Ergebnisse unterstützen Literaturangaben, welche die arterielle Hypertonie und den Diabetes mellitus als wesentliche Risikofaktoren für eine zerebrale Mikroangiopathie betrachten.

Zusätzlich zeigte sich eine Verminderung der vaskulären Reagibilität (Stimulation vs. Ruhebedingung) in der Patientengruppe in Übereinstimmung mit histologischen und physiologischen Untersuchungen. Die genannten Veränderungen waren bei den Patienten spezifisch mit den neuropsychologischen Defiziten, insbesondere der exekutiven Dysfunktion, korreliert. Für die morphologische Ausprägung der zerebralen Mikroangiopathie, wie sie im anatomischen MRT analysiert wurde, fand sich kein solcher Zusammenhang.

Zusammengefaßt scheint die zerebrale Mikroangiopathie jene bereits durch das Altern ausgelösten Prozesse zu beschleunigen und zu einer Beeinträchtigung der Autoregulation zu führen. Weiterhin zeigen die Ergebnisse, daß die Untersuchung spontaner Oszillationen mit einer Spektralanalyse wesentlich sensitiver für durch den Alterungsprozeß bzw. eine zerebrale Mikroangiopathie bedingte Alterationen als eine herkömmliche Zeitreihenanalyse ist.

Die letzten Experimente konnten den dritten Fragekomplex beantworten, indem sie zeigten, daß kognitive ereigniskorrelierte fNIRS-Studien mit Kindern, älteren Probanden und Patienten möglich sind. Zusätzlich konnte gezeigt werden, daß die optische Bildgebung aufgrund ihrer hohen zeitlichen Auflösung besonders für die Untersuchung von spontanen Oszillationen geeignet ist.

Inhaltlich konnten die in der Einleitung hervorgebrachten Vorteile der optischen Bildgebung offensichtlich zur Geltung gebracht werden. Bisher nutzten fNIRS-Studien jedoch

verschiedene Analyseverfahren. Um eine weitere erfolgreiche Anwendung der optischen Bildgebung zu ermöglichen, sollte das letzte Experiment die Frage beantworten, welche statistischen Verfahren als Standardverfahren für die optische Bildgebung geeignet sein könnten. Hierzu wurden zwei visuelle Paradigmen verwendet, die sich bezüglich der Verwendung von sich bewegenden Stimulationsreizen unterschieden. Für die bewegten Stimulationsreize erwarteten wir eine spezifische Aktivierung der Region V5 im okzipitotemporalen Übergang. Um die Aktivierung in diesem Areal messen zu können, wählten wir ein optisches Imaging-Gerät zur zweidimensionalen Darstellung der Hirnaktivität.

Als Analyseverfahren benutzten wir das in fMRT-Studien verbreitete allgemeine lineare Modell und eine Spektral(kohärenz)analyse (letztere nach Normalisierung der Daten). Beide Verfahren sind unabhängig von dem intra- und interindividuell hochvariablen differentiellen Weglängenfaktor und insofern besonders für die optische Bildgebung geeignet.

Die Auswertung mit dem allgemeinen linearen Modell ergab tatsächlich eine spezifische Aktivierung des Areals V5 bei der Stimulation mit bewegten Stimulationsreizen. Die Spektralanalyse zeigte, daß bei hoher Kohärenz die hämodynamische Antwort in V5 im Verhältnis zum primären visuellen Kortex um einige Sekunden verzögert war.

In Beantwortung des vierten Fragekomplexes möchten wir die Analyse mit Effektstärken, die Normalisierung von Powerspektren und die Anwendung des linearen Modells als Standardmethoden für die optische Bildgebung vorschlagen, da diese drei Verfahren vom hochvariablen differentiellen Weglängenfaktor unabhängig sind.

3. Zusammenfassung

Unsere Untersuchungen ordnen sich in die internationalen Bemühungen ein, die optische Bildgebung als Standardverfahren in der kognitiven Neurowissenschaft zu etablieren. Nachdem wir die neurovaskuläre Kopplung in einem multimodalen Experiment untersucht hatten, zeigten wir, daß ereigniskorrelierte kognitive Studien bei gesunden Erwachsenen, Kindern, älteren Probanden und neuropsychiatrischen Patienten möglich sind und im Vergleich mit anderen bildgebenden Verfahren auch neuartige Erkenntnisse erbringen können. Zuletzt schlugen wir drei verschiedene Standardverfahren für die optische Bildgebung vor.

Bisher sind nach Recherchen in Medline und Current Contents 58 kognitive fNIRS-Studien publiziert worden. Diese Studien untersuchten im wesentlichen exekutive Funktionen,

Sprachprozesse, Prozesse der kognitiven Entwicklung und psychiatrische Patienten. Insofern können die von uns gewählten Populationen in einen allgemeinen Trend eingeordnet werden, der die schrittweise Etablierung der optischen Bildgebung in diesen Bereichen betrifft.

Aus den am Anfang diskutierten Vorteilen der Methode und den bisherigen Studienergebnissen kann geschlußfolgert werden, daß die Methode aufgrund der relativ geringen Artefaktanfälligkeit und der geringen Inanspruchnahme der Probanden besonders für psychiatrische und neurologische Patienten sowie Entwicklungs- und Altersstudien geeignet ist. Weiterhin ist die Methode bei Studien, welche Kognitionen in bezug zu Handlungen untersuchen wollen, also bezüglich exekutiver Funktionen zu empfehlen. Ein weiteres Gebiet eröffnet sich mit der Erforschung von therapeutischen Effekten, wofür die Methode prädestiniert scheint.

In der Zukunft wäre nach noch ausstehenden methodischen Entwicklungen die Möglichkeit gegeben, zusätzlich die zweidimensionale Bildgebung intrazellulärer Parameter (Cytochromoxidase) einzubeziehen.

Eidesstattliche Erklärung

Hiermit versichere ich an Eides statt, daß ich die vorliegende Habilitation ohne unerlaubte Hilfe angefertigt, das benutzte Schrifttum vollständig erwähnt habe und daß die Habilitation noch von keiner anderen Fakultät abgelehnt worden ist.

Die in dieser Arbeit angegebenen Experimente sind nach entsprechender Anleitung durch Herrn Prof. D. Yves von Cramon von mir selbst am Max-Planck-Institut für Kognitions- und Neurowissenschaften durchgeführt und ausgewertet worden. Die in den Kapiteln 2.2. und 2.5.1. beschriebenen Experimente wurden gemeinsam mit Herrn Thomas Kupka, jene in den Kapiteln 2.6.3., 2.7.2. und 2.8. gemeinsam mit Herrn Markus Bücheler durchgeführt und ausgewertet.

Lebenslauf

Persönliche Angaben

Name	Dr. med. habil. Matthias L. Schroeter, M.A.
Adresse	Max-Planck-Institut für Kognitions- und Neurowissenschaften Stephanstr. 1A, 04103 Leipzig, Germany
Telephon	++49-341-9724982
Fax	++49-341-9940221
e-mail	schroet@cbs.mpg.de
Geburtsdatum	22. Oktober 1965
Nationalität	Deutsch

Berufliche Tätigkeit

Mai 2004	Facharzt für Psychiatrie & Psychotherapie
Sept 2000 – dato	Wissenschaftlicher Mitarbeiter Max-Planck-Institut für Kognitions- und Neurowissenschaften Abteilung Kognitive Neurologie, Leipzig
April 2003 – dato	Wissenschaftlicher Mitarbeiter/Facharzt Tagesklinik für kognitive Neurologie, Universität Leipzig
Aug 1994 – Sept 2002	Ausbildung in Psychotherapie: Systemische und Familientherapie Kognitive Verhaltenstherapie
Aug 1998 – Juli 2000	Assistenzarzt Abteilung für Psychiatrie, Königin-Elisabeth-Krankenhaus/ Humboldt-Universität Berlin
Nov 1998	Promotion (Dr. med.) Humboldt-Universität Berlin
Aug 1996 – Aug 2000	Mitglied im Graduiertenkolleg Schadensmechanismen im zentralen Nervensystem – Einsatz bildgebender Verfahren
Mai 1996 – Juni 1998	Wissenschaftlicher Mitarbeiter Forschungsinstitut für Molekulare Pharmakologie Berlin Abteilung Signaltransduktion/Molekulare Medizin
Nov 1994 – April 1996	Arzt im Praktikum Abteilung für Psychiatrie, Königin-Elisabeth-Krankenhaus/ Humboldt-Universität Berlin
Sept 1987 – Okt 1994	Studium der Humanmedizin, Humboldt-Universität Berlin (Charité)
Sept 1993 – Aug 1999	Studium der Philosophie, Technische Universität Berlin, Freie Universität und Humboldt-Universität Berlin
Sept 1972 – Aug 1984	Schulbesuch, Abitur, Gymnasium zum Grauen Kloster in Berlin
Sept 1984 – Aug 1987	Arbeit als Pfleger und Absolvierung der Wehrpflicht

MPI Series in Human Cognitive and Brain Sciences:

- 1 Anja Hahne
Charakteristika syntaktischer und semantischer Prozesse bei der auditiven Sprachverarbeitung: Evidenz aus ereigniskorrelierten Potentialstudien
- 2 Ricarda Schubotz
Erinnern kurzer Zeitdauern: Behaviorale und neurophysiologische Korrelate einer Arbeitsgedächtnisfunktion
- 3 Volker Bosch
Das Halten von Information im Arbeitsgedächtnis: Dissoziationen langsamer corticaler Potentiale
- 4 Jorge Jovicich
An investigation of the use of Gradient- and Spin-Echo (GRASE) imaging for functional MRI of the human brain
- 5 Rosemary C. Dymond
Spatial Specificity and Temporal Accuracy in Functional Magnetic Resonance Investigations
- 6 Stefan Zysset
Eine experimentalpsychologische Studie zu Gedächtnisabrufprozessen unter Verwendung der funktionellen Magnetresonanztomographie
- 7 Ulrich Hartmann
Ein mechanisches Finite-Elemente-Modell des menschlichen Kopfes
- 8 Bertram Opitz
Funktionelle Neuroanatomie der Verarbeitung einfacher und komplexer akustischer Reize: Integration haemodynamischer und elektrophysiologischer Maße
- 9 Gisela Müller-Plath
Formale Modellierung visueller Suchstrategien mit Anwendungen bei der Lokalisation von Hirnfunktionen und in der Diagnostik von Aufmerksamkeitsstörungen
- 10 Thomas Jacobsen
Characteristics of processing morphological structural and inherent case in language comprehension
- 11 Stefan Kölsch
Brain and Music
A contribution to the investigation of central auditory processing with a new electrophysiological approach

- 12 Stefan Frisch
Verb-Argument-Struktur, Kasus und thematische Interpretation beim Sprachverstehen
- 13 Markus Ullsperger
The role of retrieval inhibition in directed forgetting – an event-related brain potential analysis
- 14 Martin Koch
Measurement of the Self-Diffusion Tensor of Water in the Human Brain
- 15 Axel Hutt
Methoden zur Untersuchung der Dynamik raumzeitlicher Signale
- 16 Frithjof Kruggel
Detektion und Quantifizierung von Hirnaktivität mit der funktionellen Magnetresonanztomographie
- 17 Anja Dove
Lokalisierung an internen Kontrollprozessen beteiligter Hirngebiete mithilfe des Aufgabenwechselfaradigmas und der ereigniskorrelierten funktionellen Magnetresonanztomographie
- 18 Karsten Steinhauer
Hirnphysiologische Korrelate prosodischer Satzverarbeitung bei gesprochener und geschriebener Sprache
- 19 Silke Urban
Verbinformationen im Satzverstehen
- 20 Katja Werheid
Implizites Sequenzlernen bei Morbus Parkinson
- 21 Doreen Nessler
Is it Memory or Illusion? Electrophysiological Characteristics of True and False Recognition
- 22 Christoph Herrmann
Die Bedeutung von 40-Hz-Oszillationen für kognitive Prozesse
- 23 Christian Fiebach
Working Memory and Syntax during Sentence Processing.
A neurocognitive investigation with event-related brain potentials and functional magnetic resonance imaging
- 24 Grit Hein
Lokalisation von Doppelaufgabendefiziten bei gesunden älteren Personen und neurologischen Patienten

- 25 Monica de Filippis
Die visuelle Verarbeitung unbeachteter Wörter.
Ein elektro-physiologischer Ansatz
- 26 Ulrich Müller
Die katecholaminerge Modulation präfrontaler kognitiver Funktionen
beim Menschen
- 27 Kristina Uhl
Kontrollfunktion des Arbeitsgedächtnisses über interferierende Information
- 28 Ina Bornkessel
The Argument Dependency Model: A Neurocognitive Approach to Incremental
Interpretation
- 29 Sonja Lattner
Neurophysiologische Untersuchungen zur auditorischen Verarbeitung
von Stimminformationen
- 30 Christin Grünewald
Die Rolle motorischer Schemata bei der Objektrepräsentation:
Untersuchungen mit funktioneller Magnetresonanztomographie
- 31 Annett Schirmer
Emotional Speech Perception: Electrophysiological Insights into the
Processing of Emotional Prosody and Word Valence in Men and
Women
- 32 André J. Szameitat
Die Funktionalität des lateral-präfrontalen Cortex für die Verarbeitung
von Doppelaufgaben
- 33 Susanne Wagner
Verbales Arbeitsgedächtnis und die Verarbeitung ambiger Wörter in
Wort- und Satzkontexten
- 34 Sophie Manthey
Hirn und Handlung: Untersuchung der Handlungsrepräsentation im ventralen
prämotorischen Cortex mit Hilfe der funktionellen Magnet-Resonanz-
Tomographie
- 35 Stefan Heim
Towards a Common Neural Network Model of Language Production and
Comprehension: fMRI Evidence for the Processing of Phonological and
Syntactic Information in Single Words
- 36 Claudia Friedrich
Prosody and spoken word recognition: Behavioral and ERP correlates

- 37 Ulrike Lex
Sprachlateralisierung bei Rechts- und Linkshändern mit funktioneller Magnetresonanztomographie
- 38 Thomas Arnold
Computergestützte Befundung klinischer Elektroenzephalogramme
- 39 Carsten H. Wolters
Influence of Tissue Conductivity Inhomogeneity and Anisotropy on EEG/MEG based Source Localization in the Human Brain
- 40 Ansgar Hantsch
Fisch oder Karpfen? Lexikale Aktivierung von Benennungsalternativen bei der Objektbenennung
- 41 Peggy Bungert
Zentralnervöse Verarbeitung akustischer Informationen Signalidentifikation, Signallateralisation und zeitgebundene Informationsverarbeitung bei Patienten mit erworbenen Hirnschädigungen
- 42 Daniel Senkowski
Neuronal correlates of selective attention: An investigation of electrophysiological brain responses in the EEG and MEG
- 43 Gert Wollny
Analysis of Changes in Temporal Series of Medical Images
- 44 Angelika Wolf
Sprachverstehen mit Cochlea-Implantat: EKP-Studien mit postlingual ertaubten erwachsenen CI-Trägern
- 45 Kirsten G. Volz
Brain correlates of uncertain decisions: Types and degrees of uncertainty
- 46 Hagen Huttner
Magnetresonanztomographische Untersuchungen über die anatomische Variabilität des Frontallappens des menschlichen Großhirns
- 47 Dirk Köster
Morphology and Spoken Word Comprehension: Electrophysiological Investigations of Internal Compound Structure
- 48 Claudia A. Hruska
Einflüsse kontextueller und prosodischer Informationen in der auditorischen Satzverarbeitung: Untersuchungen mit ereigniskorrelierten Hirnpotentialen

- 49 Hannes Ruge
Eine Analyse des raum-zeitlichen Musters neuronaler Aktivierung im Aufgabenwechselfparadigma zur Untersuchung handlungssteuernder Prozesse
- 50 Ricarda I. Schubotz
Human premotor cortex: Beyond motor performance
- 51 Clemens von Zerssen
Bewusstes Erinnern und falsches Wiedererkennen:
Eine funktionelle MRT Studie neuroanatomischer Gedächtniskorrelate
- 52 Christiane Weber
Rhythm is Gonna Get you.
Electrophysiological Markers of Rhythmic Processing in Infants with and without Risk for Specific Language Impairment (SLI)
- 53 Marc Schönwiesner
Functional Mapping of Basic Acoustic Parameters in the Human Central Auditory System
- 54 Katja Fiehler
Temporospatial characteristics of error correction
- 55 Britta Stolterfoht
Processing Word Order Variations and Ellipses: The Interplay of Syntax and Information Structure during Sentence Comprehension
- 56 Claudia Danielmeier
Neuronale Grundlagen der Interferenz zwischen Handlung und visueller Wahrnehmung
- 57 Margret Hund-Georgiadis
Die Organisation von Sprache und ihre Reorganisation bei ausgewählten, neurologischen Erkrankungen gemessen mit funktioneller Magnetresonanztomographie – Einflüsse von Händigkeit, Läsion, Performanz und Perfusion
- 58 Jutta L. Mueller
Mechanisms of auditory sentence comprehension in first and second language: An electrophysiological miniature grammar study
- 59 Franziska Biedermann
Auditorische Diskriminationsleistungen nach unilateralen Läsionen im Di- und Telenzephalon

- 60 Shirley-Ann Rüschemeyer
The Processing of Lexical Semantic and Syntactic Information in Spoken Sentences: Neuroimaging and Behavioral Studies of Native and Non-Native Speakers
- 61 Kerstin Leuckefeld
The Development of Argument Processing Mechanisms in German. An Electrophysiological Investigation with School-Aged Children and Adults
- 62 Axel Christian Kühn
Bestimmung der Lateralisierung von Sprachprozessen unter besonderer Berücksichtigung des temporalen Cortex, gemessen mit fMRT
- 63 Ann Pannekamp
Prosodische Informationsverarbeitung bei normalsprachlichem und deviantem Satzmaterial: Untersuchungen mit ereigniskorrelierten Hirnpotentialen
- 64 Jan Derrfuß
Functional specialization in the lateral frontal cortex: The role of the inferior frontal junction in cognitive control
- 65 Andrea Mona Philipp
The cognitive representation of tasks
Exploring the role of response modalities using the task-switching paradigm
- 66 Ulrike Toepel
Contrastive Topic and Focus Information in Discourse – Prosodic Realisation and Electrophysiological Brain Correlates
- 67 Karsten Müller
Die Anwendung von Spektral- und Waveletanalyse zur Untersuchung der Dynamik von BOLD-Zeitreihen verschiedener Hirnareale
- 68 Sonja A.Kotz
The role of the basal ganglia in auditory language processing: Evidence from ERP lesion studies and functional neuroimaging
- 69 Sonja Rossi
The role of proficiency in syntactic second language processing: Evidence from event-related brain potentials in German and Italian
- 70 Birte U. Forstmann
Behavioral and neural correlates of endogenous control processes in task switching

71 Silke Paulmann

Electrophysiological Evidence on the Processing of Emotional Prosody:
Insights from Healthy and Patient Population